GEORGIA INSTITUTE OF TECHNOLOGY — OFFICE OF CONTRACT ADMINISTRATION

PROJECT ADMINISTRATION DATA SHEET

[x] ORIGINAL [ ] REVISION NO. _____

Project No. E-26-688 (continuation of E-26-672) DATE 1/11/82

Project Director: Dr. J. W. Poston* School/Lab: Nuclear Eng.

Sponsor: Department of Energy, Oak Ridge Operations

Type Agreement: Contract DE-AS05-76EV04814, Mod A009

Award Period: From 12/1/81 To 6/30/82 (Performance) _____ (Reports)

Sponsor Amount: $9,300 Contracted through: GTRI/GIT

Cost Sharing: N/A

Title: Dev. & Application of Some Fast Newtron Dosimetry Techniques Utilizing Plastic Track Detectors for Radiotherapy and Health Physics

ADMINISTRATIVE DATA OCA Contact William F. Brown x4820

1) Sponsor Technical Contact:

Dr. Robert Wood
Pollutant Characterization & Safety
Research Division ~~M/S E-201~~
Dept. of Energy
Washington, D. C. 20545

2) Sponsor Admin/Contractual Matters:

Ms. Joyce Carringer
Procurement & Contracts Division
Dept. of Energy
Oak Ridge Operations
P. O. Box E
Oak Ridge, TN 37830
(615) 576-7564

Defense Priority Rating: None Security Classification: None

RESTRICTIONS

See Attached Gov't Supplemental Information Sheet for Additional Requirements.

Travel: Foreign travel must have prior approval – Contact OCA in each case. Domestic travel requires sponsor approval where total will exceed greater of $500 or 125% of approved proposal budget category.

Equipment: Title vests with none proposed or anticipated

COMMENTS:

Mod A009 adds $9,300 and extends contract through 6/30/82. Revised total value of contract (including prior project numbers) is $271,112.

*NOTE that Project Director is changed from K. Z. Morgan to J. W. Poston

COPIES TO:

Administrative Coordinator
Research Property Management
Accounting
Procurement/EES Supply Services
Research Security Services
Reports Coordinator (OCA)
Legal Services (OCA)
Library
EES Public Relations (2)
Computer Input
Project File
Other _____

FORM OCA 4:781

GEORGIA INSTITUTE OF TECHNOLOGY OFFICE OF CONTRACT ADMINISTRATION

SPONSORED PROJECT TERMINATION/CLOSEOUT SHEET

LR. 8/84 NBF

Date 3/5/85

Project No. E-26-688 School/Lab NE

Includes Subproject No.(s)

Project Director(s) Dr. J. W. Poston GTRI XXX XXXX

Sponsor Department of Energy, Oak Ridge Operations

Title Development & Application of Some Fast Neutron Dosimetry Techniques Utilizing Plastic Track Detectors for Radiotherapy and Health Physics.

Effective Completion Date: 6/30/82 (Performance) 6/30/82 (Reports)

Grant/Contract Closeout Actions Remaining:

- [X] None
- [ ] Final Invoice or Final Fiscal Report
- [ ] Closing Documents
- [ ] Final Report of Inventions
- [ ] Govt. Property Inventory & Related Certificate
- [ ] Classified Material Certificate
- [ ] Other

Continues Project No. E-26-672 Continued by Project No.

COPIES TO:

Project Director
Research Administrative Network
Research Property Management
Accounting
Procurement/EES Supply Services
Research Security Services
Reports Coordinator (OCA)
Legal Services

Library
GTRI
Research Communications (2)
Project File
Other M. Heyser

A. Jones

Form OCA 60:1028

DEVELOPMENT AND APPLICATION OF THE ELECTROCHEMICAL ETCHING TECHNIQUE

(Contract No. DE-AS05-76EV04814)
(Our Project E-26-688

by Micheal E. Sanders

July, 1984

Program In Nuclear Engineering and Health Physics
School of Mechanical Engineering
Georgia Institute of Technology
Atlanta, Georgia 30332

TABLE OF CONTENTS

PROJECT PERSONNEL

Karl Z. Morgan, Ph.D	Principal Investigator
Micheal E. Sanders, MSHP.	Graduate Research Assistant (1979 - 1982)
Mehdi Sohrabi, MSHP.	Graduate Research Assistant (1973 - 1975)
Gary B. Stillwagon, MSHP.	Graduate Research Assistant (1975 - 1978)
Shian J. Su, MS	Graduate Research Assistant 91975 - 1979)

All the student participants obtained their Ph.D degrees with theses based in part on work done under this contract and gratefully acknowledge the support of the U.S. Department of Energy.

1. SUMMARY

This final report documents the advances achieved in the development and application of several etched damage track plastic dosimeters that can be used to measure dose-equivalent from neutrons with energies from thermac to 20 Mev. Sohrabi (1975) initiated this project with the design of a rem-responding dosimeter that measured fast (> 1 Mev) neutron dose-equivalent as a function of the damage track density directly induced within the volume of polycarbonate foils amplified by electrochemical etching. Stillwagon (1978) adapted electrochemical etching of polycarbonate foils (ECEPF) to alpha dosimetry and used the technique to determine Pu-239 uptake in human bone. Su (1979) extended the usefulness of the ECEPF neutron dosimetry technique to encompass thermal neutron dose measurement. The thermal neutron dosimeter was composed of an external radiator tablet made of ^{7}LiF in contact with a polycarbonate foil and utilized the thermal neutron-induced $^{6}Li(n, \alpha)^{3}H$ reaction to give a dose-equivalent response as a function of alpha track density registered in the detector foil. An intermediate (lev-1mev) neutron dosimeter was developed by Sanders (1982) and has been shown to give an approximately dose-equivalent response to neutrons with energies from 1 ev to 17 Mev. The intermediate neutron dosimeter consists of ^{6}LiF-Teflon/CR-39 Polymer foil assembly which is enclosed by a (Cd + In) neutron filter. The neutron dose-equivalent is measured as a variable function of the damage track density rgistered in the CR-39 detector foil due to alpha particles from the 1/v dependent $^{6}Li(n, \alpha)^{3}H$ reaction, recoil H, C, O nuclei from neutron-induced elastic scattering within the foil volume, and protons from the $^{6}Li(n, p)$ reaction for neutron energies above 2 MeV.

Summaries of the above-mentioned advances are contained in this final report. Special emphasis is given to the most recent work by Sanders (1982) since it has not been reported in previous project reports.

The complete results to date of our research in the field of electrochemical etching of polycarbonate foils (ECEPF) for the purpose of dosimetry have been accumulated and appear in ORO-4914-5 and our progress reports dated August, 1977, August, 1978, August, 1979, August, 1980, and the final report, June, 1982. These reports show the intensive research done by the investigators in the field as well as some recommendations for the solution of new problems for the advancement of this rapidly developing and interesting type of dosimetry to many new applications. The results have been presented at several scientific meetings including the American Physical Society, Auburn, Alabama, 1975, and Chattanooga, Tennessee, 1979; Health Physics Society, Denver, Colorado, 1976, San Francisco, California, 1976; Atlanta, Georgia, 1977; Minneapolis, Minnnesota, 1978; Philadelphia, Pennsylvania, 1979; Seattle, Washington, 1980; Louisville, Kentucky, 1981; Orlando, Florida, 1982; International Radiation Protection Association, Amsterdam, The Netherlands, 1975; and Jerusalem, Israel, 1980; the American Industrial Hygiene Association, Atlanta, Georgia, 1976; and the American Nuclear Society, Raleigh, North Carolina, 1977, and Gainesville, Florida, 1978. (Copies of these reports have been sent to the Washington Office of the Department of Energy.)

(Note: Since Dr. Morgan retired from Georgia Tech some years ago, this report has been edited by Dr. John W. Poston). This report is a condensation of part of a Ph.D thesis of Mr. Micheal E. Sanders, presented in June 1982).

2. INTERMEDIATE NEUTRON DOSIMETER DEVELOPMENT

During the course of this research a rem-responding neutron personnel dosimeter, useable in the 1 eV to 1 MeV neutron energy region, has been developed and applied to the measurement of dose-equivalent in several different neutron spectra. The intermediate neutron dosimeter utilizes neutron-induced damage-track registration in CR-39 polymer foils and damage-track amplification by combined chemical-electrochemical etching. The optimum chemical and electrochemical etching parameters as well as the most neutron sensitive type of CR-39 have been established. Due to the inherent contribution of recoil protons and alpha particles in the intermediate neutron dosimeter designed in this research, several parameters relating to the track registration of these particles in CR-39 have been evaluated. Finally, by combining the intermediate neutron dosimeter of this research with other damage-track dosimetry techniques, a heretofore unachievable investigation of the neutron contamination generated outside and within the patient undergoing high-energy accelerator x-ray therapy has been successfuly completed for several representative medical therapy accelerators.

The results of the experimental investigations that led to the aforementioned developments are discussed in this section.

2.1 Design and Optimization of an Intermediate Neutron Dosimeter

The following sections describe the design of an intermediate neutron dosimeter and its subsequent calibration in several different neutron energy spectra. Because the dosimeter utilizes neutron-induced damage-track formation in CR-39 polymer foils from both an external alpha particle radiator and internal recoil nuclei, some etching characteristics of CR-39 foils exposed to alpha particles and proton fluences are described. Finally, the optimum combined chemical-electrochemical etching parameters are presented.

2.1.1 Optimization of Combined Etching Parameters for CR-39 Polymer Foils

Chemical and electrochemical etching parameters that affect the response of a polymer to a particular charged particle have been discussed in the open literature (see bibliography). In this section, some particular tests are reported which ultimately led to the optimization of combined chemical-electrochemical etching parameters for the CR-39 polymer foils used in the intermediate neutron dosimeter design.

2.1.1.1 Effects of CR-39 Types, Curing Times, and Thickness

As is the case with most polymers used in damage-track dosimetry, CR-39 polymer foils are not especially made by commercial manufacturers for dosimetric uses. Consequently, the reproducibility of damage-track response and background response can vary appreciably within the same sheet of CR-39 due to inhomogeneity, imperfections, surface contaminants, and thickness variations. When CR-39 is the polymer of choice, this situation is aggravated due to the small number of commercial vendors. Therefore, to deter-

mine the optimum CR-39 polymer foil, its curing time, and thickness for use in neutron and alpha particle dosimetry studies, CR-39 manufactured by three vendors was examined. These vendors are the ones most commonly listed in the literature as sources of high quality CR-39. The three are: SGL Homalite (Division of PPG Industries, Inc.), Wilmington, Delaware; Pershore Mouldings Limited, Pershore, Worcestershire, England; and American Acrylics and Plastics, Inc., Stratford, Connecticut.

Commercial CR-39 polymer sheets are made by dissolving a peroxide initiator such as benzoyl peroxide or di-isopropyl peroxydicarbonate (IPP) into the liquid monomer, allyl diglycol carbonate. The initiated solution is injected between glass plates separated by a vinyl gasket. The assembly is then tightly clamped together and its temperature is gradually raised until polymerization is complete. The rate of polymerization is determined by the amount and type of initiator used and by the temperature of the monomer. As far as it is known, only one type of allyl diglycol carbonate monomer is made. Pittsburgh Plate Glass Co. makes all the monomer used in the USA and Arinor, Ltée., Paris, under license to PPG, makes the monomer for Pershore Mouldings Ltd. Even though it is unstable at room temperature, IPP is the initiator most commonly used and is exclusively used in the CR-39 investigated in this study. Thus, since the polymer ingredients are essentially the same in all three CR-39 polymer foils examined here, any differences in response etc. must be attributed to the manufacturing process. Very thick, large-area, tempered glass plates are used to hold the CR-39 during polymerization to minimize breakage of the brittle polymer and to maximize production rate. The use of this type of glass plate results in two problems: (1) if the thermal curing cycle is not carefully programmed, the inefficient transfer of heat through the thick glass can cause high

temperature areas and large thermal gradients in the hardening polymer and result in stressed or microcracked areas, (2) unless a chemical mold release agent is used, the polymer sheets tend to stick to the glass plates. It is believed that large thermal gradients within the polymerizing sample, termination of the cure time before polymerization is complete, and chemical effects on the polymer surface at the polymer-glass interface are the primary factors in the response, background, and thickness variations seen in different CR-39 polymer foils. Two other factors may also contribute to the difficulty in obtaining a high-quality detector foil: the monomer must not be allowed to come in contact with oxygen or polymerization will be inhibited and, unless a suitably flexible gasket is employed, the 14 percent shrinkage seen in the polymer during polymerization can cause nonuniformities and cracking.

The first, and ultimately most important, task in damage-track dosimetry is to determine the best suited track-recording polymer. To achieve this goal CR-39 samples from each of the three vendors were subjected to the following series of tests. Sets consisting of three foils from each vendor were exposed for durations of 12, 24, and 40 hours to a 4μ g Cf-252 neutron source. The foils were positioned normal to the fluence and 25 cm away from the stainless steel encapsulated source. Similar sets of foils were exposed to an alpha particle fluence for durations of 5, 10, 15, and 20 seconds. The foils were placed 1.9 cm away from a 2 Ci Pu-239 alpha particle source. Each neutron-irradiated CR-39 foil was etched chemically in 45 percent KOH at 70°C for one and one-half hours, while each alpha irradiated foil was etched chemically in 45 percent KOH at 70°C for one hour. Then all the CR-39 foils were etched electrochemically in 45 percent KOH at 254°C, 2 kHz, and 20 kV/cm for two hours. The foils were cleaned, dried, and evaluated

for track density using the magnification of a standard microfiche reader. The results, plotted in Figures 1 and 2, clearly indicate that American Acrylics CR-39 foil offers superior registration of both neutron-induced and alpha-induced damage-tracks.

Reproducibility of damage-track response was examined in the three different CR-39 polymers by exposing two stacks of seven foils from each of the vendors to equal fluences of neutrons generated in the Brown-Boveri 45 MeV accelerator x-ray beam. The foil stacks were situated at a target-to-source (TSD) distance of 110 cm and normal to the primary x-ray beam. An x-ray dose of 500 rads measured at the depth of maximum dose build-up was delivered to the foils. All the foils were etched under the same conditions, i.e. a chemical etch in 45 percent KOH at 70°C for one and one-half hours followed by an electrochemical etch in 45 percent KOH at 25°C, 2 kHz, and 20 kV/cm for two hours. Reproducibility was measured as a function of $\pm$ one standard deviation for each set of 14 CR-39 foils per vendor. The 14 neutron-induced measurements recorded in the American Acrylics CR-39 were reproducible to within $\pm$ 6.3 percent, while the same tolerance for the Pershore CR-39 was $\pm$ 9.8 percent and that for the Homalite was $\pm$ 14.1 percent.

A desirable characteristic of any dosimeter is a low background response. The three investigated CR-39 polymers were evaluated to determine their respective background characteristics by subjecting seven foils of each to the same combined etch of one and one-half hours in 45 percent KOH at 60°C and then electrochemical etching for two and one-half hours in 45 percent KOH at 25°C, 2 kHz, and 20 kV/cm. The American Acrylics foils had by far the lowest background response at 7.1 $\pm$ 0.6 tracks/cm^2, while the Pershore 16-hour cure C-39 exhibited 69.6 $\pm$ 10.4 tracks/cm^2, and the

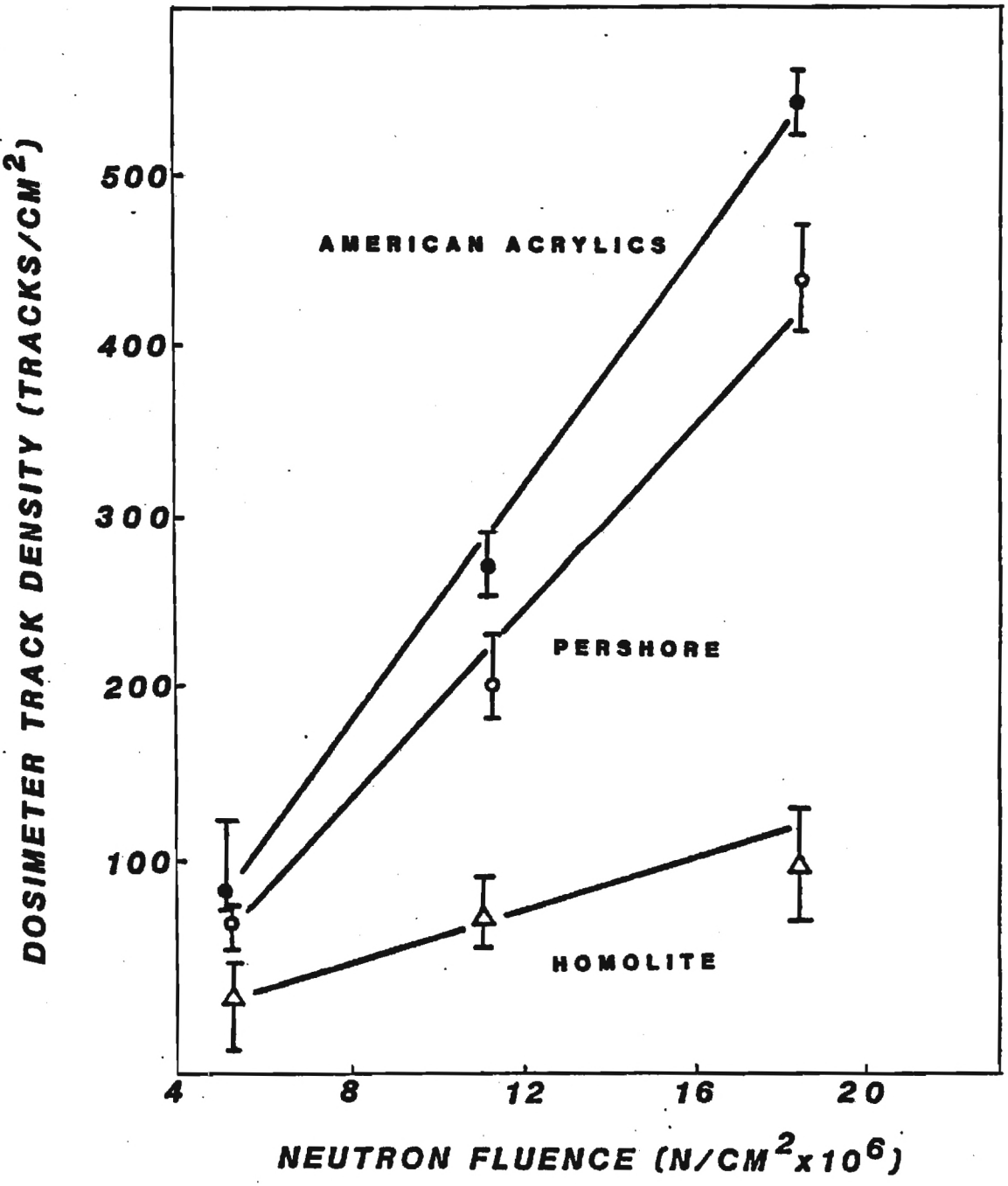

Figure 1. Comparison of Neutron-Induced Track Response in Etched CR-39 Foils Obtained from Three Different Vendors

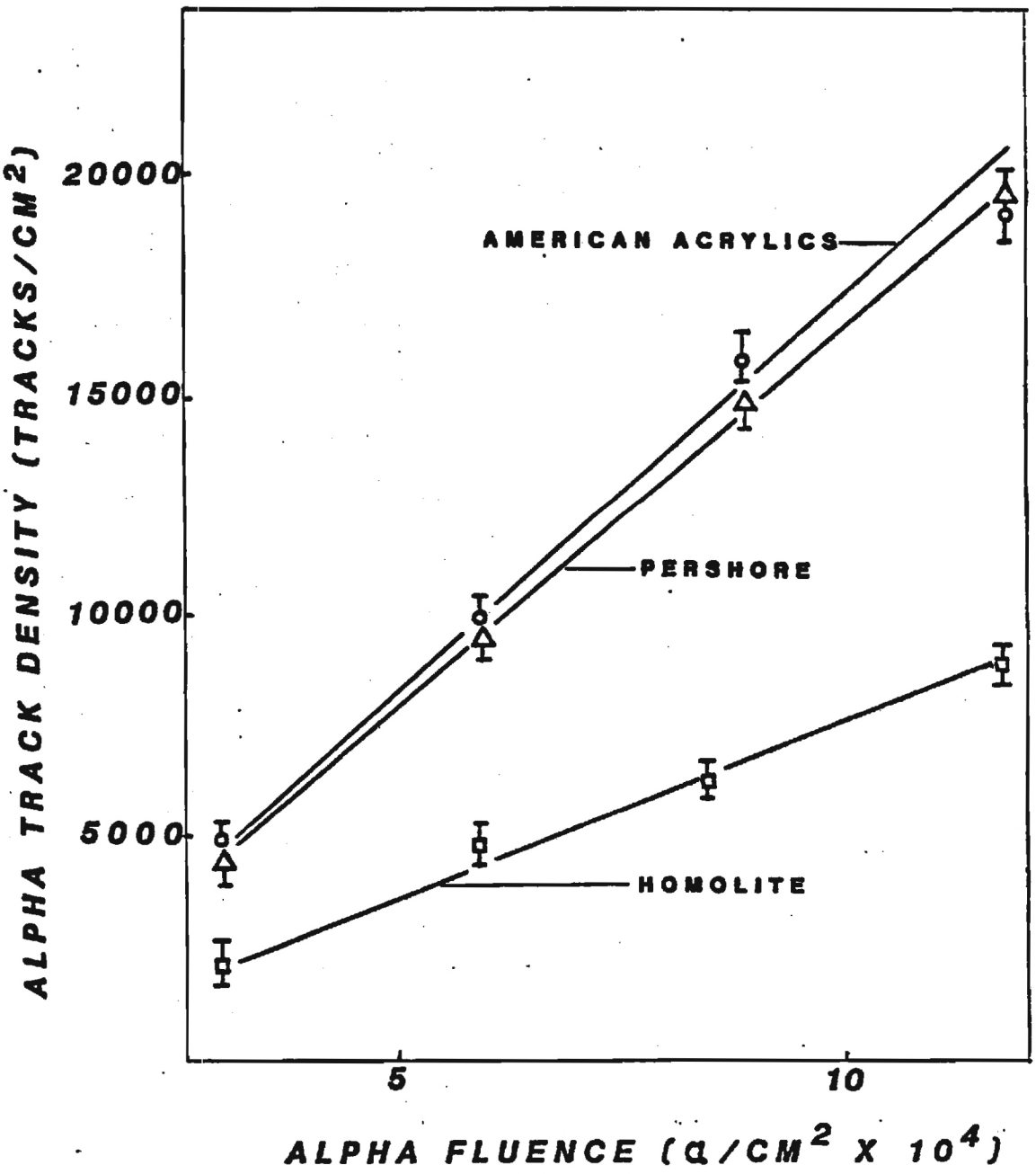

Figure 2. Comparison of Alpha Particle Track Response in Etched CR-39 Foils Obtained from Three Different Vendors

Homalite 70.0 ± 12 tracks/cm^2. The dramatic difference in background response found using American Acrylics CR-39 is primarily due to its availability in sheets that are protected by 40μ m thick polyethylene film on each surface. When the American Acrylics CR-39 foils are stored without the protective film, the background can increase from around 5 tracks/cm^2 to as high as 50 tracks/cm^2 over a period of 60 to 90 days.

Since CR-39 is a thermoset polymer, more cross-linking of the long chain polymer molecules occurs as the curing time increases. Only one of the three CR-39 polymers investigated was available with different curing times. The CR-39 obtained from Pershore Mouldings can be purchased with curing times of 8, 16, 32, and 96 hours. The CR-39 sheets are cured by holding the initiated monomer containing plate glass molds vertically in a water bath kept at 65° ± 3°C for the particular duration. The effect of curing time on foil detector sensitivity, track diameter, and background was investigated for CR-39 foils having different curing times available from Pershore. The damage-track response as a function of curing time was determined by exposing three foils of each curing duration to Pu-239 alpha particles. The foils were placed 1.9 cm away from a 2 μCi 2.0 cm diameter Pu-239 source and irradiated for five seconds. Each foil was subjected to a combined etch of one-half hour in 45 percent KOH at 60°C followed by an electrochemical etching cycle of two and one-half hours in 45 percent KOH at 25°C, 2 kHz, and 23 kV/cm. The CR-39 damage-track sensitivity does not appear to be affected by curing time, as can be seen in Table 1. However, Figure 3 shows that curing time does affect the track size after electrochemical etching. The average diameter of an alpha particle damage-track in the 8 hour cured CR-39 is approximately four times the diameter of the damage-track in the 96 hour cured samples. This is probably due to the

Table 1. Sensitivity of Pershore CR-39 Foils Irradiated with Pu-239 Alpha Particles as a Function of Curing Time

Curing Time (Hr)	CR-39 Detector Sensitivity (Tracks/Alpha)
8	$2.5 \times 10^{-3} \pm 8\%$
16	$2.8 \times 10^{-3} \pm 8\%$
32	$2.45 \times 10^{-3} \pm 10\%$
96	$3.0 \times 10^{-3} \pm 20\%$

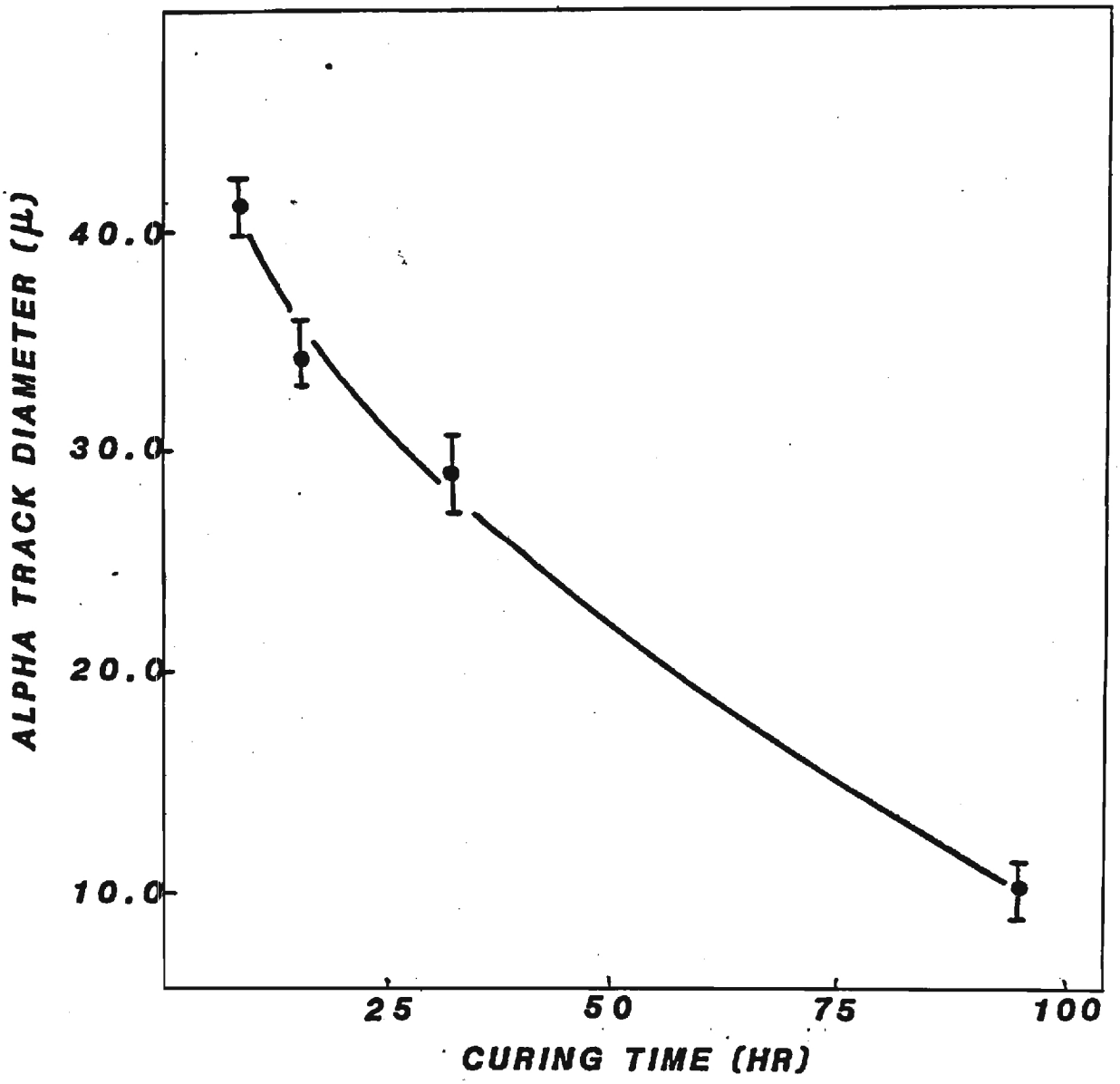

Figure 3. Effect of Curing Time of Pershore CR-39 Foils on the Combined Etch Alpha Particle Track Diameter

higher degree of cross-linking evident in the longer cured foils which may tend to inhibit electric tree growth at the chemically etched pit tips. Although the longer curing time does not significantly affect the CR-39 track registration sensitivity, the smaller track size and, in some cases, rather incomplete electrochemical etching damage-track appearance, results in a more tedious track counting procedure. Even under optimum etching conditions, this situation can lead to statistical counting errors. The small track diameter cam be compensated for by simply extending the electrochemical etching time. Background response as a function or CR-39 curing time is exhibited in Figure 4. Interestingly, the background track density measured in 14 CR-39 foils increased with extended curing time. This response was unexpected since, according to thermal annealing studies in polycarbonate, the curing process in CR-39 would be expected to anneal-out background tracks. A possible explanation of this effect is that the CR-39 sheets may register damage-tracks from alpha particles emanating from the glass plate molds in which they were contained during the cure process.

Larger variations in thickness than those quoted by the vendors were observed in all three CR-39 polymers investigated (see Figure 5). The variations charted in each histogram shown in the figure represent thickness differences observed within the same sheet of CR-39; however, thickness variations measured between different sheets tend to be greater. The following series of tests were performed to determine the effect of CR-39 thickness variations on detector foil response, track diameter, and background response. Unirradiated CR-39 foils with incremental thicknesses varying between 200 μ m and 500 μ m were etched electrochemically in 45 percent KOH at 25^{o}C, 2 kHz, and 23 kV/cm for two and one-half hours. The foils were evaluated for background response using the standard track

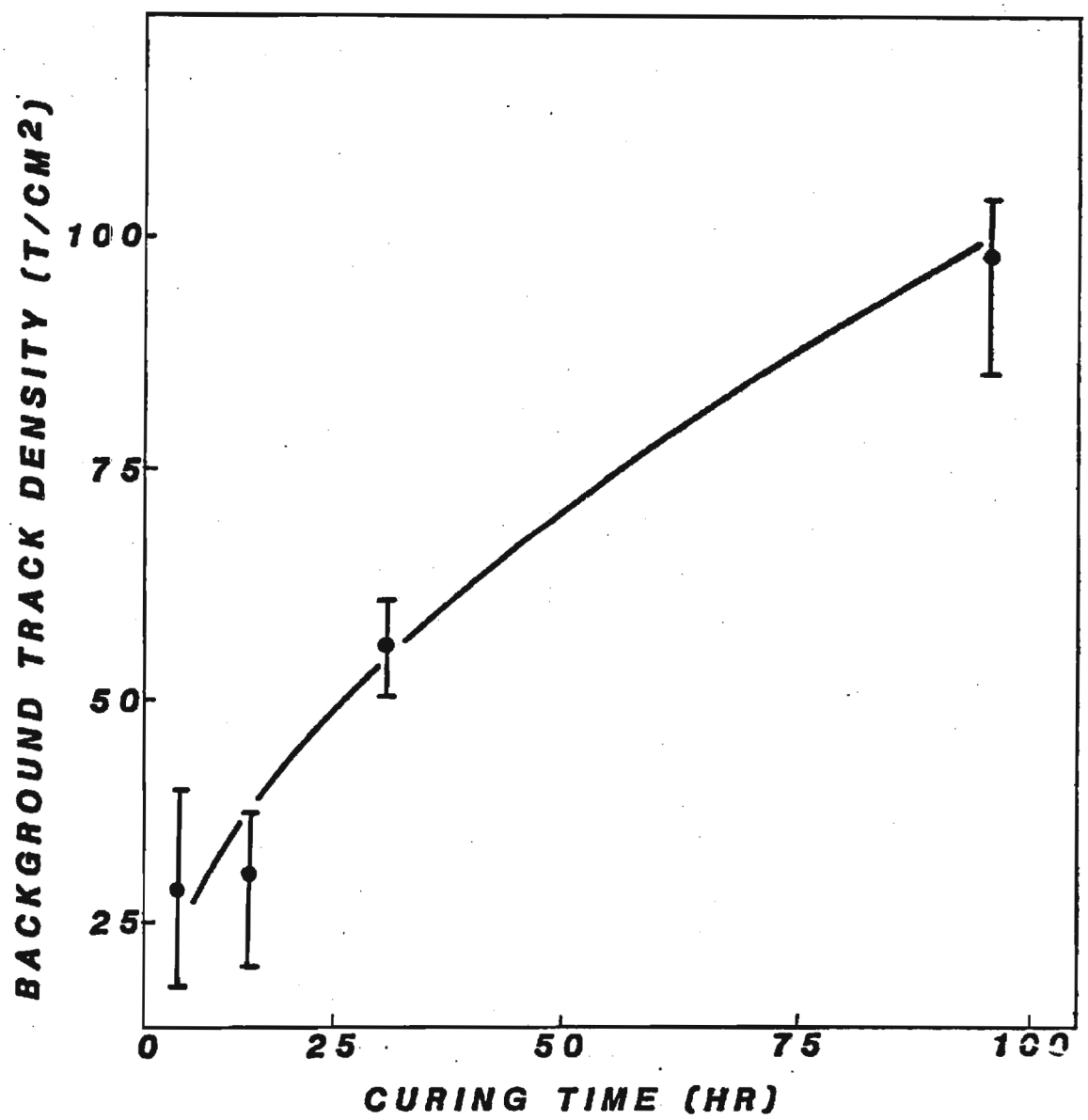

Figure 4. Background Response Found in Etched Pershore CR-39 as a Function of Curing Time

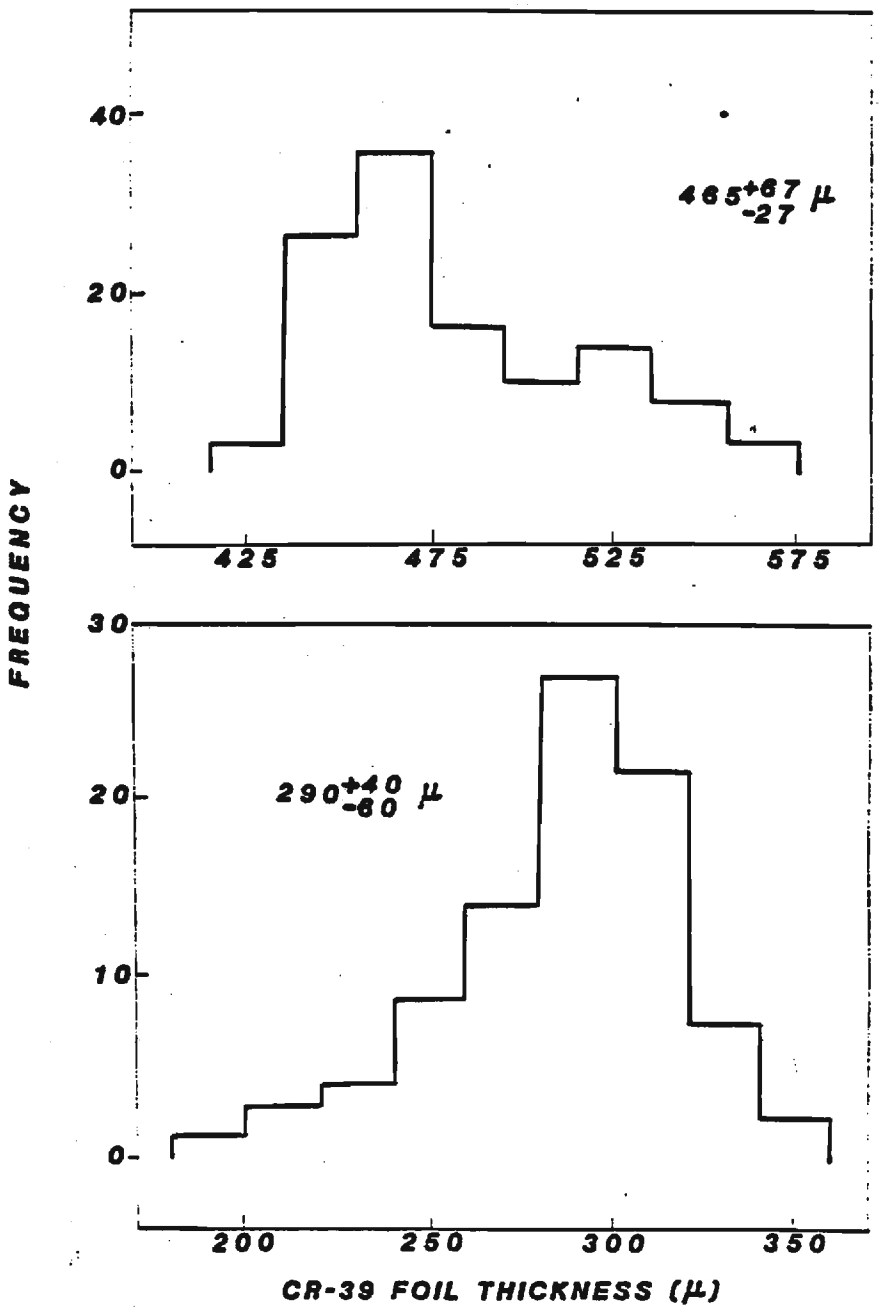

Figure 5. Histograms of Foil Thickness Variations Seen in Two Different Sheets of American Acrylics CR-39 Polymer

counting procedure. Figure 6 shows that the background response varied significantly with detector foil thickness at CR-39 thicknesses less than approximately 300 μm. The large, almost exponential, increase seen as the foil becomes very thin is most likely due to electrical breakdowns in the polymer foil volume which subsequently lead to "spontaneous" electrical treeing as the electrochemical bulk etching process proceeds. This increase in background response for very thin foils, when etched electrochemically, has been observed by others using bisphenol-A polycarbonate as the detector foil (Somogyi et al., 1979).

Damage-track sensitivity response as a function of CR-39 foil thickness was determined by irradiating several foils of incremental thicknesses between 300 μm and 600 μm for five seconds with Pu-239 alpha particles from a 2 Ci source. Each foil was approximately 2.5 cm x 2.5 cm in size. The irradiated foils were etched chemically in 45 percent KOH at 60°C for 30 minutes and etched electro-chemically in 45 percent KOH at 25°C, 2 kHz, and 23 kV/cm for two and one-half hours. The damage-track sensitivity nesses between 300 m and 600 m for five seconds with Pu-239 alpha response as a function of detector foil thickness is shown in Figure 7 and exhibits no significant decrease with increasing CR-39 thickness. Thus, as along as the thickness variation over the area of the dosimeter foil is less than ± 10 percent, no significant response variation should be encountered. All of the CR-39 foil samples used in this study had a thickness variation of not more than ± 10 percent for a given type.

Figure 8 exhibits the damage-track diameter variation as a function of foil thickness. The same CR-39 foils used in the response versus foil thickness study described above were used in this investigation. Track diameters were measured using a binocular phase contrast microscope at 100X

magnification equipped with a Filar micrometer. The results show that a decrease of ~50 percent in track diameters is apparernt between foils of 300 μ m and 600 μ m thicknesses. However, this variation is primarily seen in foils thinner than ~ 400 μ m. Track diameter variation only in the thinner foils may indicate an electrical breakdown process within the thin foil volume similar to that which predicates the large background increases observed in these same foils or a difference in the contribution of the chemical or electrochemical etching processes.

One of the most often reported problems associated with using CR-39 as a dosimeter is also encountered with many other polymers and is related to the thickness differences found within the same CR-39 sheet, inhomogeneities within the polymer foil volume, surface abrasions, etc. These problems were investigated here and we can offer some suggestions on how to best choose CR-39 for use in dosimetry. We found that Pershore Mouldings CR39 and American Acrylics CR-39 was the foil of choice in this research because of the dramatically lower background response compared to the others. Since all of the CR-39 sheets tested exhibited thickness variations imposed on CR-39 manufacture, each individual dosimeter foil should be measured for thickness and categorized for use with foils of similar thick ness. In this research, a $\pm$ 25 μm criterion ws used to separate dosimeter foils into select sets.

2.1.1.2 Chemical Etching Parameters.

The shape of the chemically etched pit, formed during the chemical etch phase of the combined etch process, is very important to the subsequent electrochemical etch track formation efficiency. As the etch pit tip radius gets larger, that is the track shape becomes more rounded and less conical,

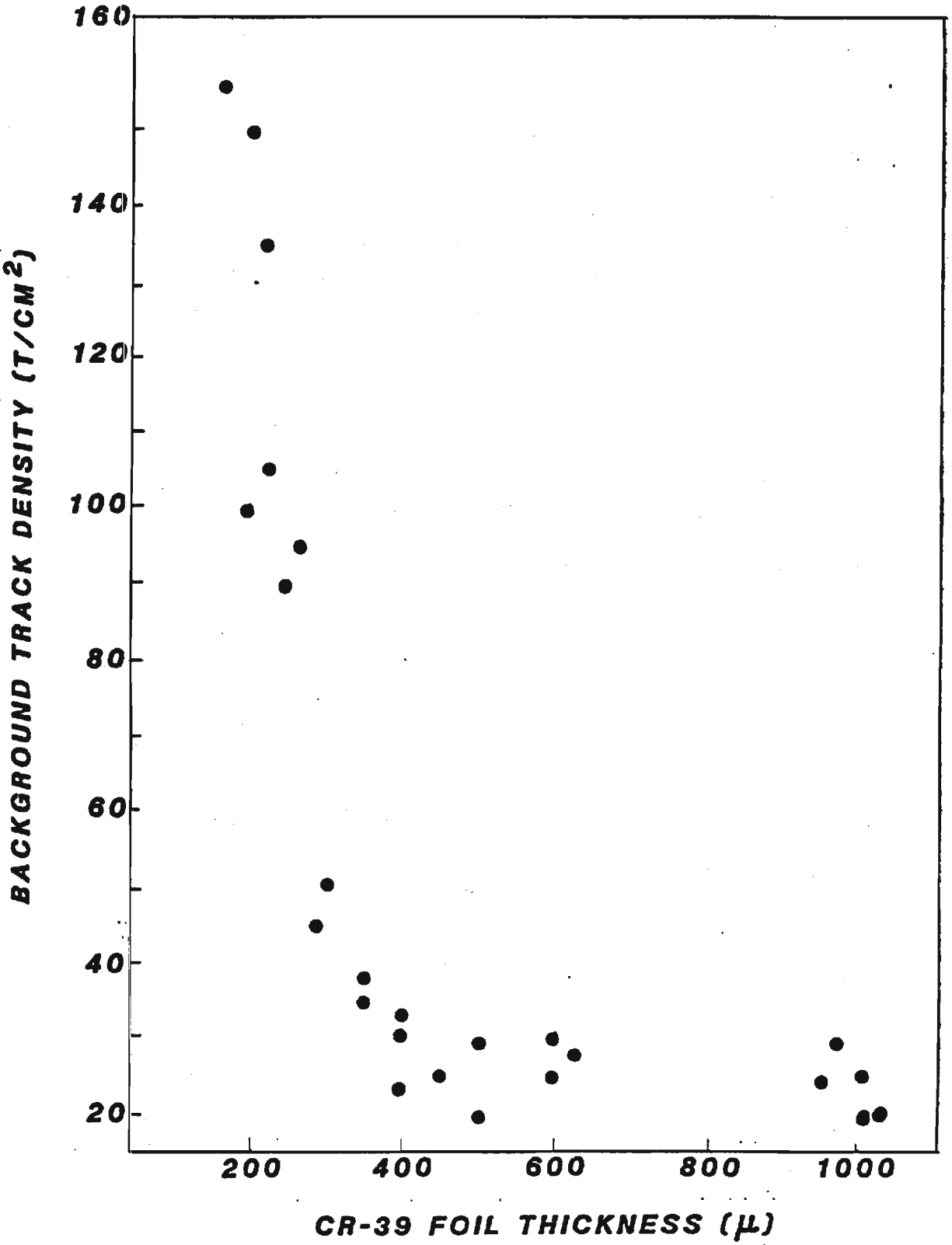

Figure 6. Background Track Density Found in Pershore CR-39 After Combined Chemical and Electrochemical Etching

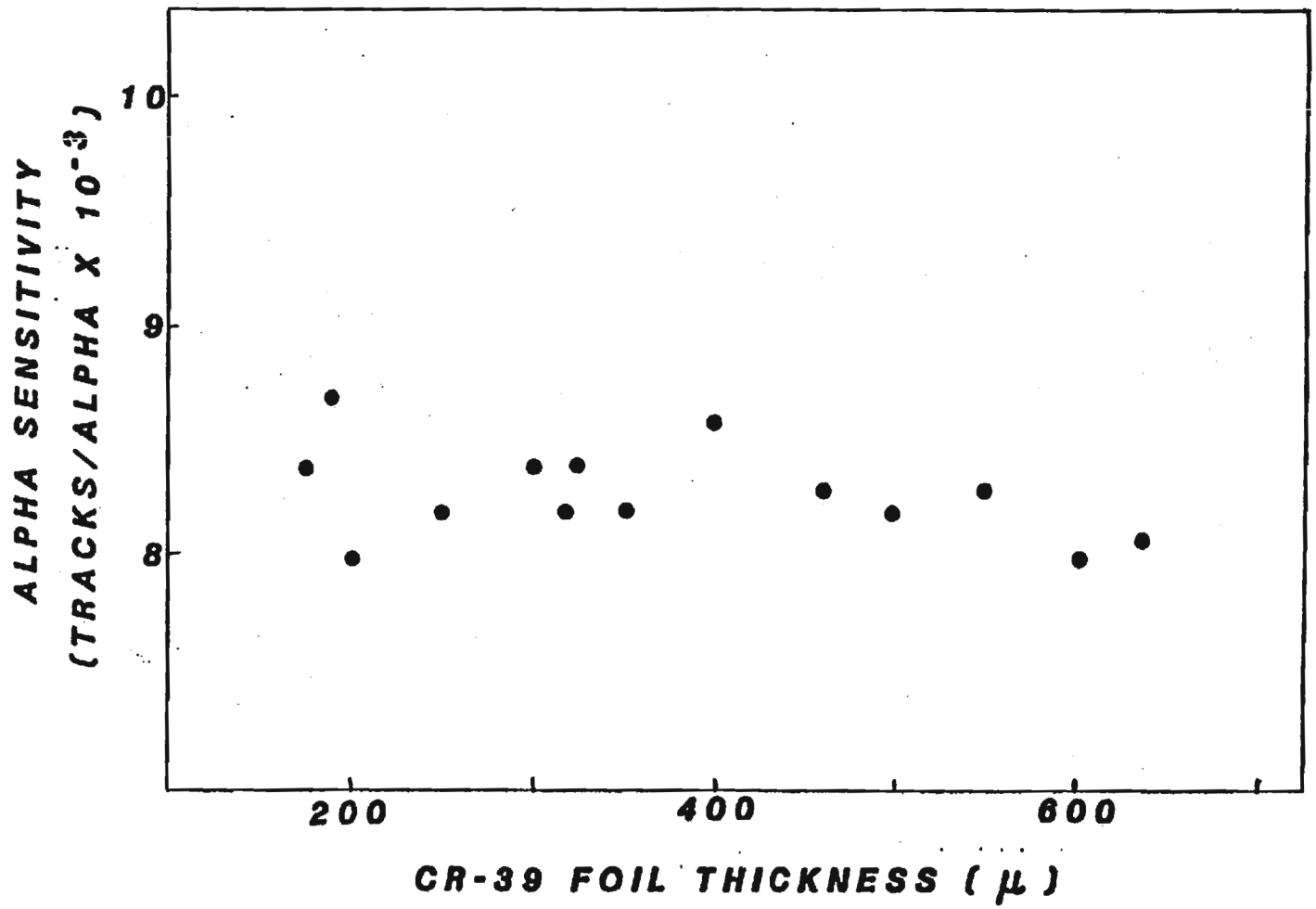

Figure 7. Alpha Track Sensitivity Seen in Etched CR-39 Foils as a Function of Foil Thickness

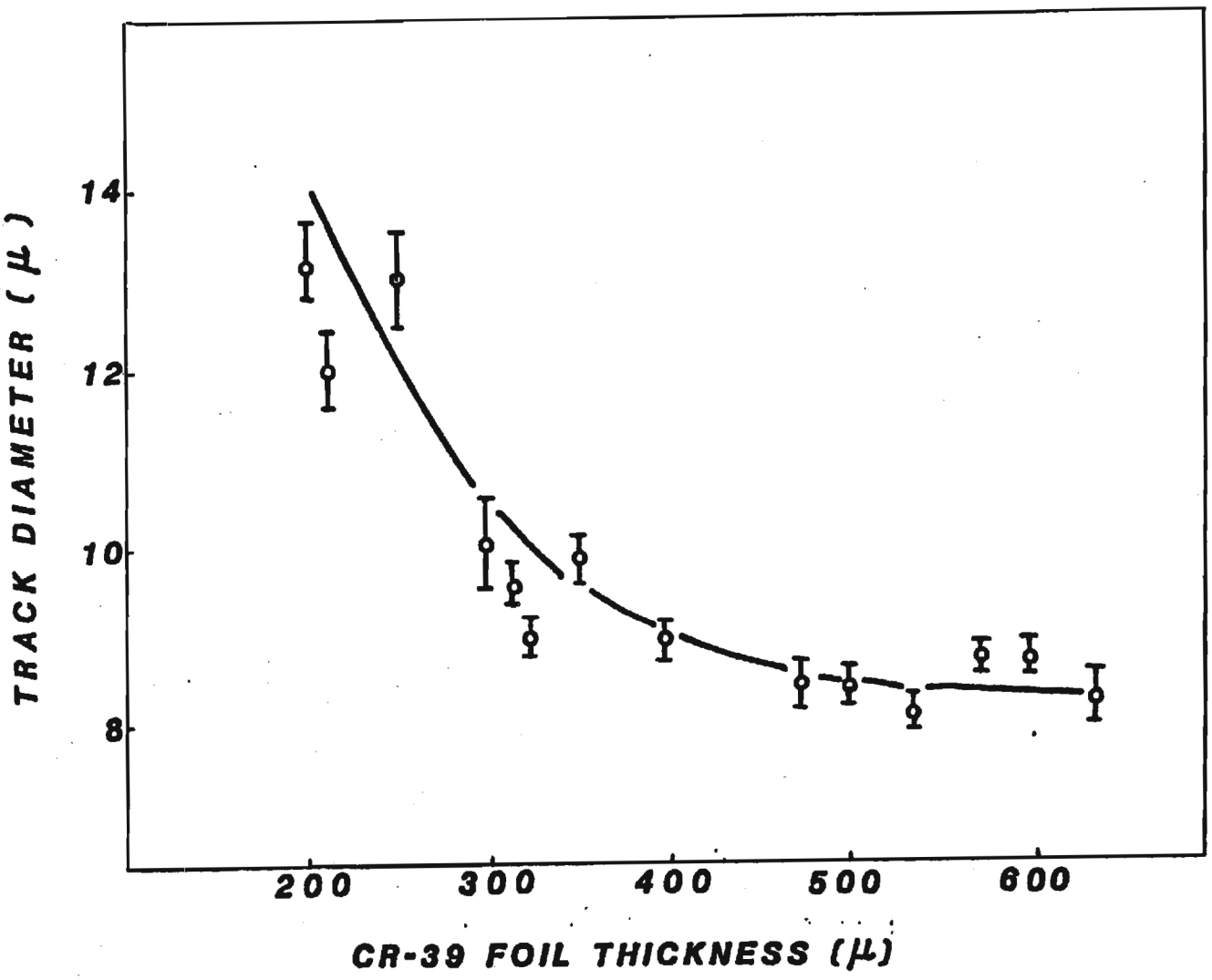

Figure 8. Variation of Alpha Particle Track Diameter Seen in Combined Chemical and Electrochemical Etched CR-39 as a Function of Foil Thickness

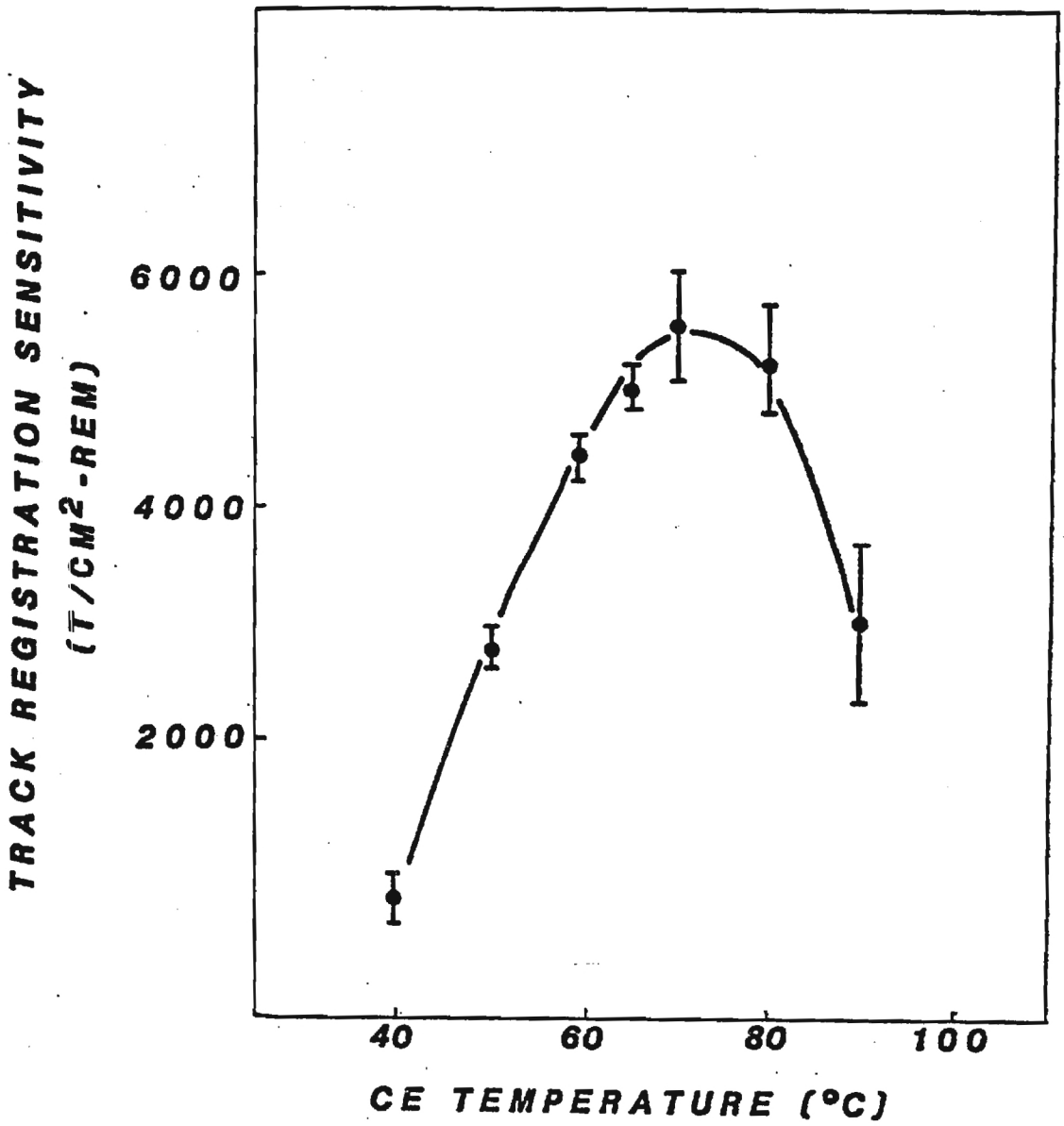

Figure 9. Sensitivity of Combined Chemical and Electrochemical Etched Neutron-Induced Track Registration in CR-39 Foils as a Function of the Chemical Etchant Temperature

the local electric field at the tip becomes smaller and the probability of electric tree propagation decreases. Therefore, control of the chemically etched pit growth is essential to obtain the highest efficiency of electrochemical etch track formation from any bombarding particle. Since elevated temperature etching is necessary for forming the etch pits in CR-39 in a reasonable time and the most critical parameter controlling chemical etchant attack is the temperature of the etchant (Fleischer et al., 1975; Sohrabi, 1975; Becker, 1973), the following test was devised to determine the optimum chemical etch duration and temperature for neutron detection. Seven stacks of seven 400 μm thick American Acrylics CR-39 foils were exposed to equal fluences of neutrons generated within the primary x-ray beam of an Allis-Chalmers 254 MeV betatron. Each set of CR-39 foils was etched chemically for one and one-half hours in 45 percent KOH and then electrochemically etched in KOH at 25°C, 2 kHz, and 20 kV/cm for two and one-half hours. Figure 9 shows that the highest electrochemical etch track formation efficiency was found when the chemical etchant temperature was between 75-80°C. However, at chemical etchant temperatures greater than about 60°C, the build-up of etch product on the foil surface tends to influence the light transmissibility of the detector. Thus, track density evaluation by light microscopy becomes more tedious and the errors associated with the evaluation increase. The chemical etchant is stirred magnetically during the chemical etch cycle and the foil detectors are removed periodically from the etchant to be washed in a warm water bath to help reduce the etch-product layer build-up. This technique works relatively well up to etchant temperatures of about 60°C; thus, this temperature was used for the chemical etch cycle in most of this research.

Once the etchant temperature was chosen for the chemical etch, an optimum chemical etch duration was determined. In this test, $\sim 400\mu m$ thick American Acrylics CR-39 foils, which had been neutron irradiated in the Allis-Chalmers 25 MeV betatron x-ray beam, were etched chemically in 45 percent KOH at 60°kC for times ranging from 30 minutes to 4 hours. After electrochemically etching in 45 percent KOH at 25°C, 2 kHz, and 23 kV/cm for two and one-half hours, all detector foils were evaluated for damage-track formation efficiency. Figure 10 shows that a peak is achieved after an etch time of two hours. In the foils that result in the formation of this peak, approximately as many etch pits have been etched past the optimum etch pit shape as have been etched to that shape during the chemical etch phase. Build-up of etch-product layer on the CR-39 foil surface begins to degrade the electrochemical etch track formation efficiency and the ease of track evaluation in the detector at etch time greater than about four hours. Figure 11 displays the electrochemically etched damage-track diameter growth as a function of chemical etching duration. The background response seen on unirradiated CR-39 foils generally decreases as the chemical etch duration increases. The higher background response after approximately two hours, seen in Figure 12, may be associated with build-up of etch product on the foil surface.

2.1.1.3 Electrochemical Etching Parameters.

A dramatic increase in damage-track amplification can be realized by utilizing electrochemical etching. To achieve the maximum sensitivity, electric tree propagation, and lowest background response, the electric field strength and its frequency must be optimized for the CR-39 detector foils. The electrochemical etch duration is also an important

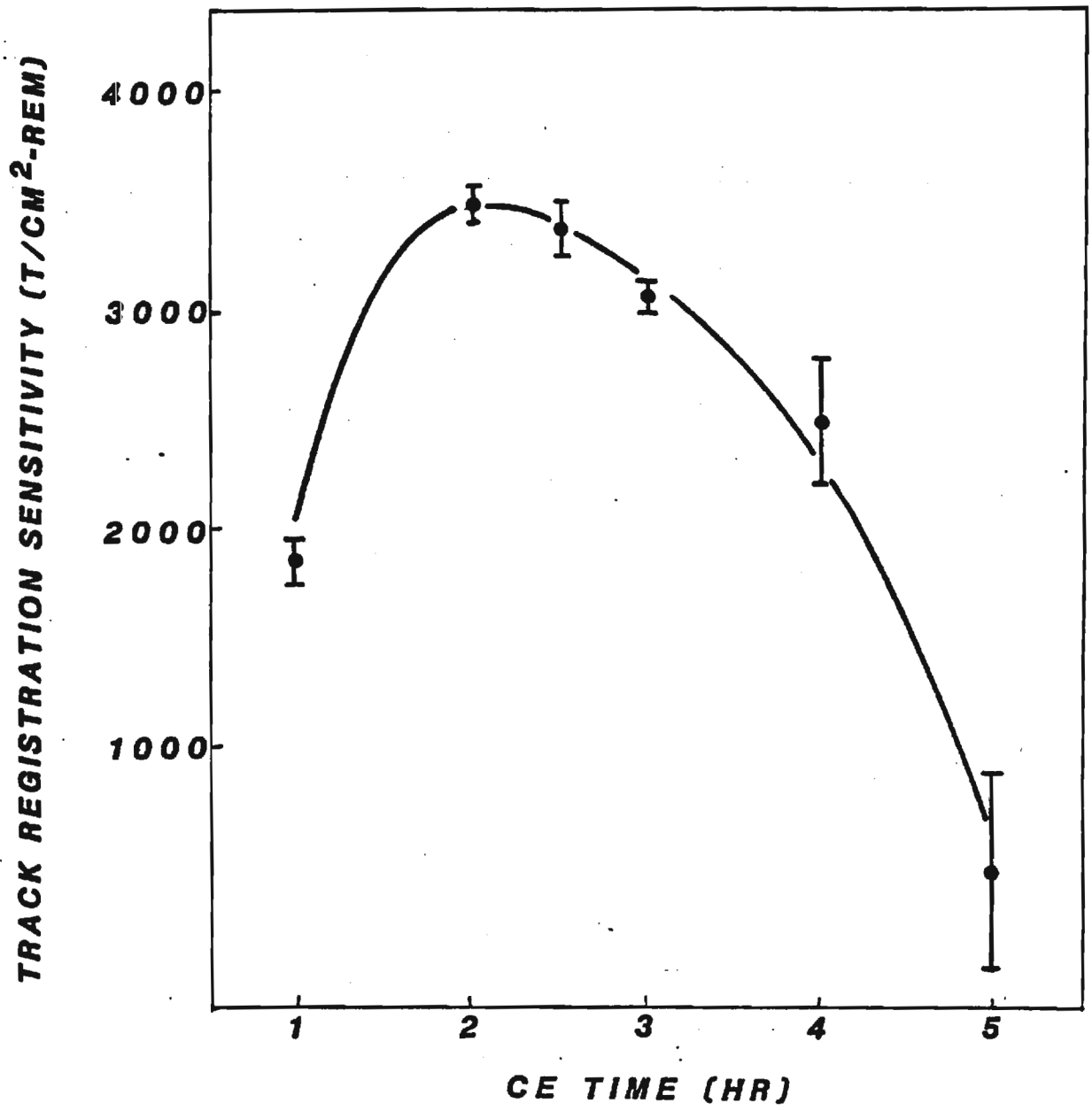

Figure 10. Sensitivity of Combined Chemical and Electrochemical Etched CR-39 Foils to Neutron-Induced Track Registration as a Function of Chemical Etching Time

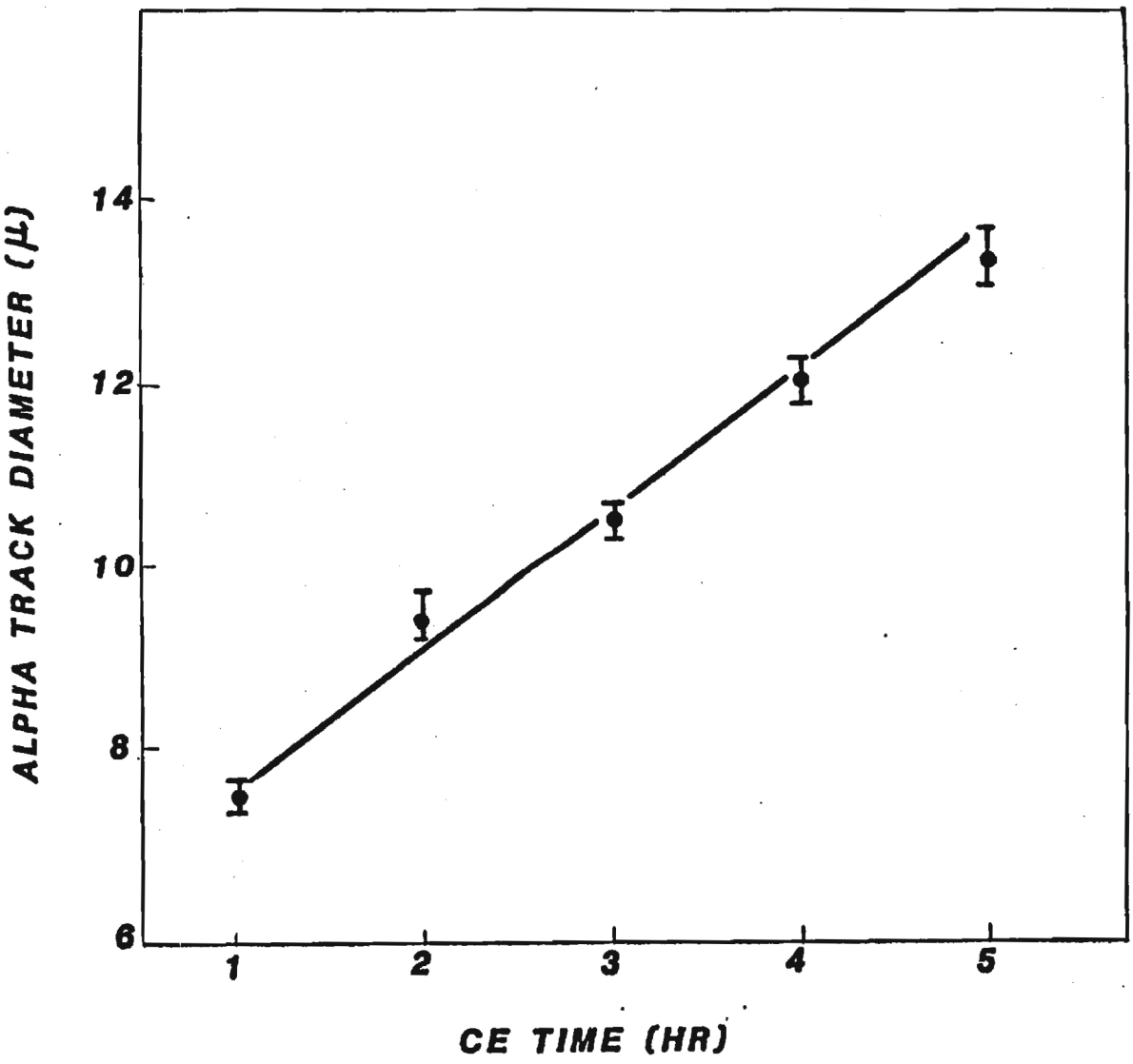

Figure 11. Alpha Track Diameter Variation in Combined Chemical and Electrochemical Etched CR-39 Foils as a Function of Chemical Etching Time

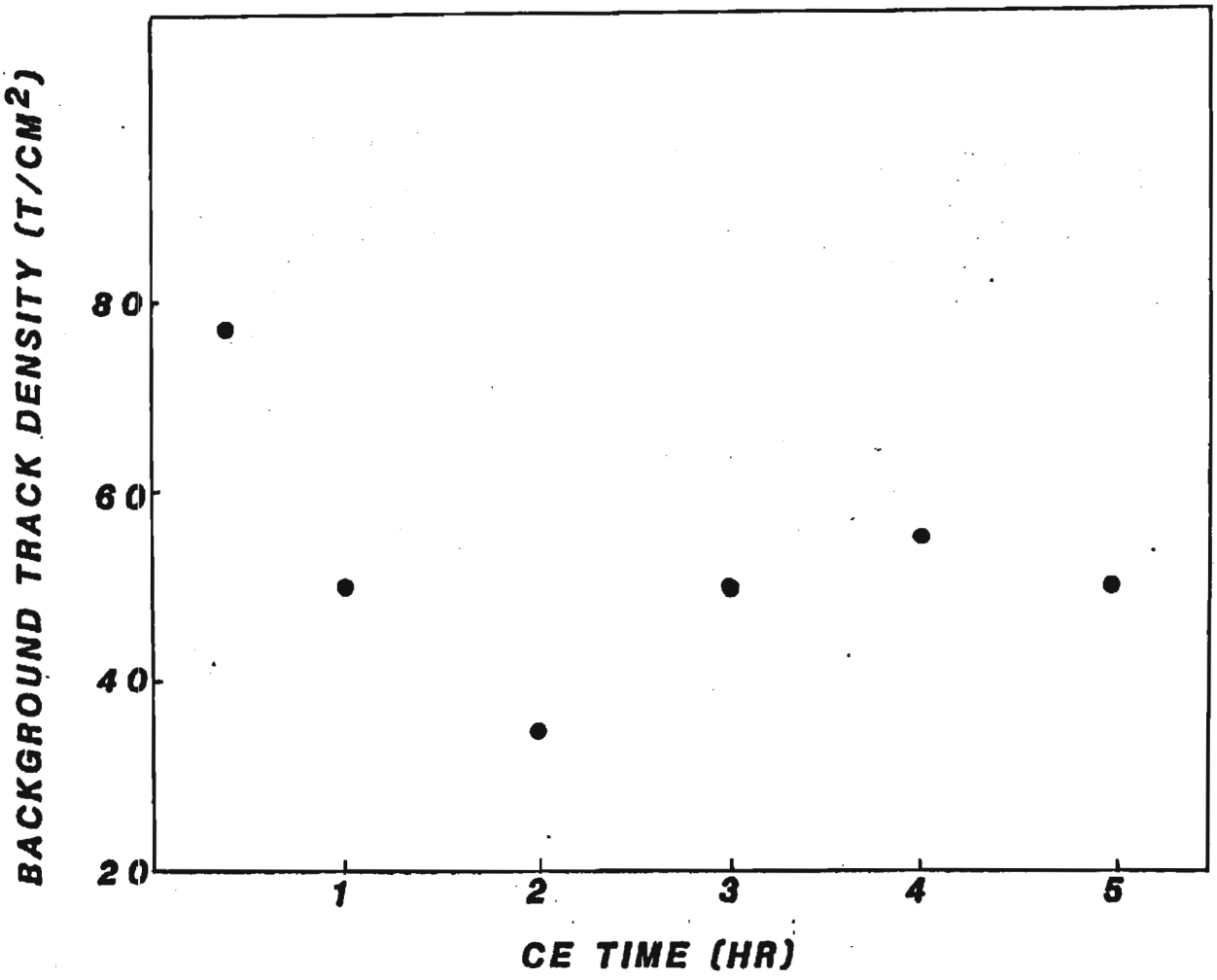

Figure 12. Background Track Density Seen in Combined Etch CR-39 Foils as a Function of Chemical Etching Time

consideration in the efficiency of damage-track revelation and track diameter growth and thus should be selected carefully.

Pershore Mouldings' 32 hour cured, ~400μm thick CR-39 foils were exposed to equal fluences of photoneutrons generated in the x-ray beam of a Brown-Boveri 45 MeV betatron. All the detector foils were etched chemically in 45 percent KOH at 60°C for two hours. Sets of seven of the chemically etched foils were etched electrochemically in 45 percent KOH at 25°C, 2 kHz, for two hours at one of five intervals of electric field strength between 16 kV/cm and 36 kV/cm. The damage-track formation sensitivity as a function of electric field strength in Figure 14. From these data the optimum electric field strength for neutron induced track revelation in CR-39 foils would appear to be about 26 kV/cm. However, as can be seen in Figure 15, which shows data taken using the identical combined etching procedure but upon unirradiated CR-39 foils, the measured background track density increases rapidly as the electric field strength is raised above 20 kV/cm. The increase in background at higher electric field strength has been observed by other researchers, albeit in bisphenol-A polycarbonate (Somogyi et al., 1979; 1980). This phenomenon is most likely caused by electrical breakdowns at structurally weak areas or in homogeneities in the polymer volume. These stressed points become candidates for electrical treeing and the resultant spontaneous "background" generation. Therefore, an electric field strength of 23 kV/cm as applied across the CR-39 polymer foils, in most of the tests in this research, is a compromise between optimum sensitivity rsesonse and low background.

The frequency of the electric field was also varied while all other parameters were held constant, to determine its effect upon background, damage-track revelation, and track diameter growth. Pershore Mouldings' 32

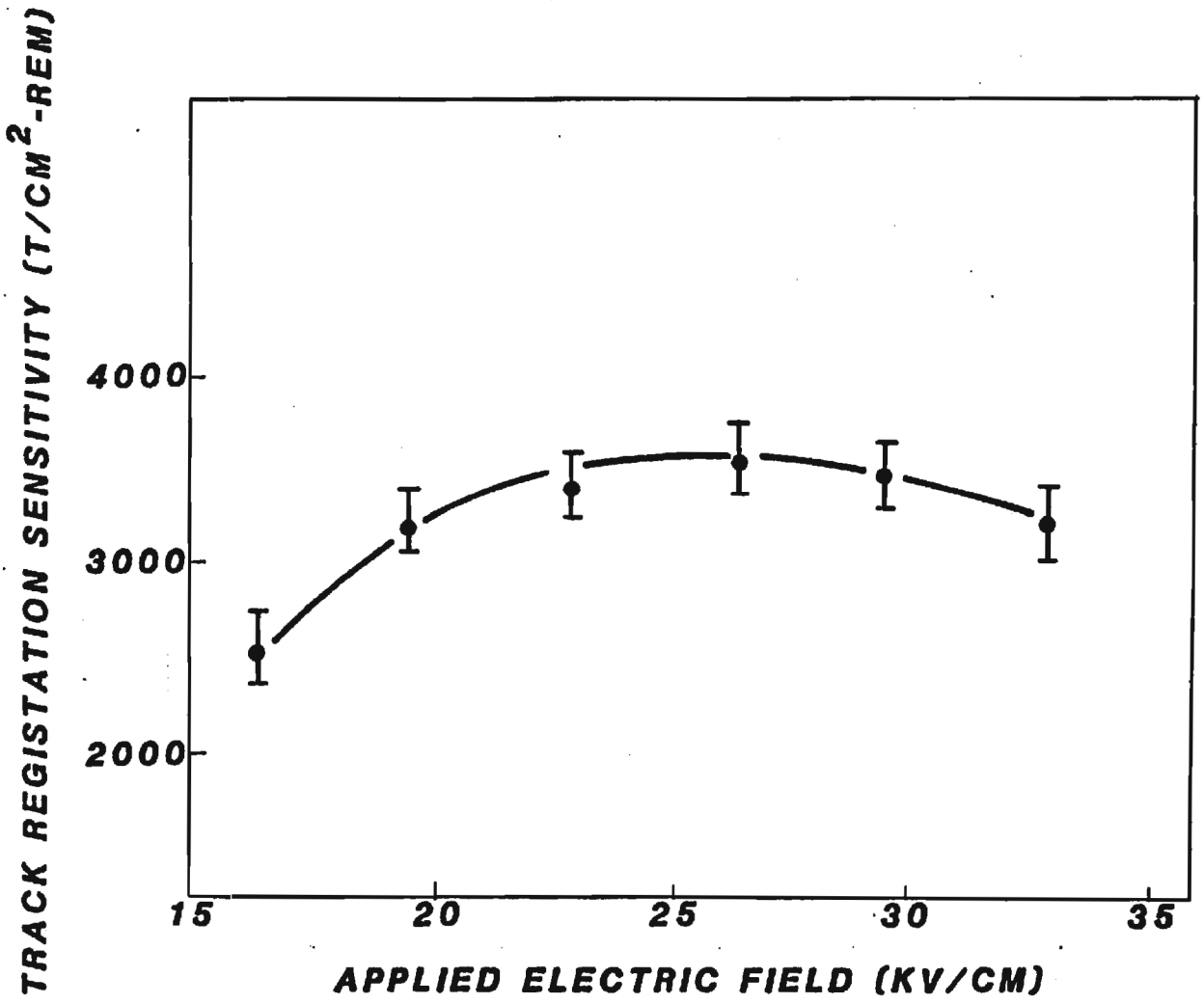

Figure 14. Neutron-Induced Track Sensitivity Seen in Combined Etch CR-39 Foils as a Function of Applied Electric Field Strength

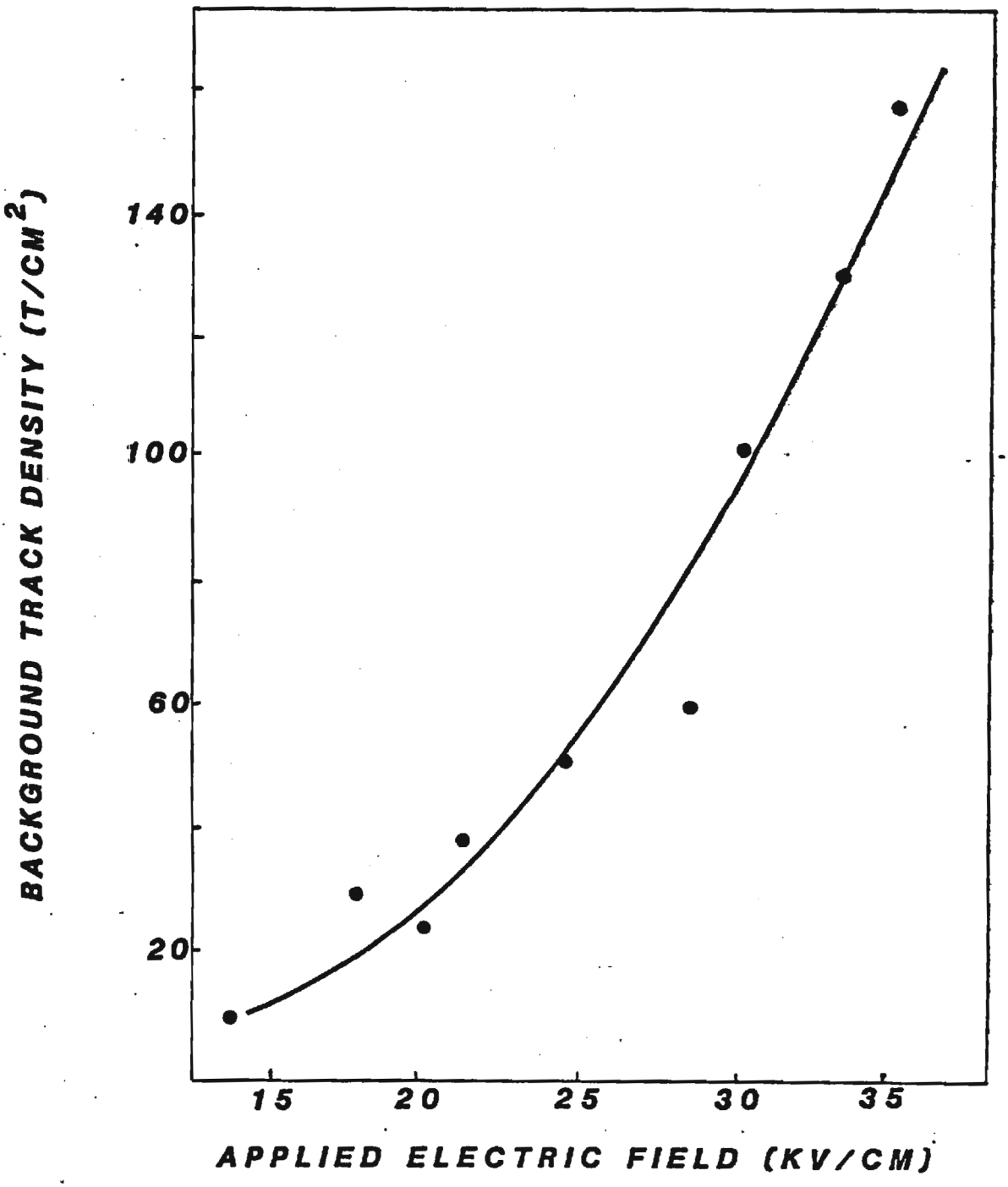

Figure 15. Background Track Density Found in Combined Etch CR-39 Foils as a Function of Applied Electric Field Strength

hour cured, 400μm thick, CR-39 foils were etched chemically in 45 percent KOH at 60^{o}C for two hours and etched electrochemically in 45 percent KOH at 25^{o}C, 23 kV/cm for two hours at one of five intervals in frequency between 1.0 kHz and 3.0 kHz. Figures 16 and 17 indicate that optimum track sensitivity and track diameter are found at approximately 2 kHz. The background response is a decreasing function of applied frequency as shown in Figure 18. Actually, from other research (Somogyi, 1980; Al Najjar et al., 1980), the background response has been shown to increase again above 5 kHz and thus the background response measured utilizing a frequency of 2 kHz represent a minimum. On the basis of the above tests, 2 kHz was chosen as the applied frequency when all other electrical parameters are as indicated.

Figures 19 and 20 display neutron-induced damage-track sensitivity and track diameter, respectively, as a function of the electrochemical etching duration. All other combined etching parameters were held constant as neutron irradiated 400μm thick CR-39 foils were etched electrochemically under standard conditions for intervals between two and five hours. Figure 19 indicates that the shortest electrochemical etching time that will allow the highest sensitivity is two and one-half hours which will result in the formation of 8-10μm diameter amplified damage-tracks (see Figure 20).

2.1.1.4 Surfactant Studies

Several researchers have found that the addition of an organic solvent to the electrochemical etching bath results in increased damage-track revelation and track diameter growth in bisphenol-A polycarbonate (Hassib et al., 1977; Somogyi, 1977; and Su, 1979). The attack of an organic solvent differs from that of a degrading agent, such as the alkali hydroxides, in that the solvent disperses the long chain polymer molecules into solution

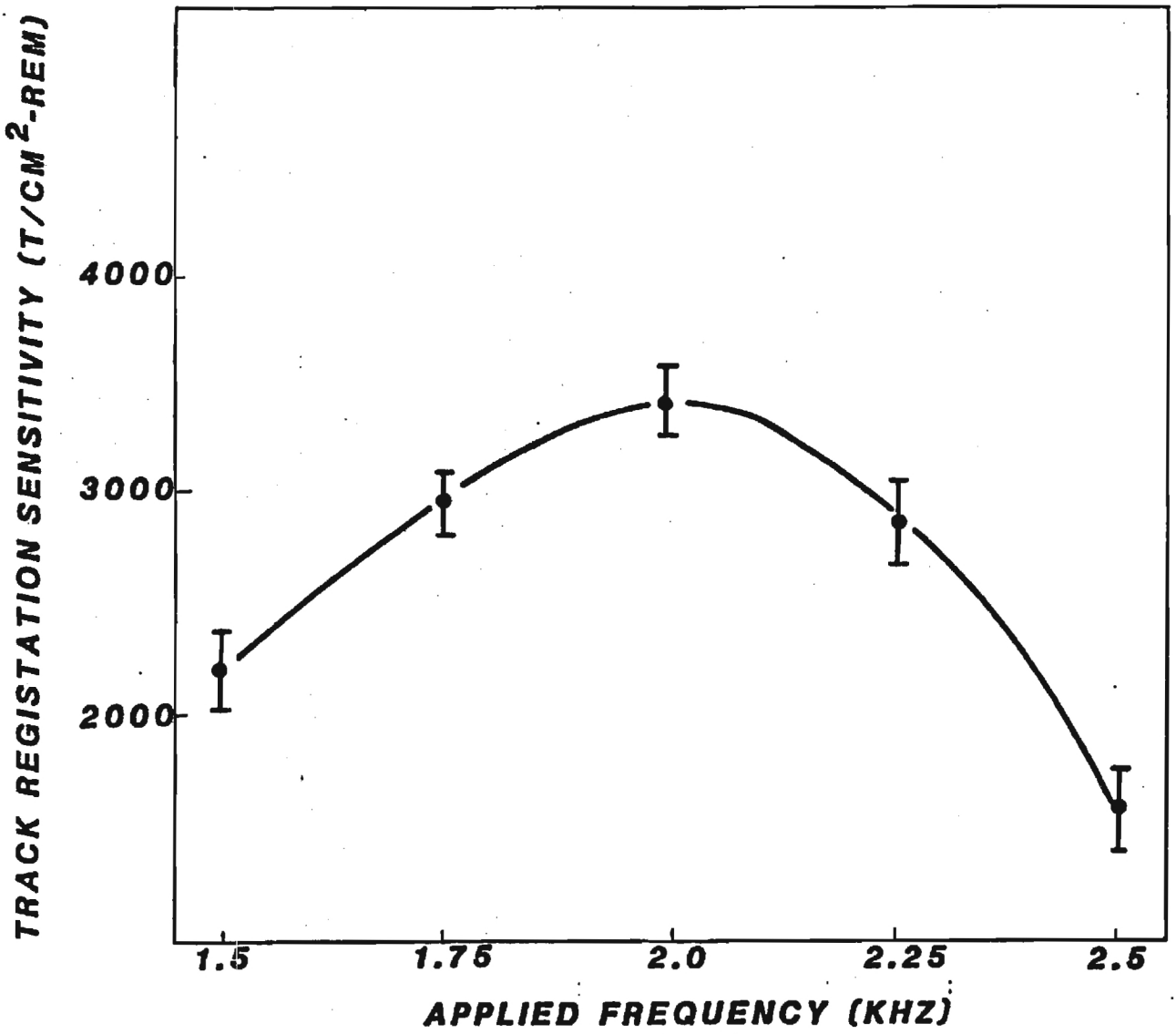

Figure 16. Neutron-Induced Track Sensitivity Seen in CR-39 Foils After Combined Etching and as a Function of Applied Frequency

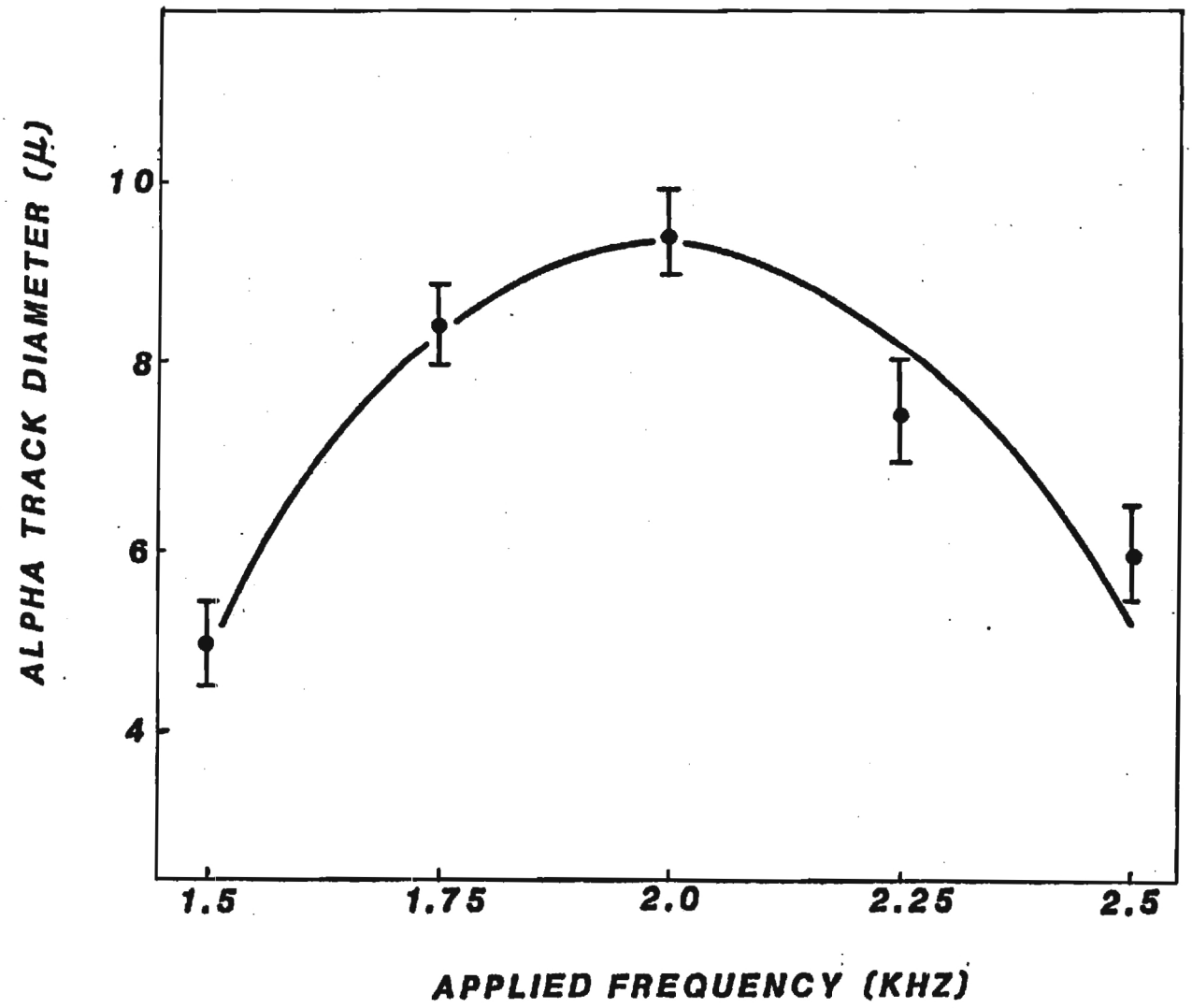

Figure 17. Variation in Track Diameter Seen in Combined Chemical and Electrochemically Etched CR-39 Foils as a Function of Applied Frequency

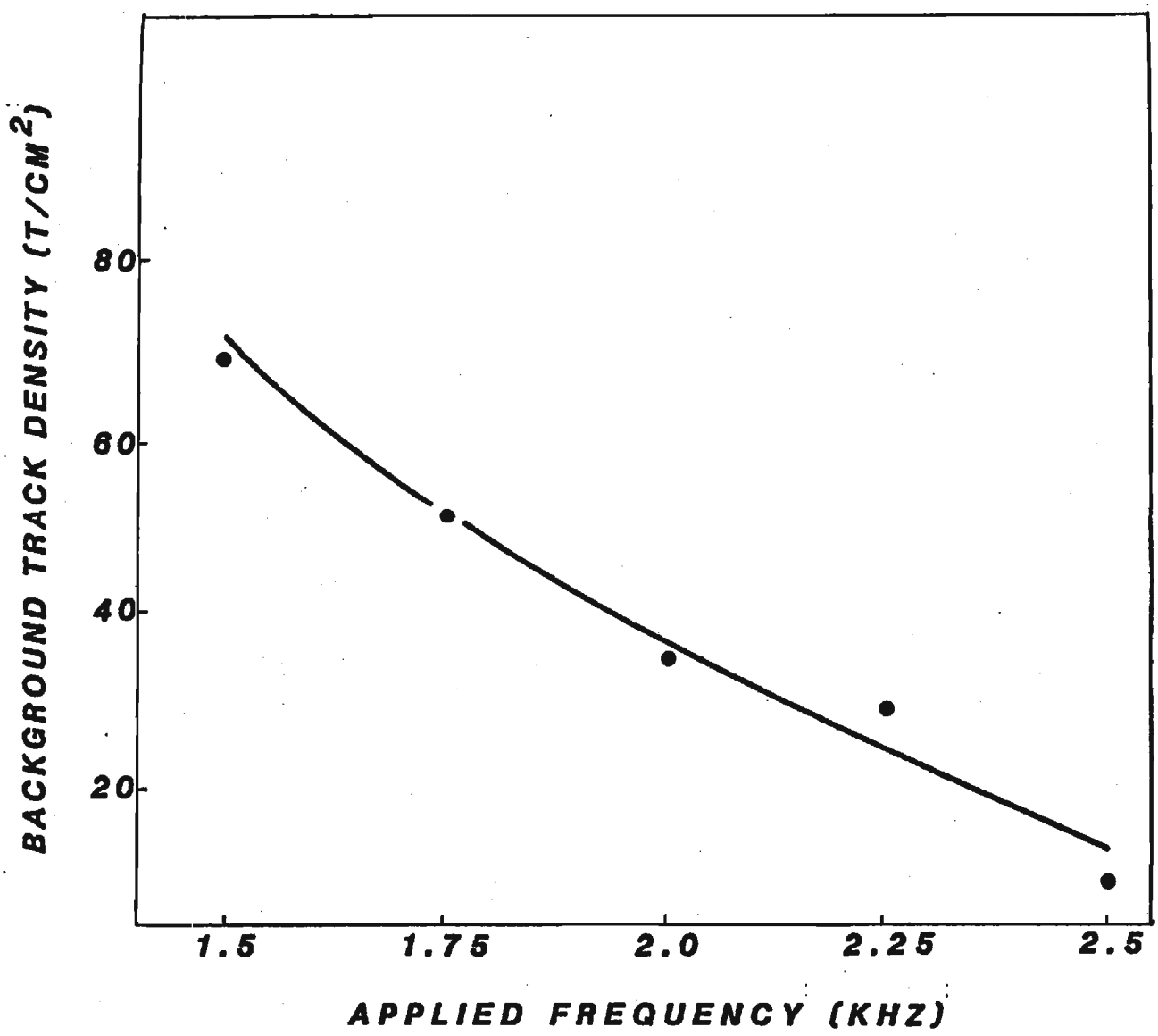

Figure 18. Background Response Observed in CR-39 Foils After Combined Etching and as a Function of Applied Frequency

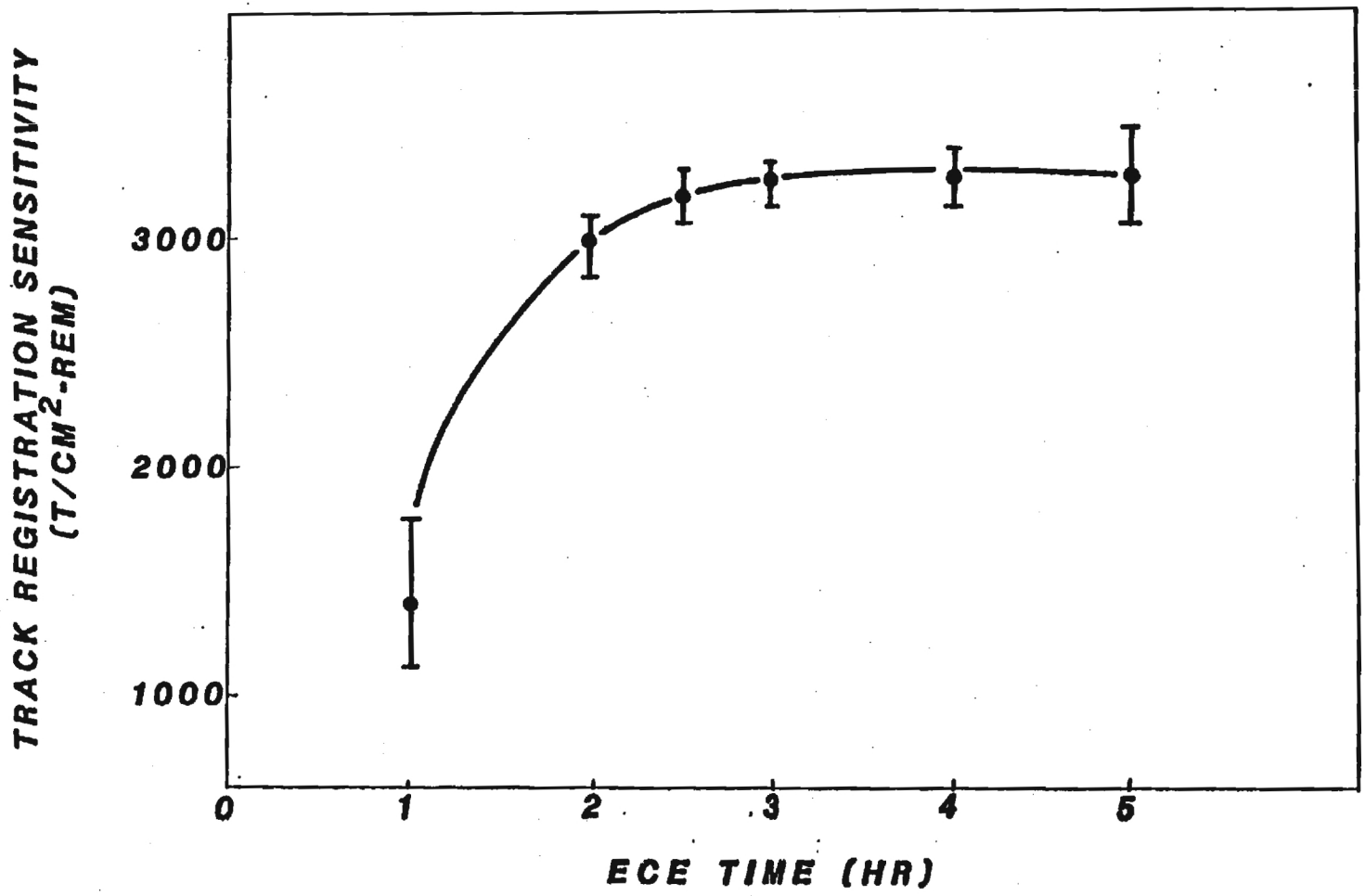

Figure 19. Neutron-Induced Damage-Track Sensitivity as a Function of the Electrochemical Etching Time in CR-39 Foils Subjected to a Combined Chemical and Electrochemical Etch Procedure

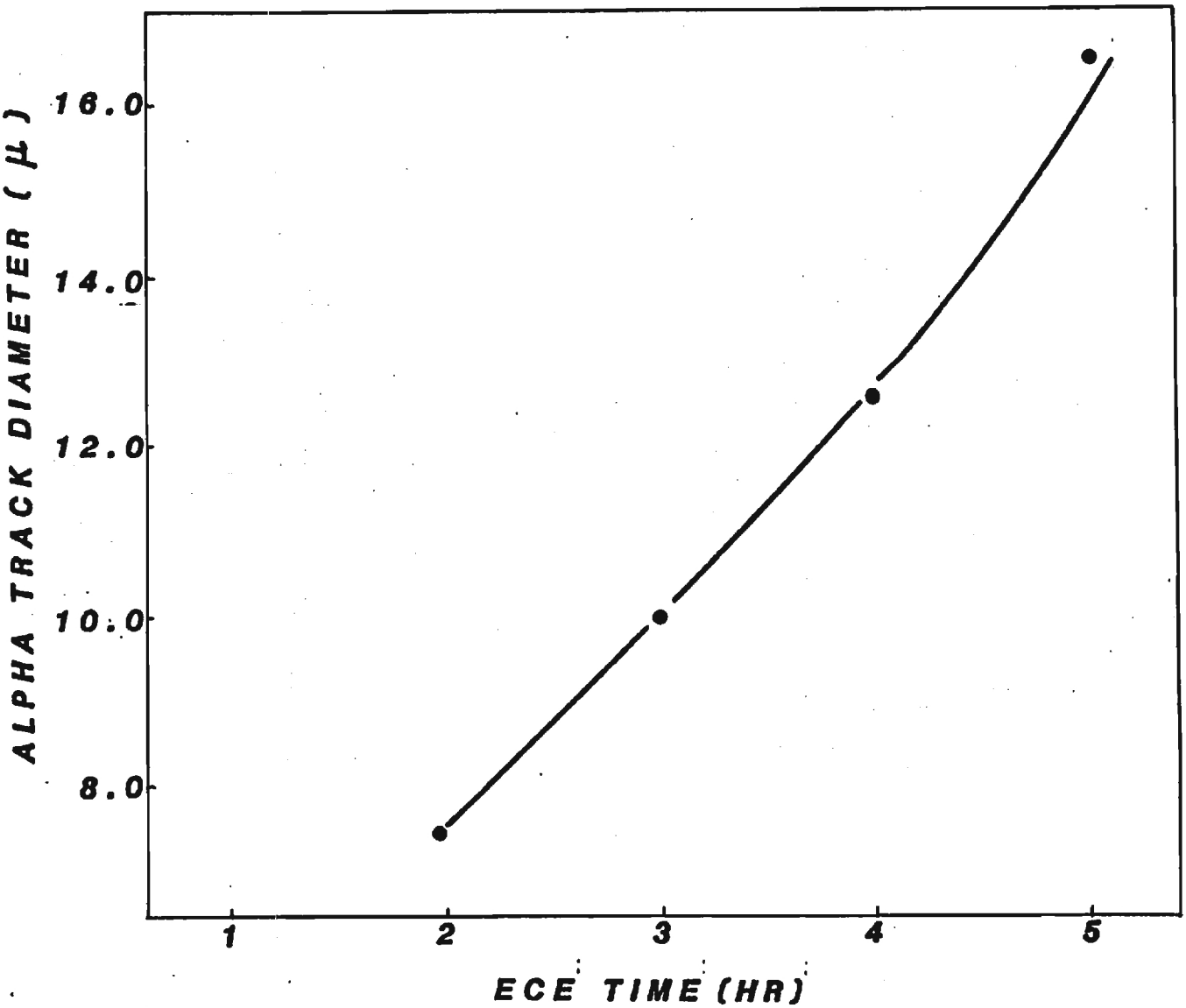

Figure 20. Variation in Combined Etch Track Diameter in CR-39 Foils as a Function of Electrochemical Etching Time

while the degrading agent randomly breaks the polymer chain along its length. In alkali hydroxide etching of any polymer, it is assumed that the rate of etching is a function of the number of unhydrated hydroxide ions available. The concentration of this species increases as the concentration of "free water" (water molecules which are not strongly bound to other species) decreases. Addition of organic solvents which do not solvate the hydroxide ion, but can bind to the water molecules, results in a marked increase in etch rate. The increased preferential etching of charged particle tracks, as seen in bisphenol-A polycarbonate, is probably associated with the solvent in solution with the etchant perferentially carrying slightly damaged long chain polymer molecules away from the areas of local moderate damage surrounding the charged particle latent track. This phenomenon enhances the preferential etch rate realized with only an alkali hydroxide degrading etchant. Several different solvents were added to the standard 45 percent KOH electrochemical etchant to decide if any enhancement could be realized in the preferential etching of CR-39 polymer foils.

Ethyl and methyl alcohol are two organic solvents that have been used to increase the preferential electrochemical etching characteristics of bisphenol-A polycarbonate. Kumanoto (1982) has found that the electrochemical etching duration necessary for damage-track revelation in bisphenol-A polycarbonate can be as short as 30 minutes when methyl alcohol is used in aqueous solution with KOH. An equal volume solution of C_2H_5OH and 45 percent KOH was used to etch electrochemically seven 400 μm thick CR-39 foils that had been irradiated previously with Pu-239 alpha particles and etched chemically in 45 percent KOH at 60°C for 30 minutes. Another set of the same type of CR-39 foils was exposed to the alpha source and subjected

to the identical combined etching parameters, except 45 percent KOH was used as the electrochemical etchant with no solvent added. The photomicrographs shown in Figures 21 and 22 illustrate the resultant alpha damage-track densities found using 45 percent KOH and C_2H_5OH + 45 percent KOH, respectively. The addition of C_2H_5OH to the electrochemical etchant drastically decreases the efficiency of alpha damage-track revelation and appears to have reacted with the CR-39 foil surface.

Several concentrated surfactants manufactured by DuPont under the brand name "Zonyl" were tested in solution with 45 percent KOH to determine their effect on electrochemical etching of CR-39. The Zonyl surfactants are fluorocarbon-based solvents as opposed to the hydrocarbon-type solvents, such as the alcohols. The fluorocarbon portion of their molecules gives the surfactants an extreme tendency to orient at interfaces. Consequently the Zonyl surfactants lower the surface tensions of solutions more than alcohols and provide a powerful wetting action. Unfortunately, the Zonyl surfactants have very low solubilities in KOH and surfactant concentrations on the order of 0.1 percent or less were difficult to attain. the surfactants were added directly to the 45 percent KOH etchant, to distilled water which was then mixed with KOH to a 45 percent KOH solution, and to C_2H_5OH which was added to 45 percent KOH; however, any Zonyl surfactant concentration over approximately 0.05 percent tended to precipitate out of the solution. DuPont suggests that Zonyl surfactant concentrations on the order of 01 percent or less are, in many cases, sufficient to achieve the desired effects of the surfactant. Thus, several tests were undertaken using six different Zonyl surfactants at 0.1 percent or less concentrations in 45 percent KOH as the electrochemical etchant. Figure 23 illustrates the effects of the different surfactant-KOH etchant solution on alpha irra-

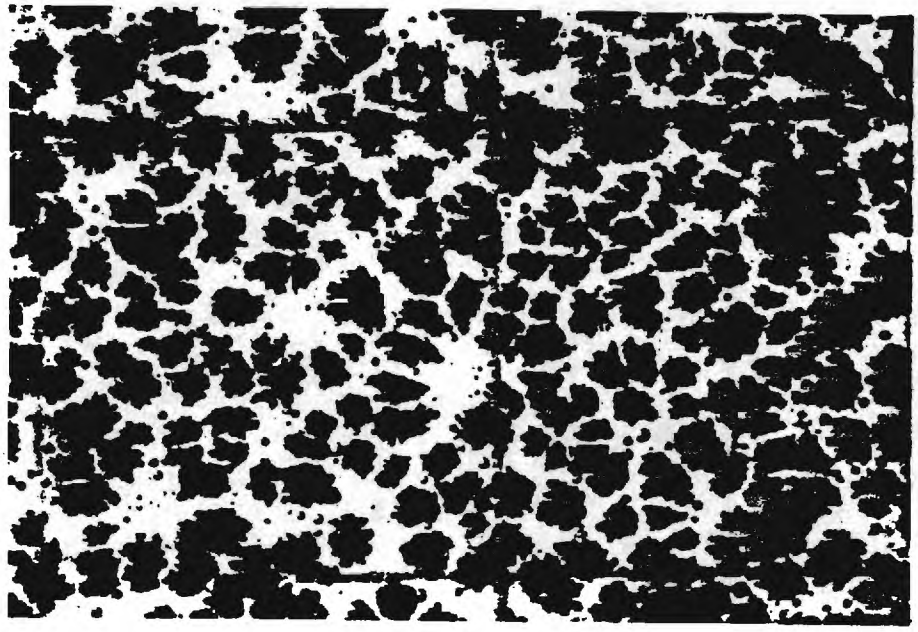

Figure 21. Microphotograph of Alpha Particle Damage-Tracks Registered in 400 μm CR-39 Foil After Combined Chemical and Electrochemical Etching in 45 Percent KOH

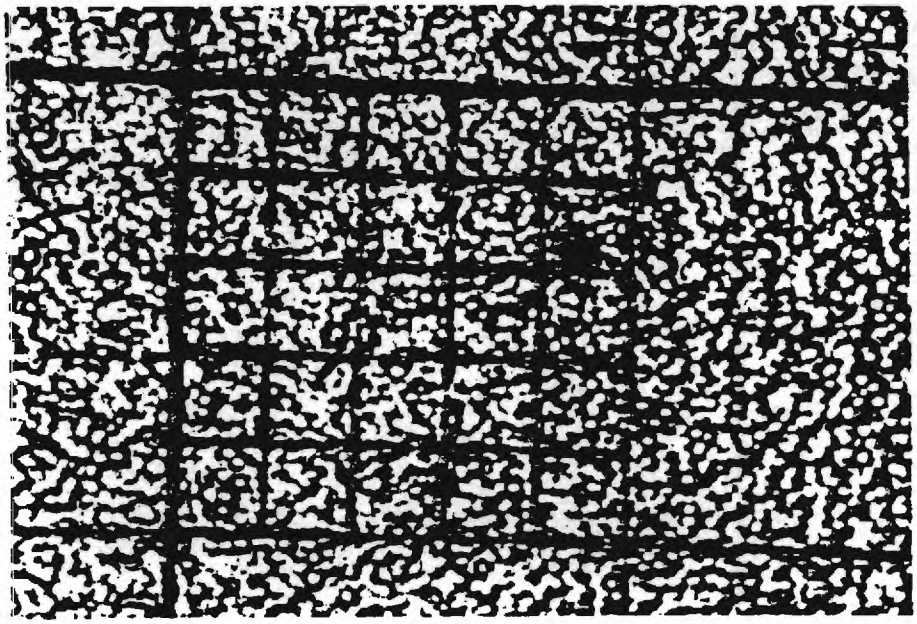

Figure 22. Microphotograph of Effect of C_2H_5OH on Alpha Particle Track Registration in 400 μm CR-39 Foil Subjected to Identical Conditions as Those Shown in Figure 53, Except $\frac{1}{2}C_2H_5OH$ + ½ 45 Percent KOH Was Used as the Electrochemical Etchant

diated CR-39 foils and compares them with the damage-track revelation found using only 45 percent KOH as the electrochemical etchant. Only one of the surfactant solutions, the FSC-KOH solution, exhibited any preferential etching enhancement and then only slightly. All other surfactant-KOH solutions showed either no enhancement or inhibition of damage-track revelation.

The nature of the thermoset CR-39 cross-linked polymer molecule and the difference in chemical attack between solvents and degrading agents may help explain why no solvent-related enhancement is seen in the damage-track revelation efficiency of CR-39. CR-39 polymer is made by the polymerization of the oxydi-2, 1-ethanediyl di-2-propanyl ester of carbonic acid. Catalysis is achieved by mixing the liquid monomer with a small percentage by weight of an initiator such as di-isopropyl peroxydicarbonate. The monomer is an allyl resin (allyl diglycol carbonate), which means it contains the functional group: (CH_2=CH-CH_2). The monomer contains two of these functional groups and has the following structure:

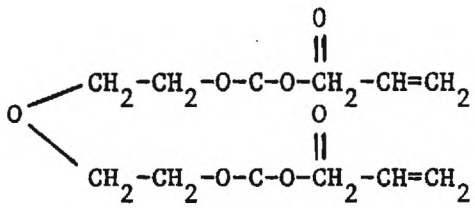

The presence of two allyl functional groups allows the monomer not only to polymerize but also to cross-link. This results in a thermoset plastic rather than a thermoplastic, such as bisphenol-A polycarbonate. One of the characteristics of thermoplastics is that they have no strong bonds between macromolecules. In contrast, thermoset plastics such as CR-39 are characterized by having covalent bonds that tie together all molecular

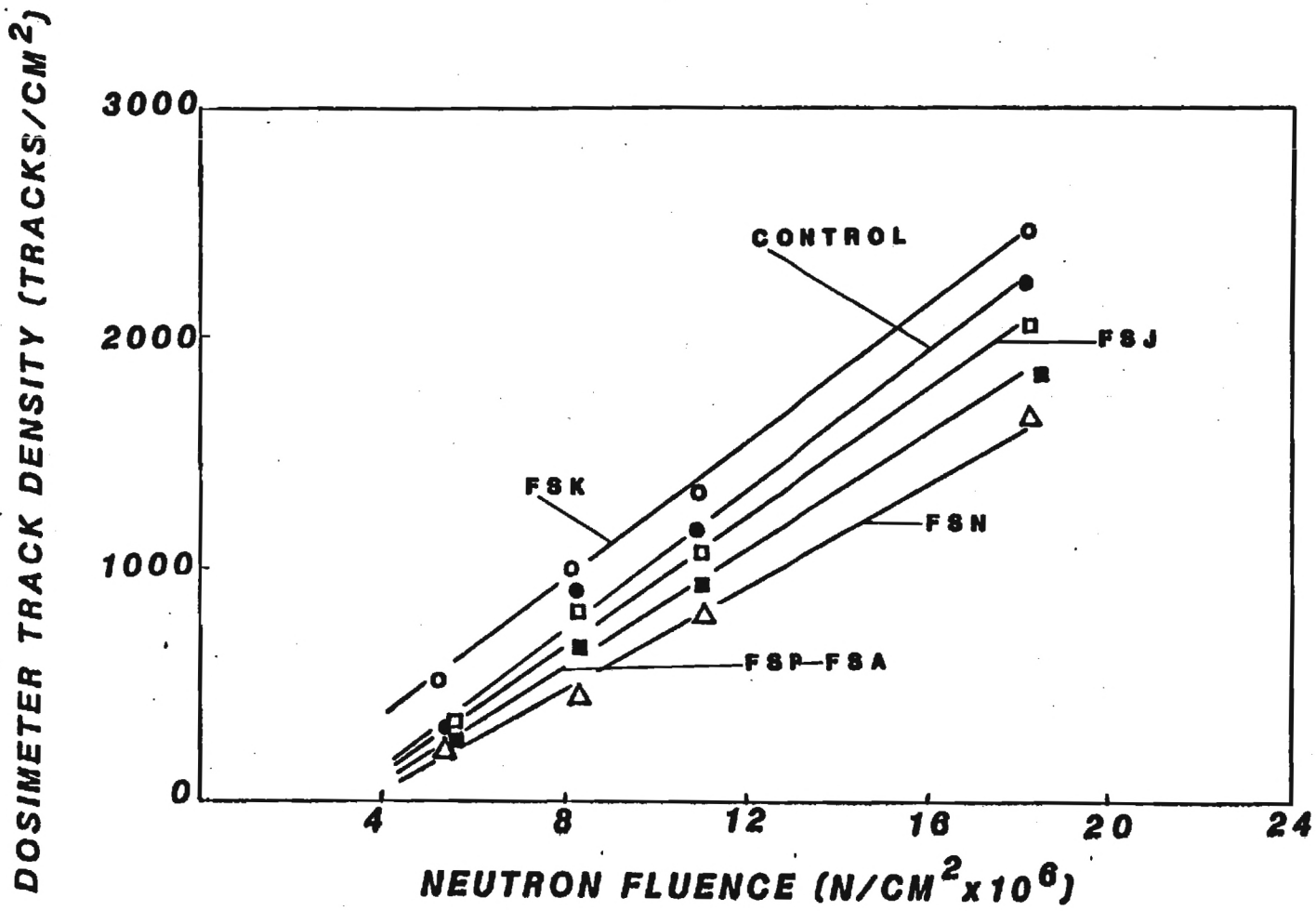

Figure 23. Effects of Different DuPont Fluorocarbon Surfactants on Combined Etch CR-39 Alpha Track Registration When the Surfactant Is Added to the Electrochemical Etchant

chains of the polymer. In effect, the polymer is not thought of as being composed of individual coiled linear molecules, but as a three-dimenesional latticework where the individual molecule is no longer taken as the smallest unit of the material.

The charged particle track left in CR-39 is characterized by a well-defined cylindrical path of highly damaged polymer surrounded by a largely undamaged cross-linked polymer matrix. This sharp division betweem damaged and undamaged polymer results in the well-defined circular etch pits seen in chemically etched CR-39. The addition of a solvent to the degrading etchant will have little or no significant damage-track revelation enhancement since any slightly damaged long-chain polymer molecules are still tightly bound by cross-linking to the surrounding polymer matrix and cannot be carried into solution by solvation. The inhibitory effect on electro chemical damage-track revelation imposed by some of the organic solvents may be explained by another phenomenon peculiar to the etching of CR-39. Polyallyl alcohol (PAA) is one of the etch products resulting from the degradtion of CR-39 by an alkali hydroxide. PAA has limitd solubility in the etchant, separates as a sticky brown oil, and collects on the surface and within the damage-tracks in CR-39. Addition of an organic solvent to the hydroxide etchant has been shown to lead to a greater bulk etching rate on CR-39 and to combine with the PAA etch product to form a surface gel which smooths over all the surface features and causes the damage-tracks to be rounded and indefinite (Gruhn et al., 1981). If the chemical etch pits become rounded and indefinite during electrochemical etching in the solvent-KOH solution, then the electrical treeing process is unlikely to occur in any of those tracks affected and damage-track revelation efficiency consequently decreases.

2.1.2 Proton and Alpha Particle Damage Registration Studies

The intermediate neutron dosimeter designed in this research utilizes the $^{6}Li(n, \alpha)^{3}H$ reaction in ^{6}LiF-Teflon radiator discs to generate neutron-induced alpha particles. The damage-tracks formed by these alpha particles act as a track density boost to the directly formed neutron-induced recoil tracks registered within the bulk voume of thin CR-39 foils. When neutrons of less than 1 MeV are the nonbarding particles, most of the resultant, directly formed damage-tracks registred in CR-39 are thought to be formed by elastically recoiling hydrogen nuclei (Tommasino et al., 1980). Alpha particle damage-tracks will be found only on the upper surface layers of the polymer foil while rcoil damage-tracks will be formed throughout the polymer detector volume. Thus, due to the two stage damage-track revelation process of electrochemical etching and the etchant resistant nature of CR-39, the optimum chemical-electrochemical etching parameters for alpha damage-tracks may differ significantly from those for recoil nuclei damage-tracks.

Alpha particles of various energies were generated by varying the distance from a collimated Pu-239 source to the CR-39 foil. Appropriate source-to-detector distances were selected from a calibration curve provided by Stillwagon (1978). Six sets of 400 μm thick CR-39 foils were irradiated at seven incremental source-to-detector distances between 0 and 3.5 cm. This arrangement provided alpha particles with incident energy ranging from 5.15 MeV to 0.5 MeV. A geometry correction factor equal to $f = (1/4) \ln \left[(D^2 + R^2)/D^2\right]$ was used to correct for air attenuation, where R is the collimated source radius, 0.5 cm, and D is the source-to-detector distance. The alpha-irradiated CR-39 foils were etched chemically in 45 percent KOH at 60^{o}C for durations ranging from 0 to 2 hours and then electro

chemically etched in 45 percent KOH at 25°C, 2 kHz, and 23 kV/cm for two and one-half hours. The alpha track registration sensitivity (tracks/alpha) was determined by dividing the measured damage-track density by the geometry-corrected alpha fluence. The alpha track registration sensitivity as a function of chemical etching time is shown in Figure 24. The series of etching curves indicates that the optimum chemical etching time for highest track registration sensitivity is a function of the incident alpha energy. This is due to the fact, that more energetic alpha particles leave behind narrower trails of damage that reach deeper within the CR-39 surface layer. These tracks require longer chemical etching times than the more shallow, lower-energy alpha tracks to be amplified to the size and shape necessary for optimum electrochemical treeing efficiency (Fleischer et al., 1975; Durrani and Al-Najjar, 1980). This method might easily be adapted to provide a simple method of alpha spectroscopy. For the purposes of this research, however, a chemical etching time of two hours or greater duration is necessary because the alpha particles produced in the $^{6}Li(n,\alpha)^{3}H$ reaction by neutrons between 1 eV and 1 MeV will all have energies greater than 2 MeV. Since an optimum chemical etch time of two hours had already been determined for neutron-induced recoil track registration in CR-39, this time was used for most of the tests in this research.

Since most of the directly induced recoil particle tracks in CR-39 from neutrons with energy less than 1 MeV are thought to be a result of recoil hydrogen nuclei, a series of tests was performed to determine the proton threshold energy for track formation using the standard combined etch parameters utilized in most of this research. Sets of CR-39 foils were irradiated with 50 keV, 100 keV, 150 keV, and 200 keV protons as described by Sanders (1982). Figure 25 reveals that energy threshold for proton

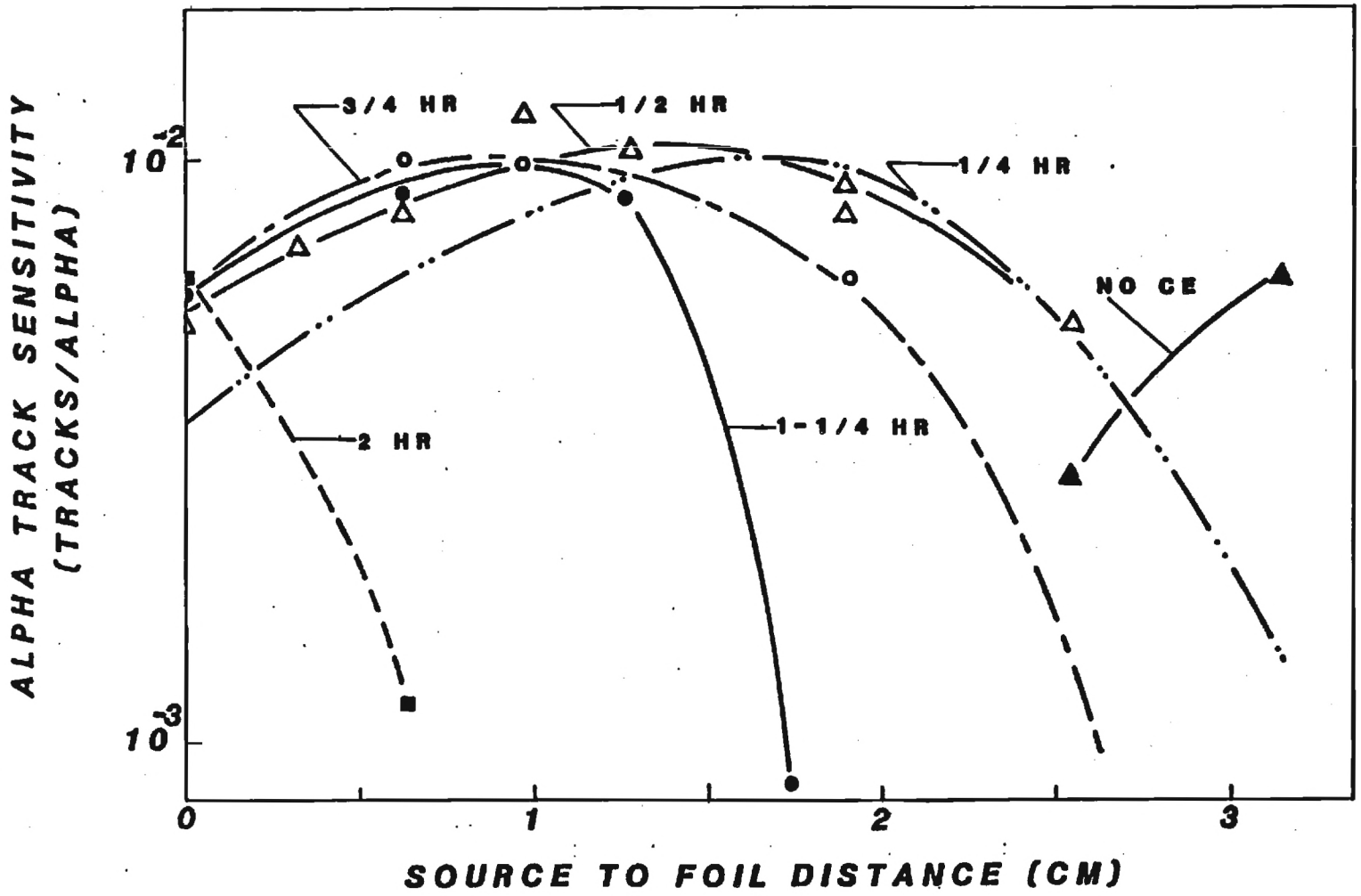

Fighre 24. Alpha Track Registration Sensitivity as a Function of Alpha Energy (source to detector distance) and Chemical Etching Time

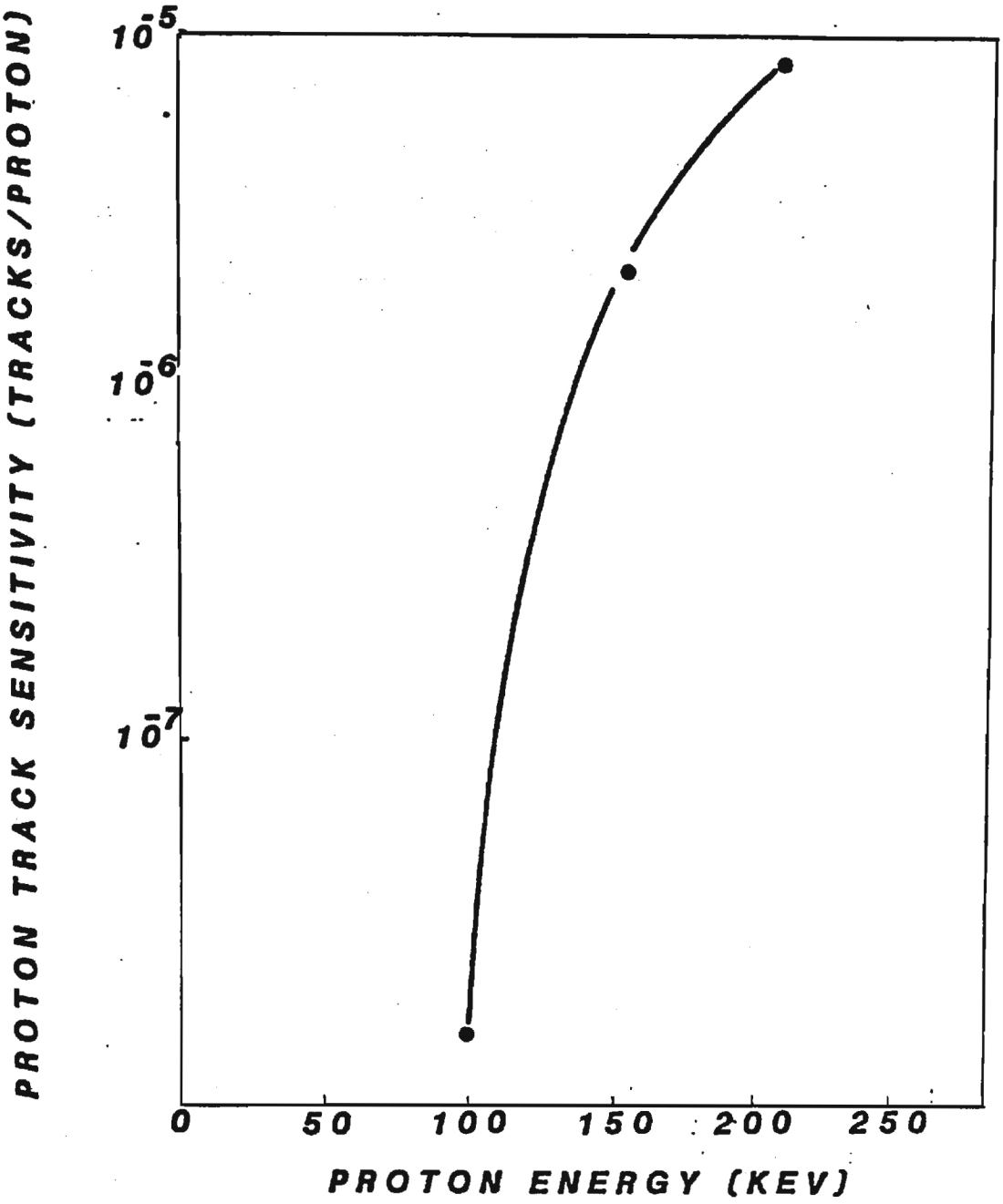

Figure 25. Proton Track Registration Energy Threshold Found in CR-39 Foils Combined Etched Using the Standard Chemical and Electrochemical Parameters Determined in This Research

damage-track formation using the standard combined etching conditions is approximately 100 keV. The rather low damage track registration sensitivities found in this test suggest that the etching conditions were not optimum. The threshold energy might be somewhat lower if the etching parameters were adjusted for optimum proton damage-track revelations. However, since no researchers have reported the observation of directly induced recoil tracks from neutrons with less than 10 keV, the 100 keV proton energy threshold for damage track formation may be a valid threshold.

2.1.3 Intermediate Neutron Dosimeter Design

The work of Sohrabi (1975)and Su (1979) has established simple and reliable damage-track techniques to measure neutron dose-equivalent in the 1 MeV to 20 MeV and thermal neutron energy ranges, respectively. The experimental investigation detailed in the following section has resulted in a rem-responding damage-track dosimeter that effectively bridges the 1 eV to 1 MeV energy gap which previously existed between these two dosimetric techniques. Measurement of dose-equivalent over the neutron energy region of thermal and 20 MeV energies is now possible.

CR-39 polymer foil was chosen as the damage-track registration medium for this investigation because of its sensitivity to neutrons with energy less than 1 MeV. Although CR-39 is much more sensitive to neutron-induced damage-track formation than bisphenol-A polycarbonate, its response as a function of neutron energy does not approximate the ICRP dose-equivalent curve. After some early studies that utilized alpha particles from the $^{6}Li(n, \alpha)^{34}H$ reaction to achieve thermal neutron-induced sensitivity in bisphenol-A polycarbonate, (Su and Sanders, 1979), it was decided to attempt a similar neutron-induced track density "boosting" technique for

use in the intermediate (1 eV to 1 MeV) neutron energy region with the more sensitive CR-39 polymer foils. The optimum "boosting" technique should not simply increase the overall neutron-induced damage-track density found in CR-39, but should increase selectively the neutron-induced damage-track response, so that the measured track density as a function of neutron fluence and neutron energy effectively follows the shape of the ICRP dose-equivalent response curve.

The neutron energy-dependent response of bare CR-39 foil decreases rapidly as the neutron energy falls below 1 MeV. Thus, the first requirement of a charged particle radiator material to be used as a track density booster must be that its neutron cross-section increases as the neutron energy decreases below 1 MeV. Figure 26 shows that the (n,α) cross-section for ^{6}Li fits this initial requirement. Thus, a suitable ^{6}Li containing radiator configuration held in close contact with a CR-39 foil, could increase the overall damage-track density response recorded in the CR-39 when irradiated with low-energy neutrons. This increase in damage-track density is a result of the addition of neutron-induced ^{6}Li reaction alpha tracks recorded on the surface of the foil to the neutron-induced recoil nuclei tracks recorded within the volume bulk of the CR-39 polymer foil.

The ^{6}LiF pressed-tablet radiators fabricated in this laboratory and used in the thermal neutron dosimeter development (Su, 1979; Su and Sanders, 1979) are extremely fragile and badly hygroscopic. Thus, a commercially available ^{6}LiF radiator disc was utilized in the intermediate neutron dosimeter development. The radiator disc is made of a ^{6}LiF and Teflon matrix by Teledyne Isotopes, Westwood, New Jersey. The 11. mm diameter and 0.4 mm thick radiator discs are much more rugged than the hand-pressed tablets

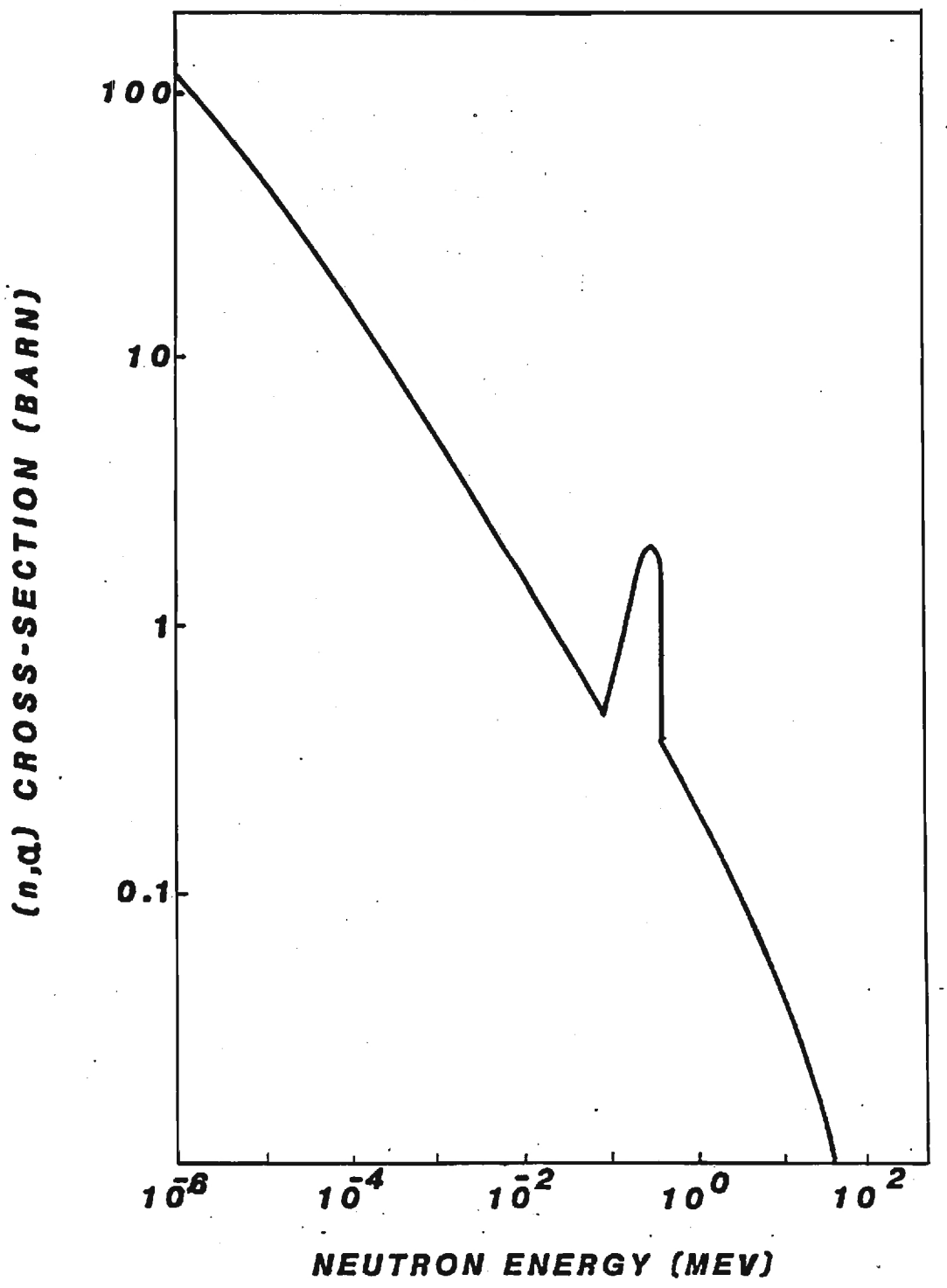

Figure 26. $^{6}Li(n,\alpha)^{3}H$ Cross-Section as a Function of Neutron Energy (BNL, 1953)

previously used and exhibit little or no hygroscopy. The ^{6}LiF-Teflon mixture results in a 30 percent ^{6}Li abundance in the radiator.

One of the major criticisms of CR-39 polymer foils used in damage-track technology is that tremendous variations in thickness, homogeneity, and background response are often found in foils taken from the same sheet of polymer. These tolerance variations are primarily the result of the CR-39 foil being manufactured for some purpose other than damage-track studies. As the demand for CR-39 for use in damage-track technology increases, the fabrication tolerances of the polymer should become more stringent. However, one of the first considerations of this investigation was the choice of the most reliable CR-39 foil to use in the intermediate neutron dosimeter design. The testing procedures which led to this choice are discussed in detail in Section 2.1.1 of this report. The CR-39 polymer chosen is manufactured by American Acrylics and Plastics, Stratford, Connecticut. The foil is old in approximately one square meter sheets at nominal thicknesses of 0.15 inch 0.025 inch, and 0.040 inch, with listed thickness tolerances of $\pm$ 0.005 inch. The 0.015 inch, or 400 μm, thick CR39 foil, sold at a cost of $160.00/sheet, was detrmined to have the latest variation in damage-track response and lowest background of all the CR-39 polymers investigated.

At this point in the research, the basic damage-track dosimeter to be used to measure neutron dose-equivalent in the 1 eV to 1 MeV energy range consisted of a sensitive 400 μm thick CRF-39 foil in contact with a ^{6}LiF-Teflon alpha radiator disc. However, this simple radiator-detector foil configuration has an inherent drawback in that it exhibits a massive over-response to neutrons with energies < 10 keV. The over-response is due to the large increase in the $^{6}Li(n,\alpha)^{3}$ cross-section as a function of energy

between 10 keV and thermal neutron energies. The cross-section increases from 2.5 barns at 10 keV to 110 barns at 1 eV and 950 barns at 0.025 eV energy.

Many high-Z nuclei have large interaction cross-sections with neutrons of less than 1 MeV energies. These interactions are primarily inelastic in nature for neutrons between 100 KeV and 1 MeV. When the incident neutron is in the thermal energy range, radiative capture is the dominant interaction seen in high-Z elements. Such interaction properties of several high-Z elements have been used in this resarch to shape the neutron spectra seen by the ^{6}Li-CR-39 dosimeter selectively so that the resultant damage-track response approximates a rem-response to neutron energies between 1 eV and 1 MeV.

For low-energy neutrons the CR-39 shows a damage-track over-response. This is due to the large 1/v dependent reaction cross-section of the particle radiator to neutrons with less than 1 eV of energy. This over-response can be eliminated effectively by wrapping the dosimeter assembly in cadmium foil. Thus, the first intermediate neutron dosimeter design to be tested in a well-characterized neutron spectrum consisted of a ^{6}LiF-Teflon radiator disc sandwiched between two 400 μm thick CR-39 foils, with the entire assembly wrapped in 0.05 cm thick cadmium foil (see Figure 27). Three sets of three of this dosimeter design were assembled for calibration in the NBS filtered reactor neutron beams, described by Sanders (1982). One each of the sets was exposed to a given fluence in either the 2 keV, 24.5 keV, or 144 keV moderated neutron beam. The dosimeters were then disassembled and the CR-39 foils were subjected to the standard combined chemical-electrochemical etching procedure. The resultant amplfied damage-tracks were counted using a binocular phase contrast microscope and Whipple disc

arrangement (Sanders 1982). The numerical data from this test are tabulated in Table 2. As can be seen in Figure 28, this damage-track dosimeter design offers a dramatic improvement in neutron-induced response in the 24 keV to 144 keV neutron energy range compared to the bare CR-39 foil response in this same region. The dosimeter response in this neutron energy region, which tends to follow the shape of the rem-response curve, is also drastically improved by the intermediate dosimeter; however, the low energy over-response has not been eliminated completely. This low-energy neutron-induced over-response probably does not become evident until the neutron energy drops below 10 keV, since this is the point on the ICRP rem-response curve where the neutron quality factor remains relatively constant at about two.

To improve the dosimeter response below 10 keV further, the neutron "filtering" characteristics of several other high-Z materials were investigated. Thin foils made of either indium, gold, or silver were placed on the CR-39 foil surface separating the CR-39 sandwich assembly from the 0.05 cm thick cadmium cover. The neutron "filters" were used either singly or in combination for this dosimeter design. The dosimeters were then exposed in the moderated neutron beams in the same procedure as the first design dosimeter. The CR-39 foils were etched under the standard combined chemical-electrochemical conditions and evaluated for track density. The numerical results of the "filtered" intermediate neutron dosimeter design are presented in Table 3. Figure 29 shows that some improvement in the neutron-induced damage-track response below 10 keV was obtained with all combinations of neutron filter foils. However, the additional filtering of the neutron spectra above 10 keV is also evident in all cases except one. The addition of a 0.02 cm thick indium foil to the cadmium thermal neutron

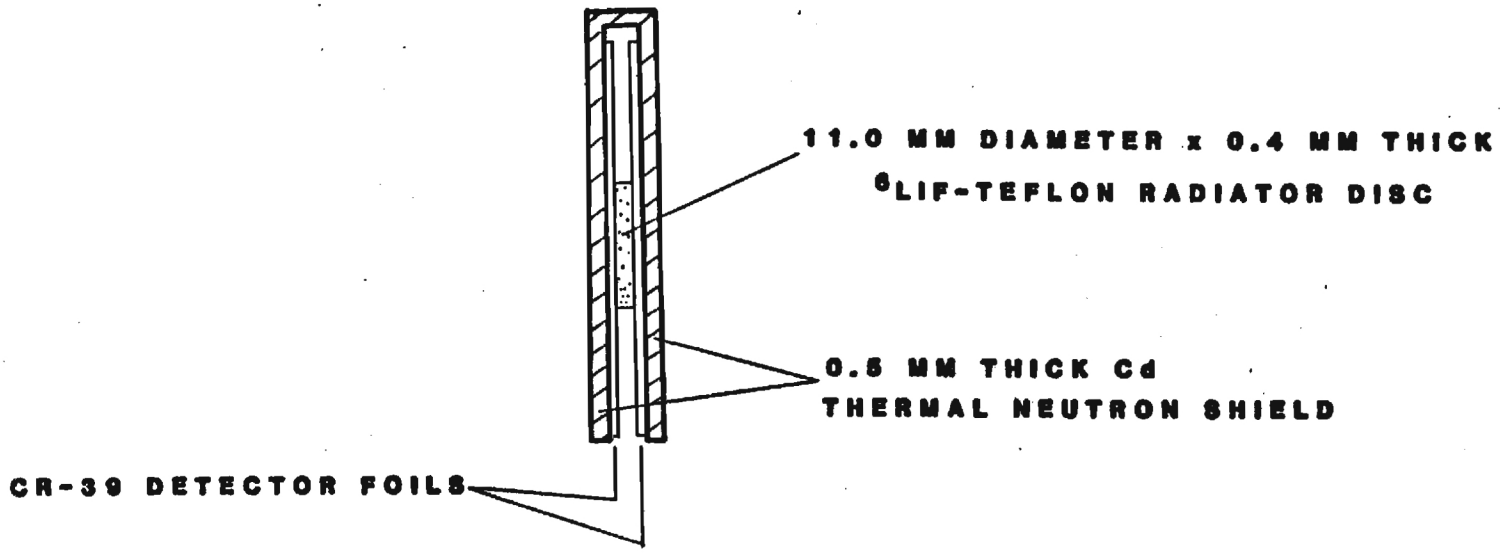

Figure 27. Initial CR-39 Dosimeter Design Consisting of Cd-Covered ^{6}LiF Radiator Disc CR-39 Assembly

Table 2. Initial Filtered Neutron Beam Irradiations of Dosimeter Configuration Shown in Figure 27.

Neutron Beam Energy (keV)	Neutron Fluence (n/cm^2)	Track Density (($t/0.49\ cm^2$) ± 1σ)
2.0	2.6×10^7	238 ± 18
2.0	2.6×10^7	244 ± 18
24.5	2.0×10^7	50 ± 4
24.5	2.0×10^7	54 ± 3
144.0	2.0×10^7	196 ± 12
144.0	2.0×10^7	192 ± 11

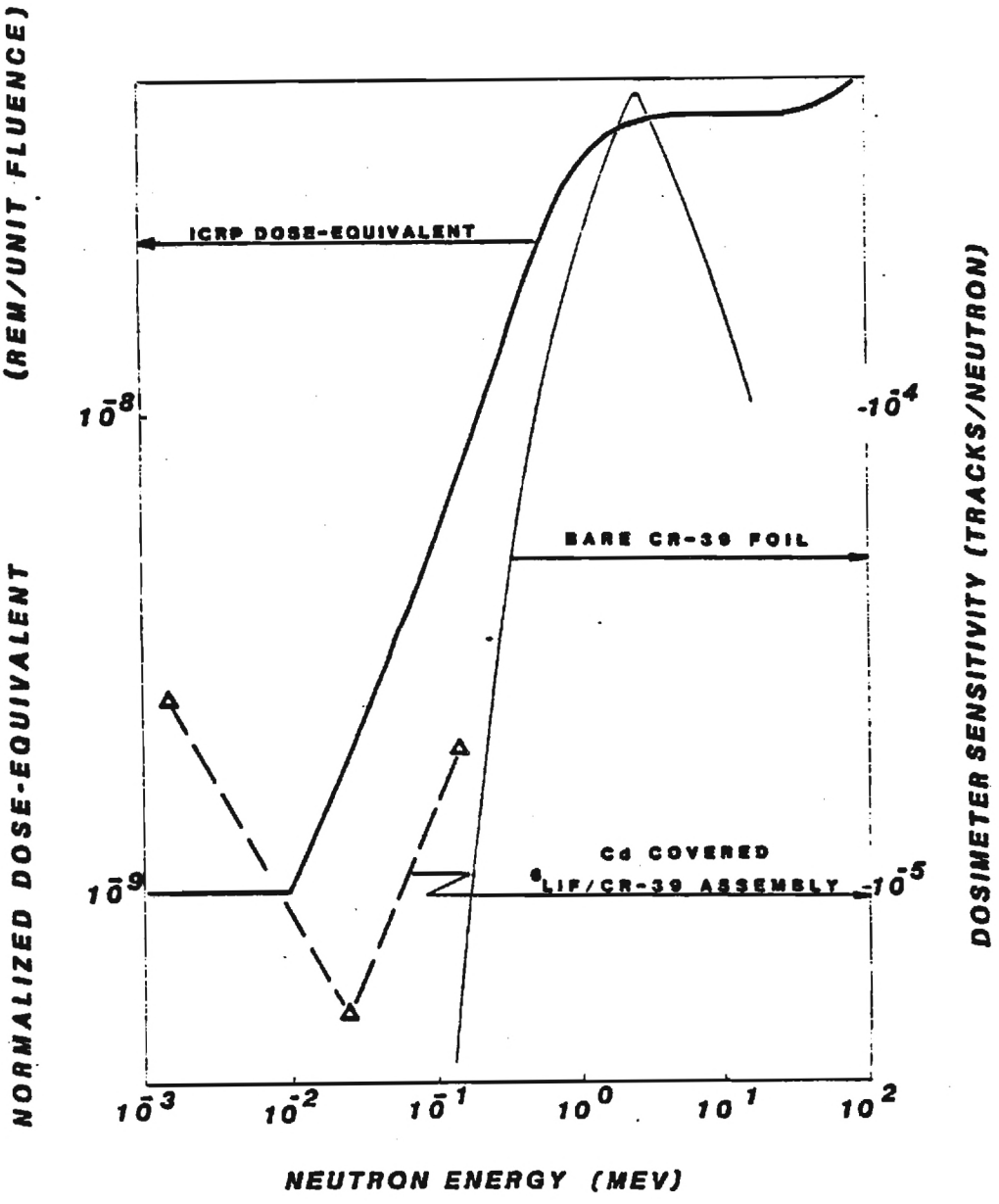

Figure 28. Sensitivity of Initial CR-39 Dosimeter to the NBS Filtered Neutron Beams Compared to the ICRP Rem Curve and the Neutron Response of Bare CR-39 Foils (ICRP, 1973; Griffith et al., 1980)

Table 3. Damage-Track Densities Recorded by the Intermediate Neutron Dosimeter Utilizing Different Thin Foil Neutron "Filters" and Exposed to the NBS Filtered Reactor Neutron Beams

Dosimeter Filter Material	Neutron Beam Energy (keV)	Neutron Fluence (n/cm^2)	Track Density (($t/0.49\ cm^2$)$\pm 1\sigma$)
Cd + Ag	2	5.3×10^7	537 ± 48 608 ± 61
Cd + Au	2	5.3×10^7	442 ± 41 436 ± 32
Cd + In	2	5.3×10^7	318 ± 28 324 ± 12
Cd + In + Au	2	5.3×10^7	292 ± 19 280 ± 17
Cd + Ag	24.5	3.9×10^7	92 ± 8 94 ± 4
Cd + Au	24.5	3.9×10^7	87 ± 10 88 ± 4
Cd + In	24.5	3.9×10^7	93 ± 6 92 ± 5
Cd + In + Au	24.5	3.9×10^7	81 ± 8 85 ± 5
Cd + Ag	144	3.9×10^7	427 ± 11 418 ± 24
Cd + Au	144	3.9×10^7	242 ± 21 250 ± 20
Cd + In	144	3.9×10^7	358 ± 24 365 ± 18
Cd + In + Au	144	3.9×10^7	185 ± 14 183 ± 18

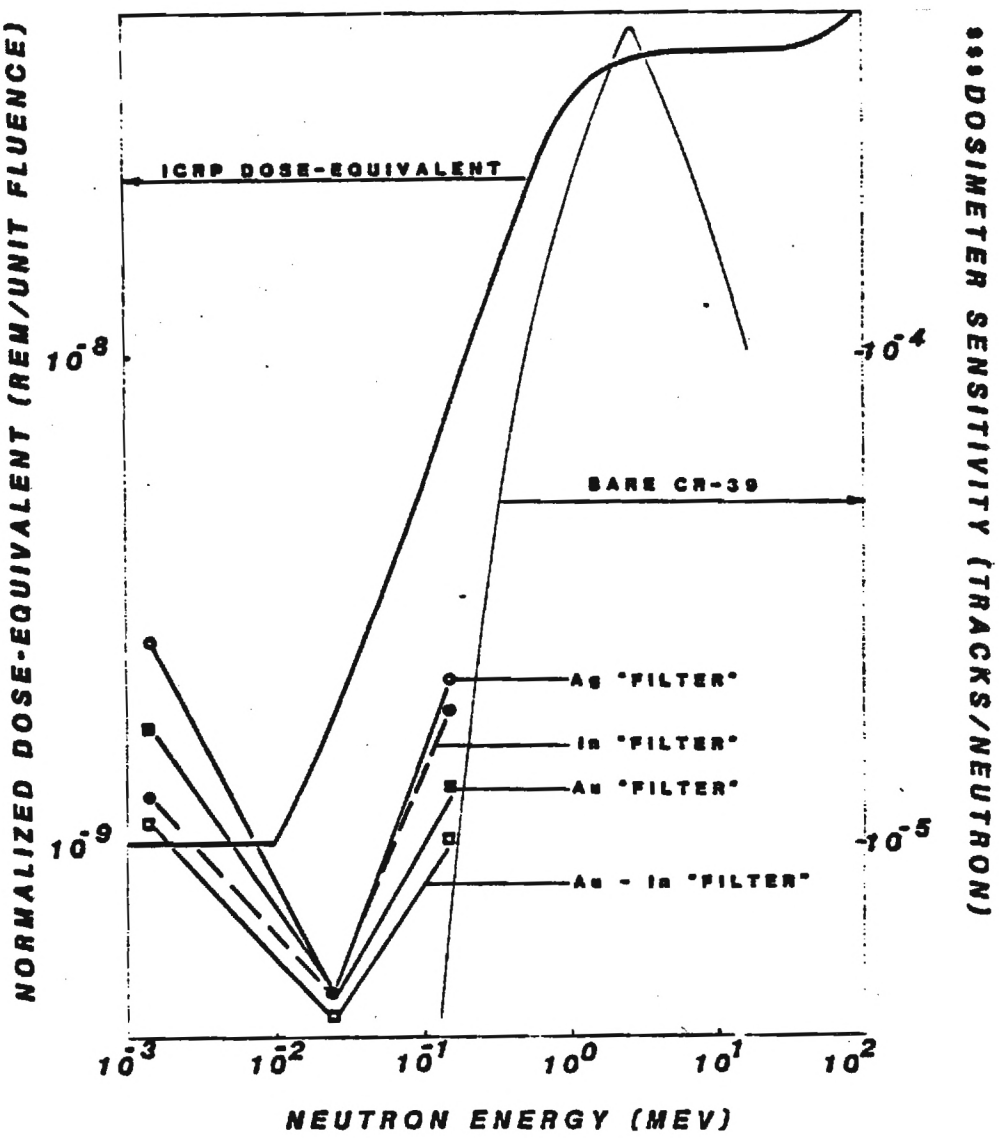

Figure 29. Sensitivity of the Intermediate Neutron Dosimeter Shielded by Different Thin Foils to the NBS Filtered Neutron Beams; Compared to the ICRP Rem Curve and the Neutron Sensitivity of Bare CR-39

filter reduced the low energy over-response by approximately 30 percent while having no significant effect on the neutron-induced damage-track response found above 10 keV. The total neutron scatter cross-sections of all the elements listed in the BNL-325 neutron cross section catalogue were examined to determine if any other element might be used to help lower the 10 keV over-response of the intermediate neutron dosimeter without deleteriously affecting the neutron response above 10 keV. No such optimally shaped cross-section ws found. Thus, the "best" design for the intermediate neutron dosimeter seems to consist of the arrangement shown in Figure 30. A 11.0 mm diameter, 0.4 mm thick ^{6}LiF-Teflon radiator disc is sandwiched between two 2.5 cm X 2.5 cm. 40 m thick, low background CR-39 foils. A 0.02 cm thick indium foil is placed on the outer surface of the CR-39 foil which will be anterior to the incident neutron beam. This assembly is enclosed in 0.05 cm thick cadmium foil and the entire dosimeter is wrapped in water repellent filament tape.

Prototypes of this intermediate neutron dosimeter were exposed to each of the filtered neutron beams to a dose-equivalent of between 50 mrem and 1500 mrem. All of the irradiated CR-39 detector foils were subjected to the standard combined etching procedure and then evaluated for track density. The measured neutron-induced track density per foil is plotted in Figure 31 as a function of neutron fluence delivered by each of the filtered neutron beams. A least squares fit of the data from each beam reveals dosimeter sensitivity values (tracks/n) which can be related to the IRP dose-equivalent curve. The dosimeter sensitivity as a function of neutron energy is shown in Figure 32.

If one assumes that the neutron-induced damage-track density registered by the ^{6}Li-CR-39 dosimeter is a function of the alpha particle tracks

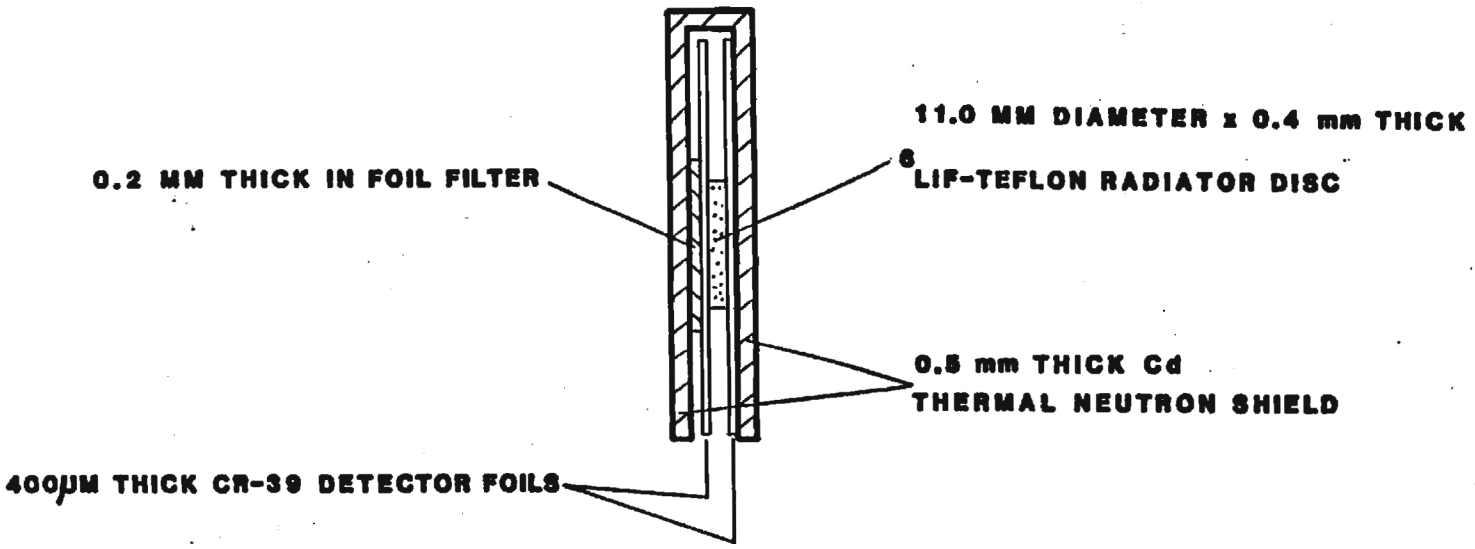

Figure 30. The Cd-In Filtered, ^{6}LiF-Teflon, CR-39 Foil Intermediate Neutron Dosimeter Designed in This Research

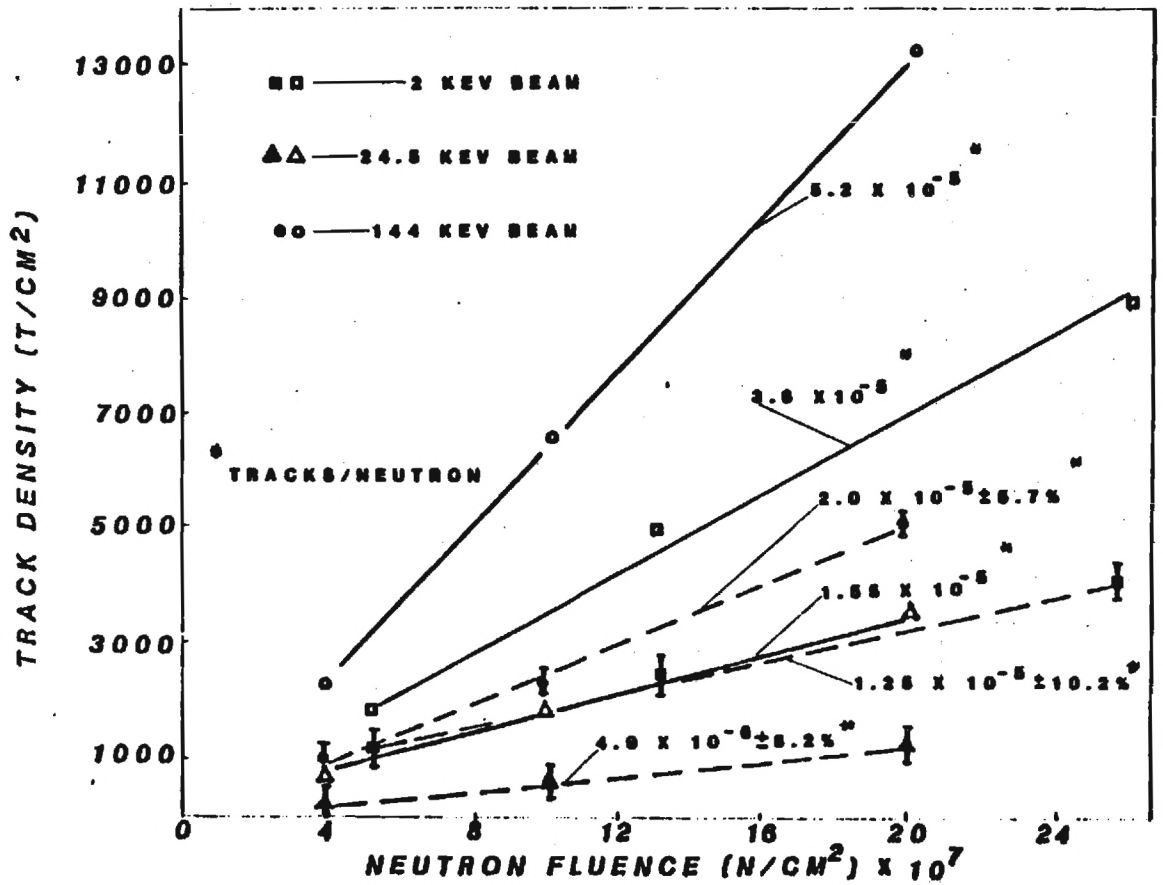

Figure 31. Neutron-Induced Track Responses Found in 400 μm CR-39 Foils Contained in the Intermediate Neutron Dosimeter Exposed to the NBS Filtered Neutron Beams (The hollow data points indicate albedo measurements and the solid points indicate "in air" measurements.)

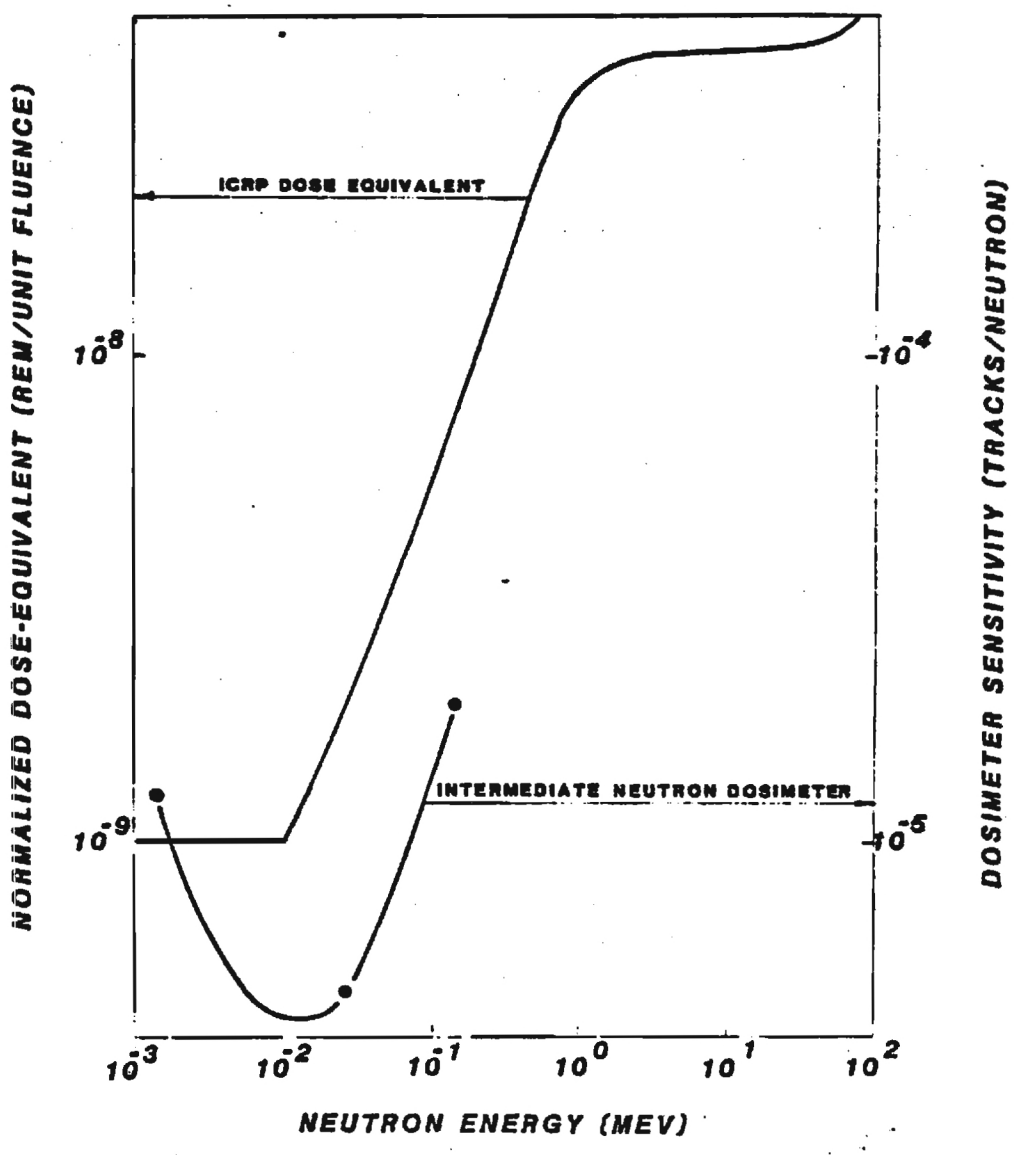

Figure 32. Intermediate Neutron Dosimeter Response as a Function of Neutron Energy Between 2 keV and 144 keV, Assuming a 1/v Response Below 24 keV

formed due to the 1/v dependent $^{6}Li(n,\alpha)^{3}H$ cross-section combined with the >100 keV neutron-induced recoil nuclei tracks formed in the CR-39 foil volume, then a curve can be drawn through the three filtered neutron beam response values as shown in Figure 32. Thus, with the help of the NBS narrow-band filtered neutron beams, the intermediate neutron dosimeter has been "calibrated" over a relatively small, but important, neutron energy range. The approximate rem-response measured between 2 keV and 144 keV offers a dramatic improvement when compared to the neutron-induced response of bare CR-309 foil. Unfortunately, no other "narrow-band" neutron sources of sufficient intensity were available between 144 keV and 1 MeV. Thus, the average neutron energies of several wide-band neutron sources were used for higher energy calibration "points." These tests not only provided further calibration data points for the intermediate neutron dosimeter, but also allowed the dosimeter dose-response to be observed for various neutron energy spectra. The dose-response tests of the intermediate neutron dosimeter to these wide-band neutron spectra are described in detail in Section 2.2. Only the values of the dosimeter neutron sensitivity in each particular fluence that was used for calibration are reported here.

The D_2O-moderated Cf-252 neutron calibration source described in Sanders (1982) has an average energy of $\sim$400 keV. Several of the intermediate neutron track dosimeters were exposed in the source fluence and a sensitivity of $6.5 \times 10^{-5} \pm 8.2$ percent tracks/neutron was determined. This value was used as a calibration point at 400 keV for the dosimeter as shown in Figure 33; however, as described later, this value may be somewhat high due to the relatively high percentage of low-energy (> 10 keV) neutrons present in the source spectrum.

A 4 μg bare Cf-252 neutron source and a 5 Ci PuBe neutron source were used to obtain average energy calibration points at ∿ 1.2 MeV and ∿ 4.1 MeV. The sensitivity response of the intermediate neutron dosimeter in these fluences was 1.33 X 10^{-4} ± 10.3 percent tracks/neutron and 1.38 X 10^{-4} (±7.1 percent) 7.1 percent tracks/neutron, respectively.

The NASA cyclotron in Cleveland, Ohio was utilized to obtain 8 MeV and 17 MeV calibration energy points for the dosimeter. The dosimeters exposed in these two high energy spectra resulted in calibration factors of 1.2 X 10^{-4} ± 13 percent tracks/neutron in the 8 MeV beam and 1.02 X 10^{-4} (± 12.5 percent) tracks/neutron in the 17 MeV beam.

Figure 33 displays the intermediate neutron dosimeter response curve which can be drawn as a function of the neutron energies described above. The track density recorded in the CR-39 detector is only a function of the 1/v dependent $^{6}Li(n,\alpha)^{3}H$ cross-section for neutron energies below ∿100 keV since no recoil nuclei tracks have been observed in bare CR-39 from neutron with energies less than 100 keV. Between ∿100 keV and ∿ 2 MeV the detector response is a function of the $^{6}Li(n,\alpha)^{3}H$ cross-section and the neutron-induced recoil nuclei track formation within the detector foil volume. Above 2 MeV neutron energies the response of the dosimeter is a function of the above interaction processes plus the contribution of the $^{6}Li(n,p)$ reaction which has a threshold at ∿ 2 MeV and a maximum cross-section of 20 millibarns at 4 MeV.

Figure 33 shows that the intermediate neutron dosimeter has an approximately dose-equivalent response when exposed to neutrons with energies of 10 keV to 4 MeV. Below 10 keV the dosimeter exhibits an over-response due to the rapid increase in the 1/v dependent $^{6}Li(n, \alpha)^{3}H$ cross-section. Above

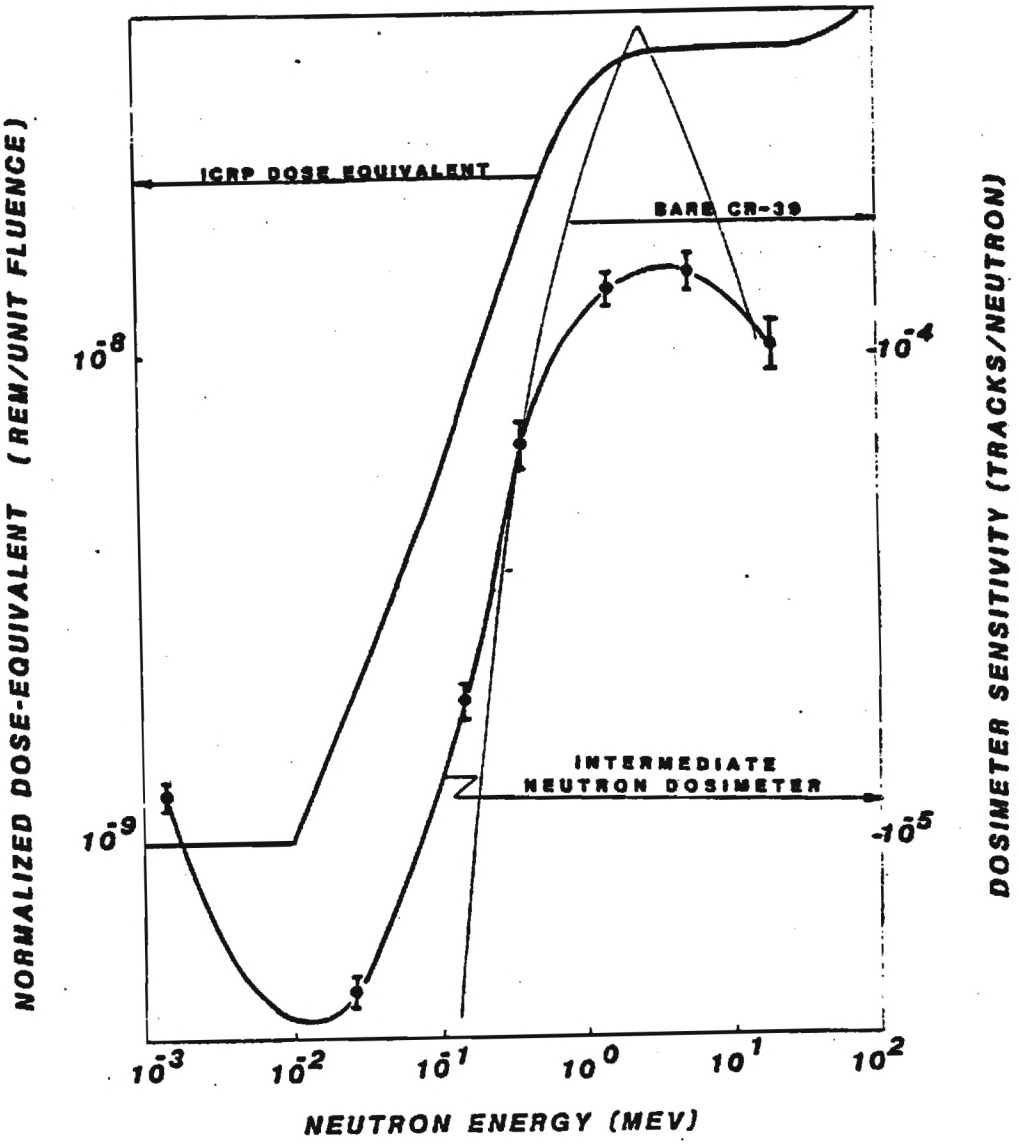

Figure 33. The Intermediate Neutron Dosimeter Neutron-Induced Response as a Function of Neutron Energy Between 2 keV and 17 MeV; Compared to the ICRP Rem Curve and the Neutron Energy Response of Bare CR-39 Foils (ICRP., 1973; Griffith et al., 1980)

4 MeV the dosimeter displays an under-response due to the decrease in probability of all the neutron-induced interaction processes mentioned above.

All of the intermediate neutron dosimeter measurements reported to this point have been "in air" measurements. The dosimeter was also irradiated in an albedo situation for all of the neutron spectra except the PuBe. The dosimeter sensitivity can be improved by a factor of 2-3 when used to measure neutron spectra with average neutron energies below approximately 1 MeV (see Figure 34). Unfortunately, the low-energy over-response increases by about the same factor as the dosimeter sensitivity. Thus, the intermediate neutron dosimeter used as an albedo dosimeter offers a higher sensitivity but has approximately the same over-response to neutrons $<$ 10 keV.

The intermediate neutron dosimeter directional response was measured by exposing seven dosimeters to the PuBe neutron spectrum. Each dosimeter was situated 12 cm away from the source and at an angle to the source of between 0° (normal) and 180° with intervals of 30°. Figure 35 shows the directional dependence of the dosimeter and reveals a $0^{\circ}/90^{\circ}$ dependence of 1.9. This is equal to or slightly better than that found in other non-fissile radiator damage-track dosimeters.

2.2 Application of the Intermediate Neutron Dosimeter to Various Neutron Spectra

The intermediate neutron dosimeter described above was applied to dose measurements in several neutron spectra typical of those found in the working environments of reactors, high-energy accelerators, and isotopic neutron sources. The results of these tests are described in this section.

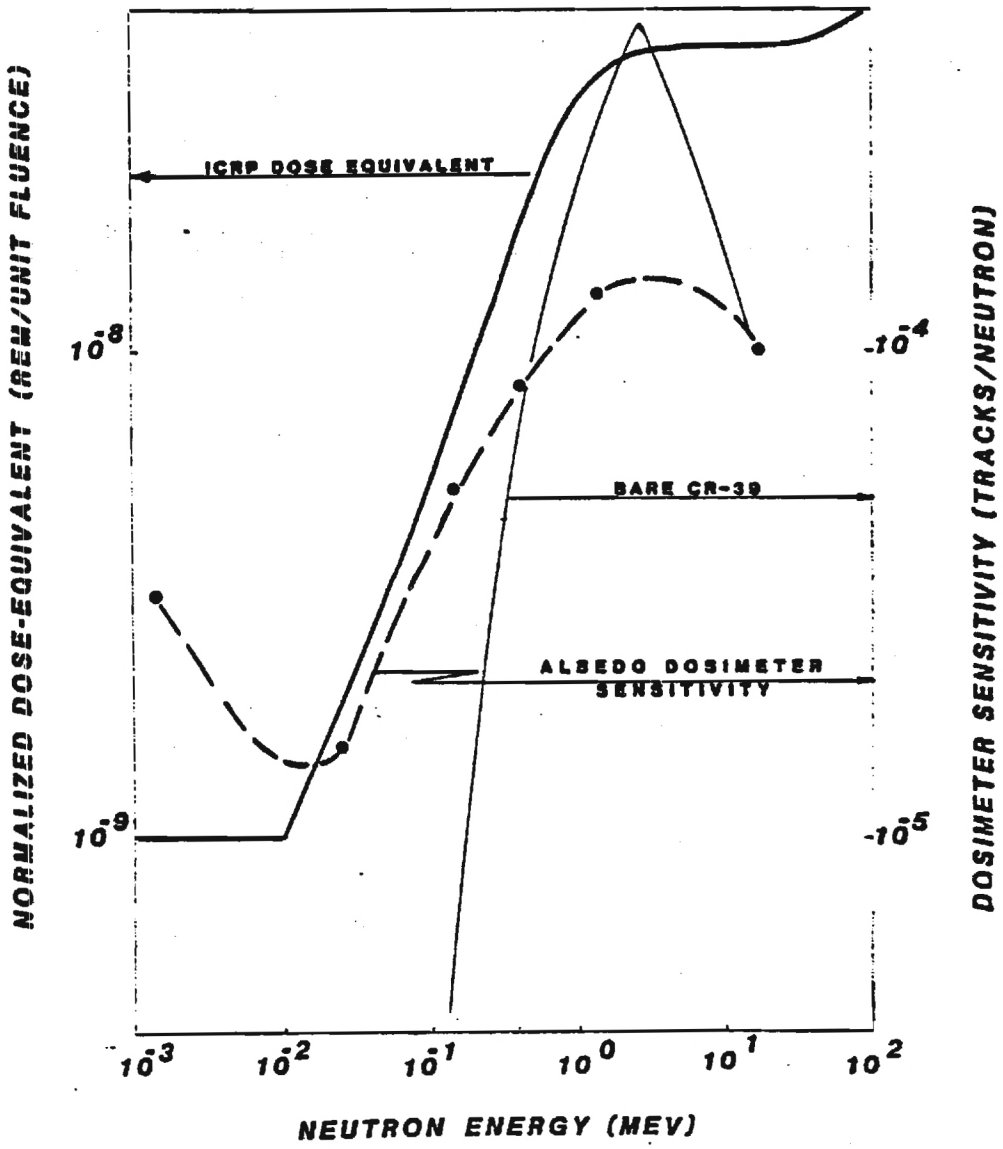

Figure 34. Albedo Response of the Intermediate Neutron Dosimeter Compared to the ICRP Rem Curve and the Neutron Energy Response of Bare CR-39 (ICRP, 1973; Griffith et al., 1980)

The effect of the low-energy over-response found in the intermediate neutron dosimeter designed in this research is evident in the dose-response measurements obtained in the D_2O-moderated Cf-252 neutron spectrum was developed to simulate the neutron energy spectra found in the vicinity of a power reactor (Schwartz and Eisenhauer, 1981). Several intermediate neutron dosimeters were mounted on either styrofoam blocks, for "in air" measurement, or on the surface of a 30 cm x 30 cm x 15 cm thick water-filled phantom, for albedo measurement. The dosimeters were exposed to a dose over the range 25 to 1000 mrem in the air and albedo situations. The CR-39 foils were etched under standard conditions. The foils were cleaned, dried, and evaluated by a phase contrast microscope and Whippl e disc arrangement using 100X magnification. The resultant data are shown numerically in Table 4, and graphically in Figure 36. If an average sensitivity factor of 3237 tracks/cm^2-rem is used (this is the average rem-conversion factor between 10 keV and 1.2 MeV as shown in Figure 33), the dosimeter shows an over-response of approximately 2.2. This over-response is probably due to the low-energy (<10 keV) over-response of the intermediate neutron dosimeter as previously discussed. However, such an over-response may not be apparent when the dosimeter is exposed to a neutron spectrum that more accurately reflects a typical differential neutron spectrum found in the working environment of a power reactor. Figure 37, depicts the differential neutron lethargy spectrum measured at the Farley, Alabama nuclear plant (Hankins and Griffith, 1978), and can be compared to the lethargy neutron spectrum of the D_2O-moderated Cf-252 spectrum. Because of practical considerations, the D_2O-moderated neutron source was constructed such that its neutron spectrum when measured by conventional neutron dosimeters and survey

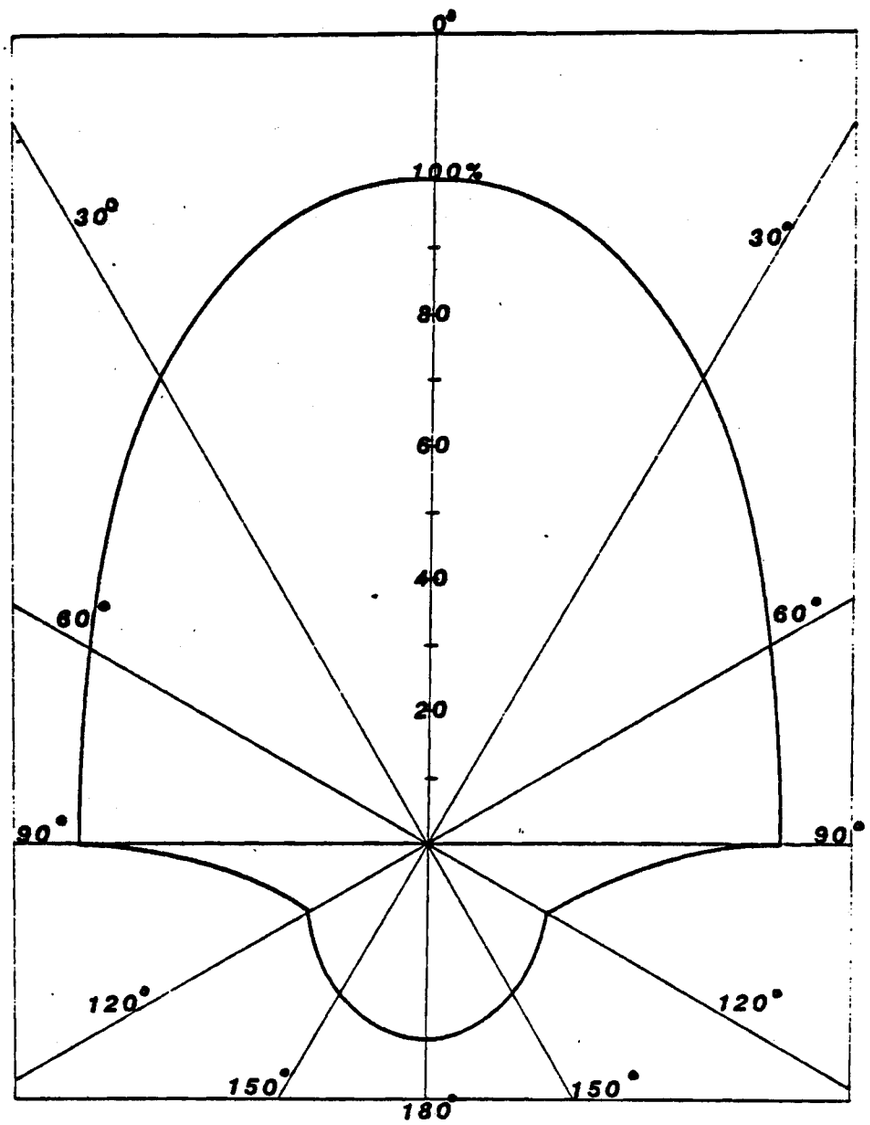

Figure 35. Directional Response of the Intermediate Neutron Dosimeter Designed in This Research

Table 4. Damage-Track Densities Recorded by the Intermediate Neutron Dosimeter When Exposed to a D_2O-Moderated Cf-252 Neutron Spectrum

Dose Equivalent Delivered (mrem)	Track Density ($(t/0.49\ cm^2) \pm 1\sigma$)
25	118 ± 11
25	125 ± 13
25	119 ± 10
25	112 ± 10
100	427 ± 17
100	442 ± 20
100	418 ± 27
100	423 ± 23
500	1707 ± 17
500	1685 ± 28
500	1798 ± 21
500	1702 ± 29
1000	3557 ± 58
1000	3502 ± 92
1000	3681 ± 109
1000	3509 ± 112

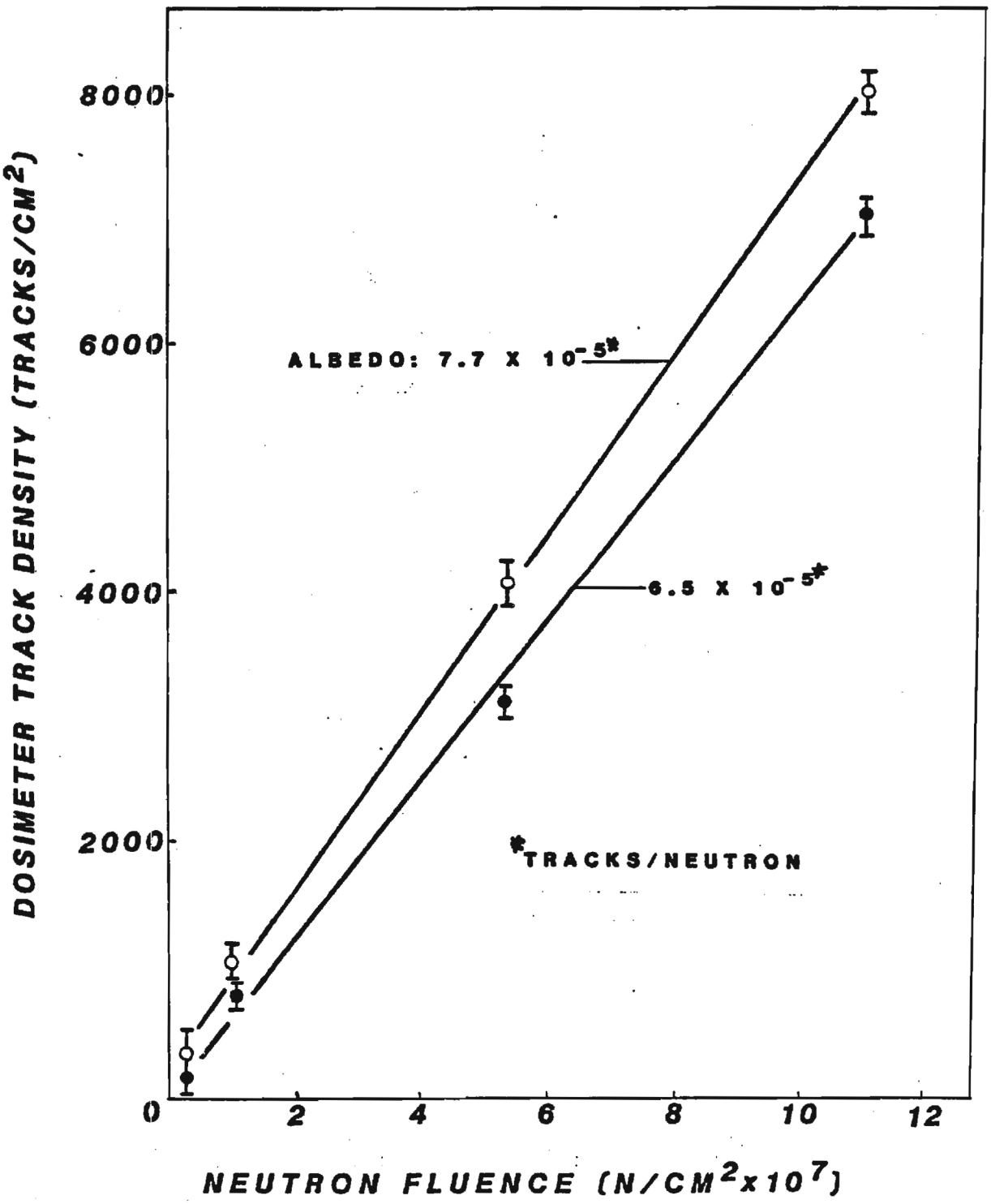

Figure 36. Dose Response of Intermediate Neutron Dosimeter in the NBS D_2O-Moderated Cf-252 Neutron Energy Spectrum

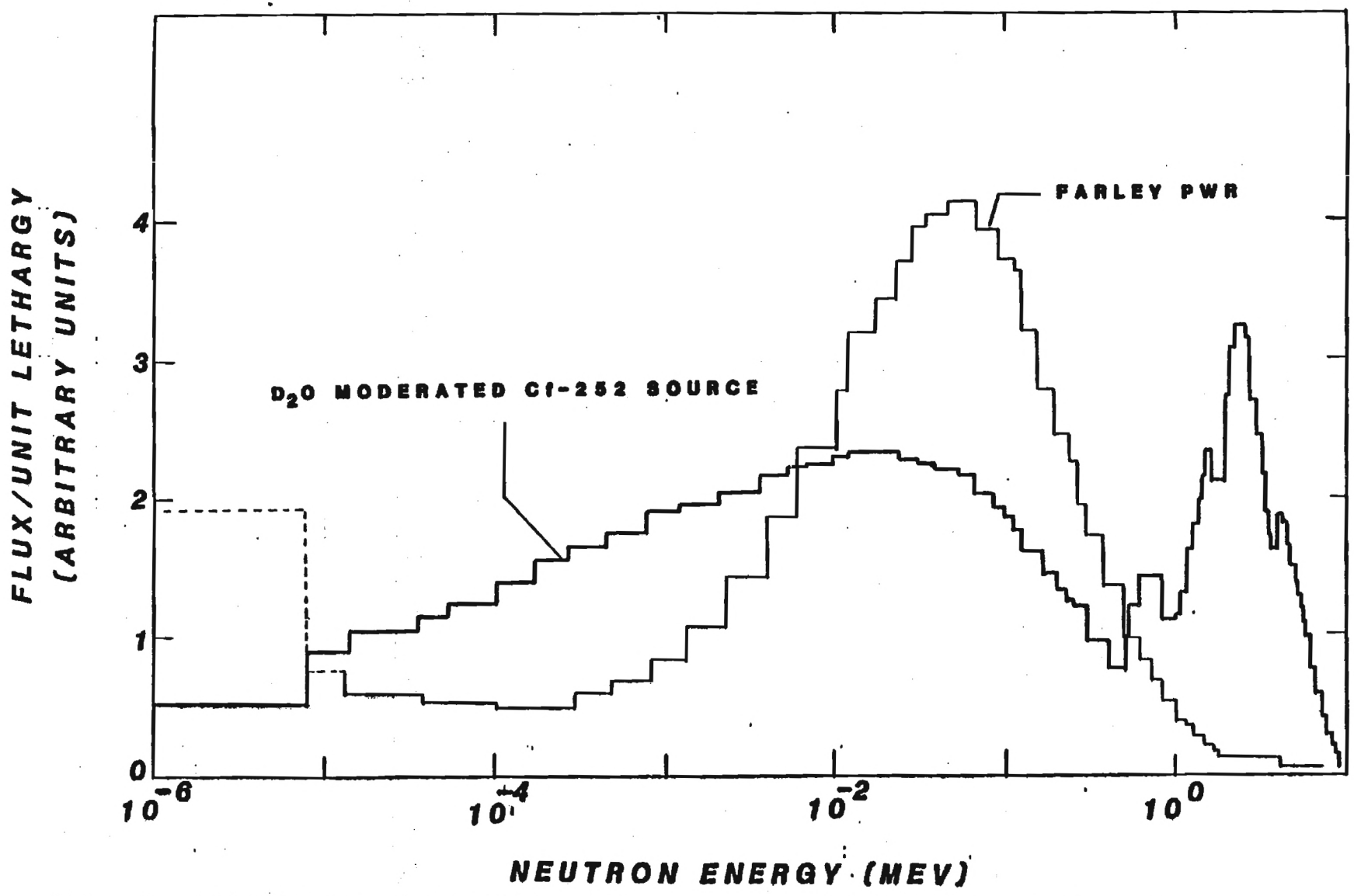

Figure 37. NBS D_2O-Moderated Cf-252 Neutron Spectrum Compared to the Neutron Lethargy Spectrum Measured at the Farley PWR (Hankins and Griffith, 1978; Schwartz and Eisenhauer, 1980)

instruments, such as an albedo dosimeter or a 9-inch sphere remmeter, would yield similar integral responses to those recorded in actual power reactor neutron lethargy spectra. Thus, the simulation quality of the D_2O-moderated neutron calibration source is limited by the rem-response sensitivity of the neutron dosimeters utilized as the criterion in its design.

The intermediate neutron dosimeter response in the absence of an excessive low-energy neutron spectrum component was evaluated with two neutron sources of higher than average energies. Two sets of dosimeters were exposed to various integral dose-equivalents in the neutron spectra of a 5μg Cf-252 source and a 5 Ci PuBe source. The CR-39 track recording foils were etched chemically and electrochemically according to the standard procedure. The evaluated neutron-induced damage-track densities are presented as a function of neutron fluence in Figures 38 and 39. If an average conversion factor of 3237 tracks/cm^2-rem (Stoddard and Hootman 1971)is assumed, the PuBe neutron dose-equivalent response measurements, shown in Figure 39, indicate that the intermediate neutron dosimeter has a slight over-response of $\sim$ 5.0 percent over the dose range measured when compared to calculated dose-equivalent values. The calculated dose-equivalent for the 4.1 MeV average neutron energy spectrum of the PuBe source was determined by using a conversion factor of 2.64 X 10^7 n/cm^2-rem (Anderson, 1967). In this case there is only a slight over-response when compared to that seen in bare CR-39 foils exposed to 4 MeV neutron irradiation. This response was better than expected and was due in part to the $^6Li(n,\alpha)^3H$ rection cross-section which is 0.1 barn at 4 MeV and also

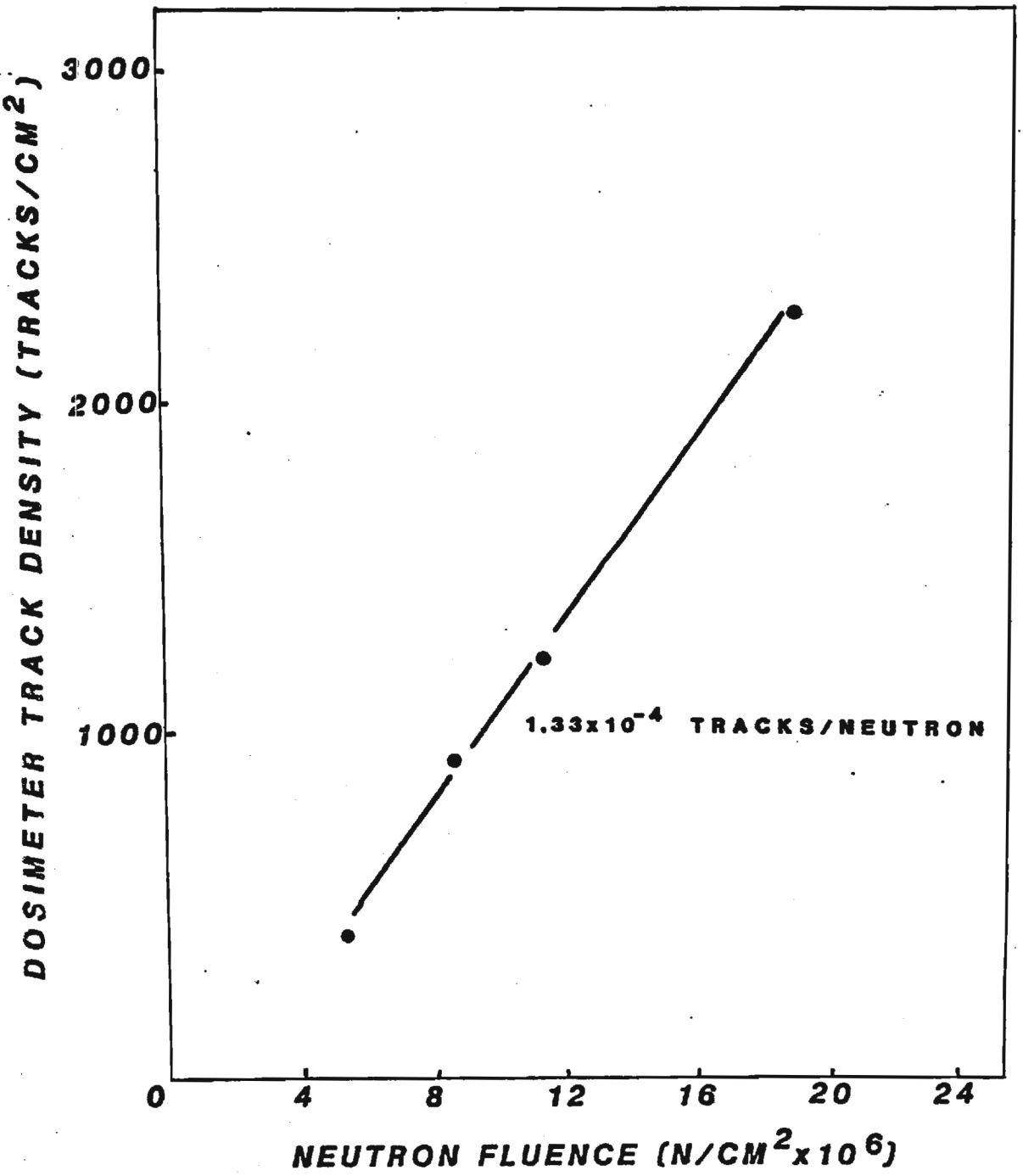

Figure 38. Dose Response of Intermediate Neutron Dosimeter in a Bare Cf-252 Neutron Energy Spectrum

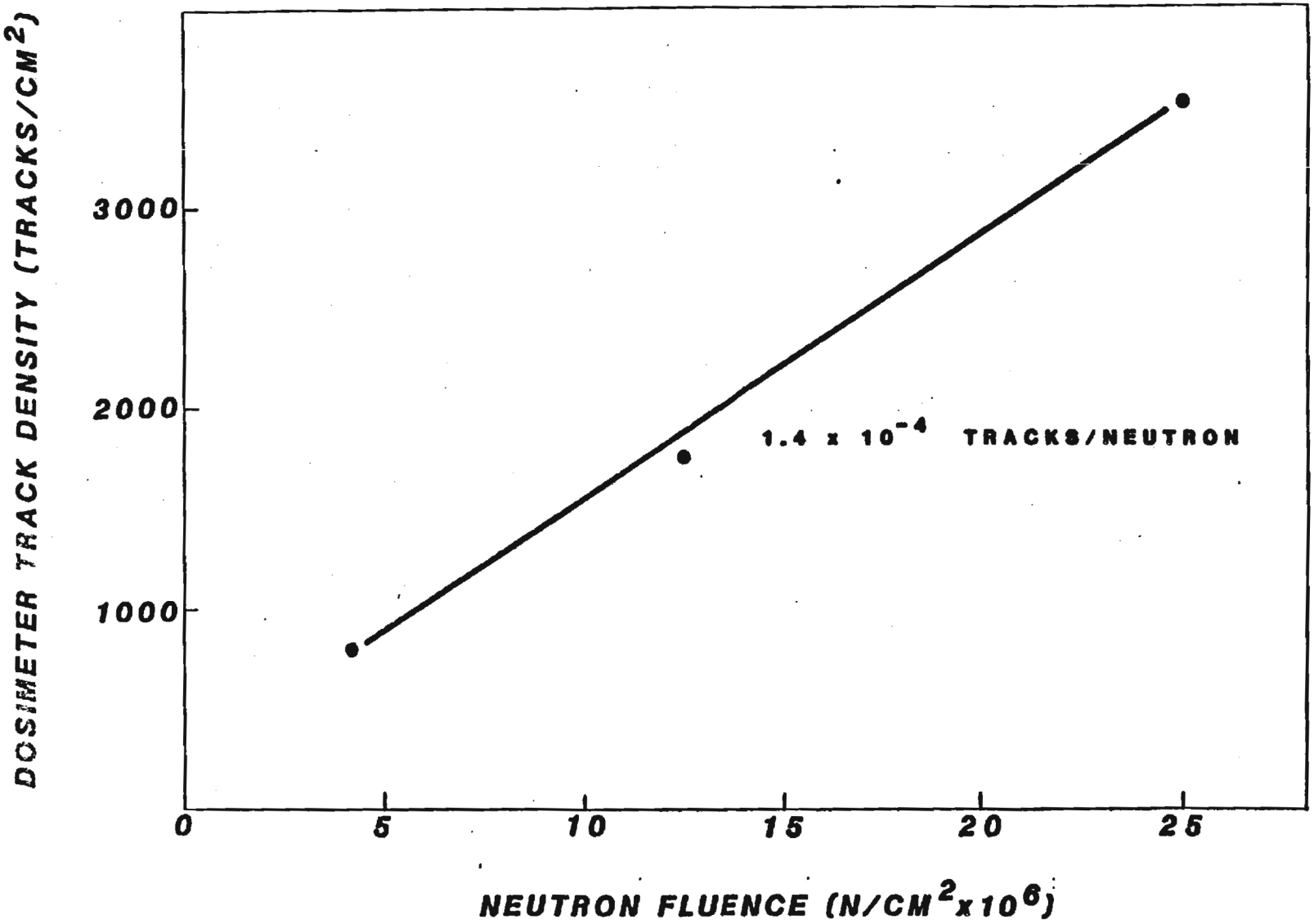

Figure 39. Dose Response of Intermediate Neutron Dosimeter in a PuBe Neutron Energy Spectrum

to a $^{6}Li(n,p)$ cross-section which has a threshold at $\sim$ 2 MeV and a maximum cross-section of 20 millibarns at 4 MeV and then gradually decreases to 10 millibarns at 30 MeV.

The $^{6}Li(n,p)$ reaction also acts as a track density boost to the CR-39 recoil nuclei track response seen in the 8 MeV and 17 MeV neutron beam exposures taken at the NASA cyclotron facility in Cleveland, Ohio. The intermediate neutron dosimeter exhibited an under-response of 10.5 percent in the 8 MeV average energy neutron beam and an under-response of 19.5 percent in the 17 MeV average energy neutron beam. Both neutron beam dose-equivalent responses are determined by using a dosimeter sensitivity conversion factor of 3237 $\pm$ 405 tracks/cm^{2}-rem and are shown in Figure 40.

Figure 33 displays a compilation of the dose-equivalent response curve slopes calculated by least squares fit for each of the neutron spectra to which the intermediate neutron dosimeter was exposed. The respective points result in a sensitivity (tracks/n) as a function of neutron energy which can be compared to the ICRP dose-equivalent curve over the same neutron energy range. The dosimeter under-response above 4 MeV and over-response below 10 keV is easily seen; however, it is also quite evident that the dosimeter offers a measured response to neutrons between 10 keV and 4 MeV that is very close to the calculated ICRP dose-equivalent response. Thus, an approximate rem-response can be achieved when the dosimeter is used to measure any neutron spectrum that is not overly rich in neutrons below 10 keV or above 4 MeV. The dosimeter is useable down to 1 eV neutron energy, albeit with an over-response of approximately a factor of 2-3 as ws shown in the BNCT neutron beam which is composed of epithermal neutrons with energies between 1 eV and 10 keV.

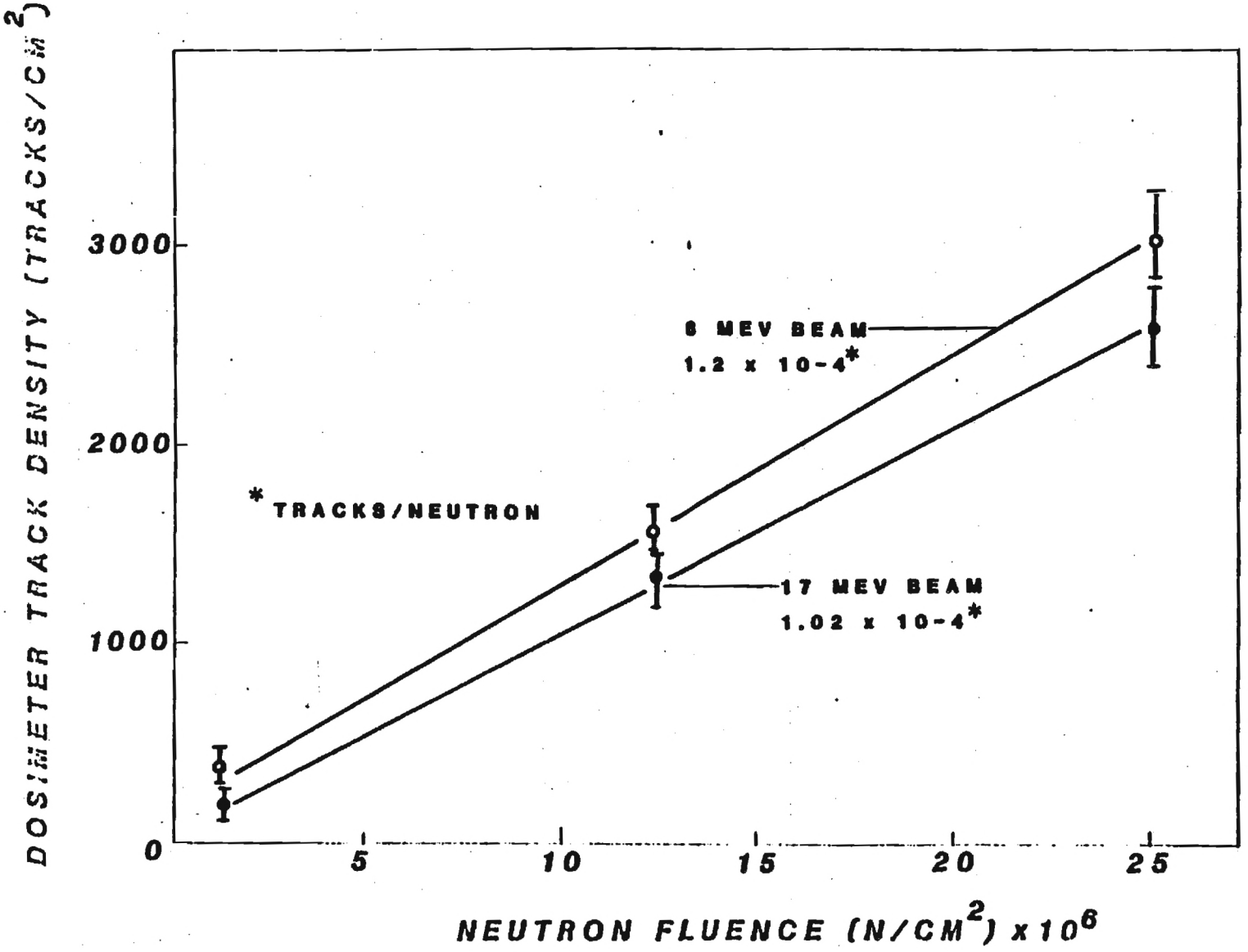

Figure 40. Dose Response of an Intermediate Neutron Dosimeter in the NASA Cyclotron Produced 8 MeV and 17 MeV Neutron Energy Spectra

2.3 Investigation of Photoneutron Contamination in Therapy Accelerator X-Ray Beams

Patient dose may be affected by photoneutrons produced by high-energy x-ray interactions with accelerator components or by reactions within the patient's body. The out-of-beam scatter from these photoneutron sources may also present a hazard to the accelerator operating personnel. An investigation of the neutron contamination generated outside and within the patient is reported in this section and elsewhere (Sanders et al., 1980: 1983).

The neutron dose-equivalent measurements reported in this study were determined by exposing damage-track dosimeters that are approximately rem-responding between thermal and 20 MeV neutron energies, to the primary treatment x-ray beam of several high-energy electron medical accelerators. The dosimeters were exposed in air to measure the neutron dose-equivalent produced by photoneutrons generated in the accelerator components touched by the x-ray beam. The dose-equivalent due to photoneutrons generated within the patient treatment volume was determined by measuring the total neutron dose deposited in a tissue-equivalent thoracic phantom and then subtracting out the "in air" neutron dose measurement. The damage-track neutron dosimeters used in this study allowed separation of the measured dose-equivalent into three neutron energy components; thermal ($<$ Cd cut-off), intermediate (1 eV to 1 MeV), and fast ($>$1 MeV).

Unless otherwise designated, the neutron dose-equivalent measured in this study is referred to in terms of percent neutron dose-equivalent, in rem, measured at the point indicated per x-ray absorbed dose, in rad, as measured at d_{max}. To determine the percent neutron absorbed dose (rad) per x-ray absorbed dose (rad) delivered, a quality factor of 2.3 can be folded

out of the thermal neutron measurements, a quality factor of 7 out of the intermediate neutron measurements, and a quality factor of ∿ 10 out of the fast neutron dose-equivalent measurements (ICRU, 1977).

Figure 41 exhibits the measured fast (>1 MeV) neutron dose-equivalent found in air due to accelerator component produced photoneutrons, the total fast neutron dose-equivalent found inside the phantom at a depth of 3.7 cm along the x-ray beam central axis (CAX), and from these measurements the phantom generated fast neutron dose-equivalent as shown by the dashed line curve. The additional dose-equivalent deposited due to the accelerator component produced photoneutrons increases from 0.2 percent in the 18 MV x-ray beam of the Clinac -20 to 1.2 percent in the 45 MV x-ray beam of the Brown-Boveri 45 MeV betatron. This results in an increase in neutron dose-equivalent between 25 MV and 45 MV of 55 percent and is considerably greater than that predicted by theory. The total number or neutrons, predicted by theory to be produced in a thin tungsten target as a function of x-ray energy, increases only by 5 percent between 25 MV and 45 MV x-ray energies. Laughlin et al., 1979; McCall and Swanson, 1979). However, the data represented in Figure 41 were taken from damage-track measurements of neutrons with energies greater than 1 MeV only and not the full spectrum of neutrons known to be present in the photoneutron spectrum. In fact, this unexpectedly large increase may be a confirmation of the greater number of high-energy neutrons predicted to be produced at higher photon interaction energies. The total accelerator component plus phantom-produced, photoneutron dose-equivalent measurements taken at a depth of 3.7 cm along the CAX increases from 0.2 percent in the 18 MV x-ray beam to 2.6 percent in the

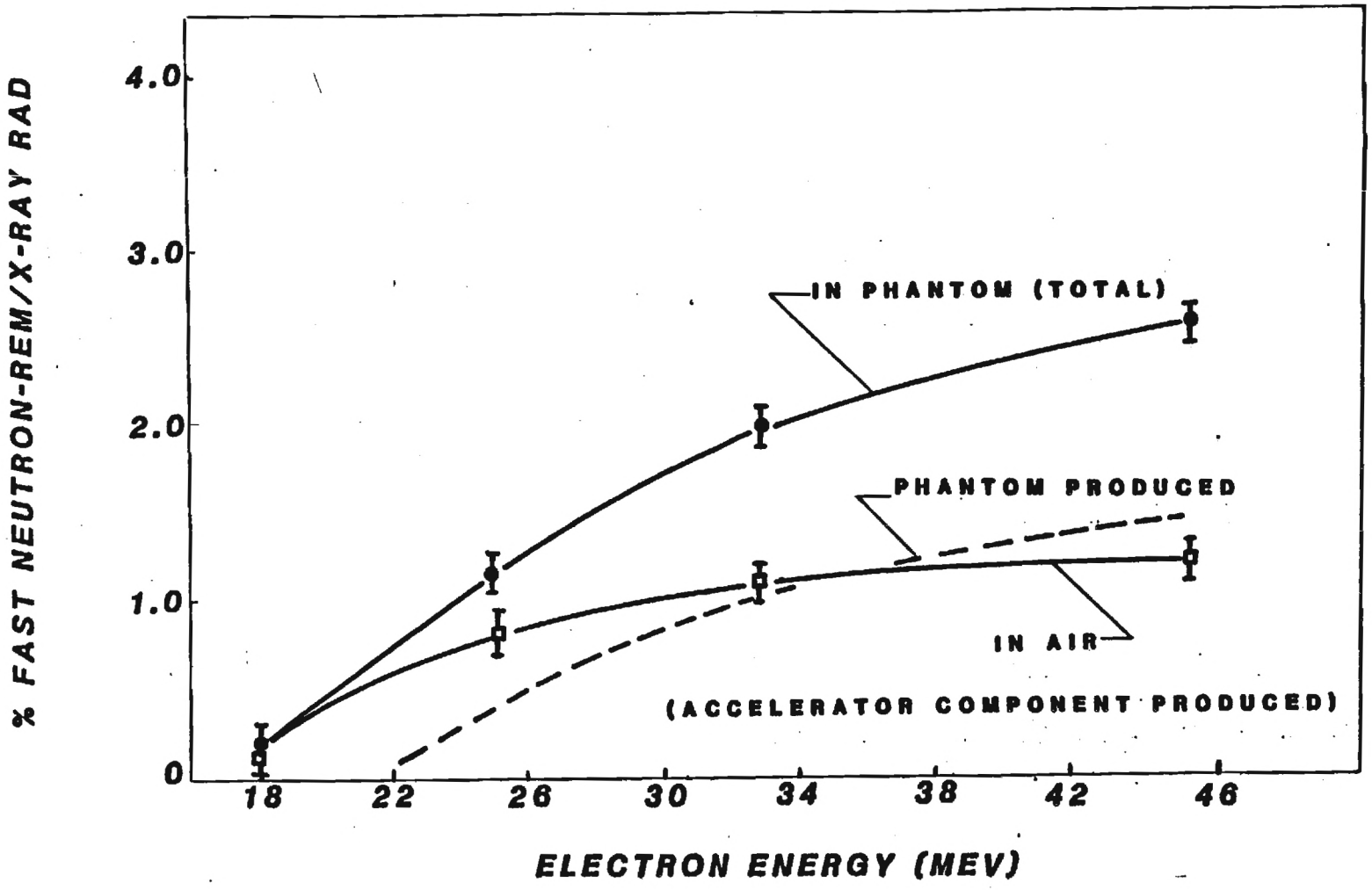

Figure 41. Additional Dose Deposited in the Patient Treatment Volume by Fast (> 1 MeV) Photoneutrons Produced in the Primary X-Ray Beam of Several Accelerators, and Measured by Damage-Track Dosimeters

45 MV x-ray beam. By subtracting the accelerator component neutron measurements from the total neutron measurements, the dose-equivalent due to the tissue phantom produced photoneutrons can be determined. The photoneutron dose-equivalent produced within the phantom is shown in the dashed curve of Figure 41 and increases as a function of x-ray beam energy from zero in the 18 MV beam to 1.4 percent in the 45 MVC beam.

Figure 42 illustrates the intermediate energy (1 eV to 1 MeV) neutron dose-equivalent measurements found due to accelerator component produced neutrons and those produced within the phantom. Interestingly, the total additional dose deposition measured due to photoneutrons between 1 eV and 1 MeV increases from 0.6 percent in the 18 MV x-ray beam to 1.0 percent in the 25 MV beam and then decreases by 20 percent to 0.8 percent in the 45 MV beam. This may be explained by the fact that there are more photoneutrons being produced as a function of x-ray energy as the beam energy is increased from 18 MV to 25 MV; however, above 25 MV approximately the same total number of neutrons is being produced but more of them are generated at higher energies due to the higher energy of the photon beam and increased incidence of photoionization neutron production. Thus, one could expect a dosimeter which is preferentially measuring the dose due to photoneutrons between 1 eV and 1 MeV to measure the dose-equivalent as a function of x-ray beam energy as illustrated in Figure 42.

The thermal neutron dose-equivalent measurements due to accelerator component and phantom produced photoneutrons are shown in Figure 43. These values are on the order of 100-500 times smaller than the dose-equivalent measured due to the more energetic neutrons generated in the treatment beam. However, these measurements do bring up an interesting sidelight in that they show the thermal neutron-induced damage-track measurements to be

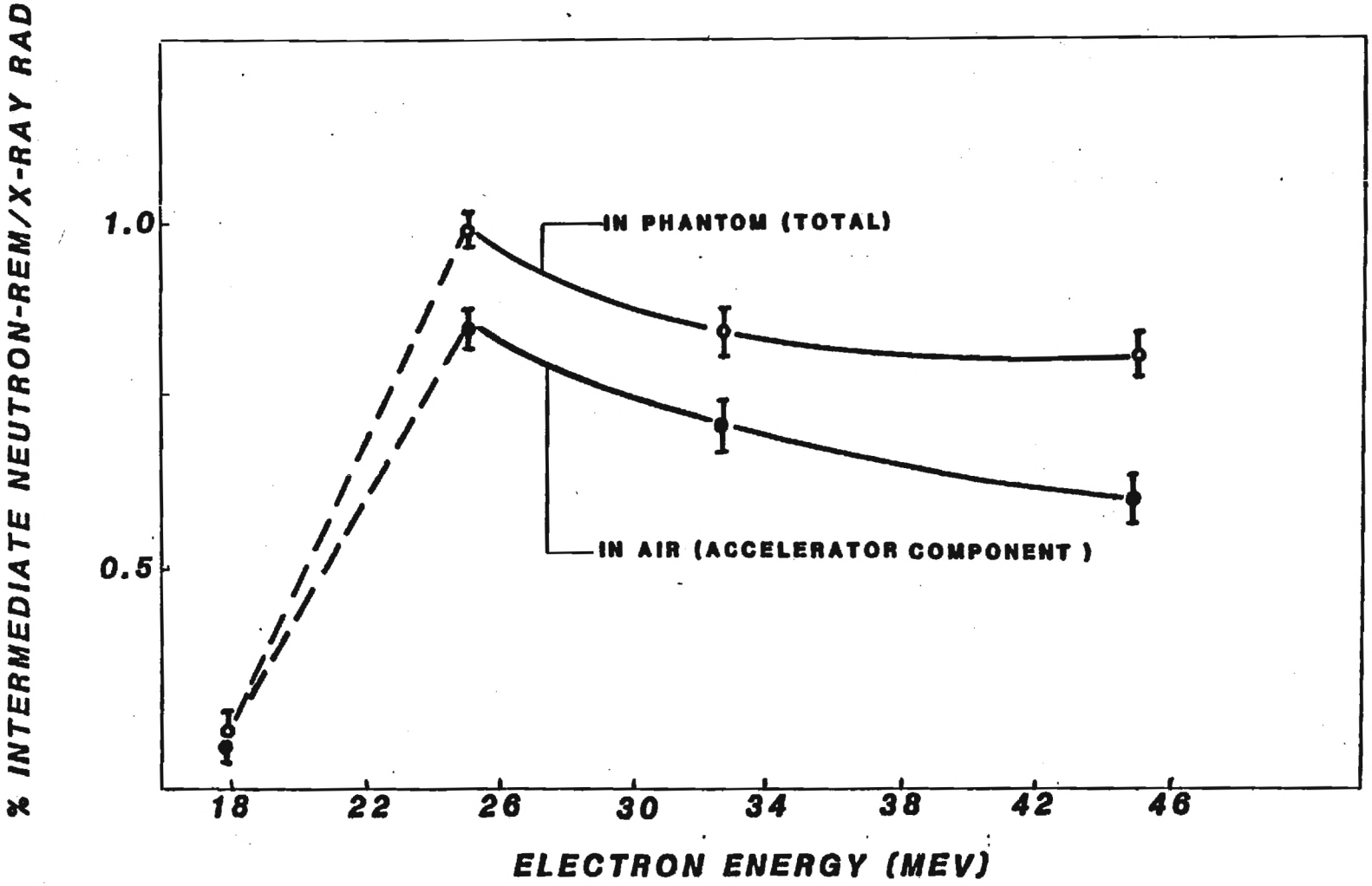

Figure 42. Additional Dose Deposited in the Patient Treatment Volume by Intermediate (1 eV - 1 MeV) Photoneutrons Produced in the Primary X-Ray Beam of Several Accelerators, and Measured with the Intermediate Neutron Dosimeter Designed in This Research

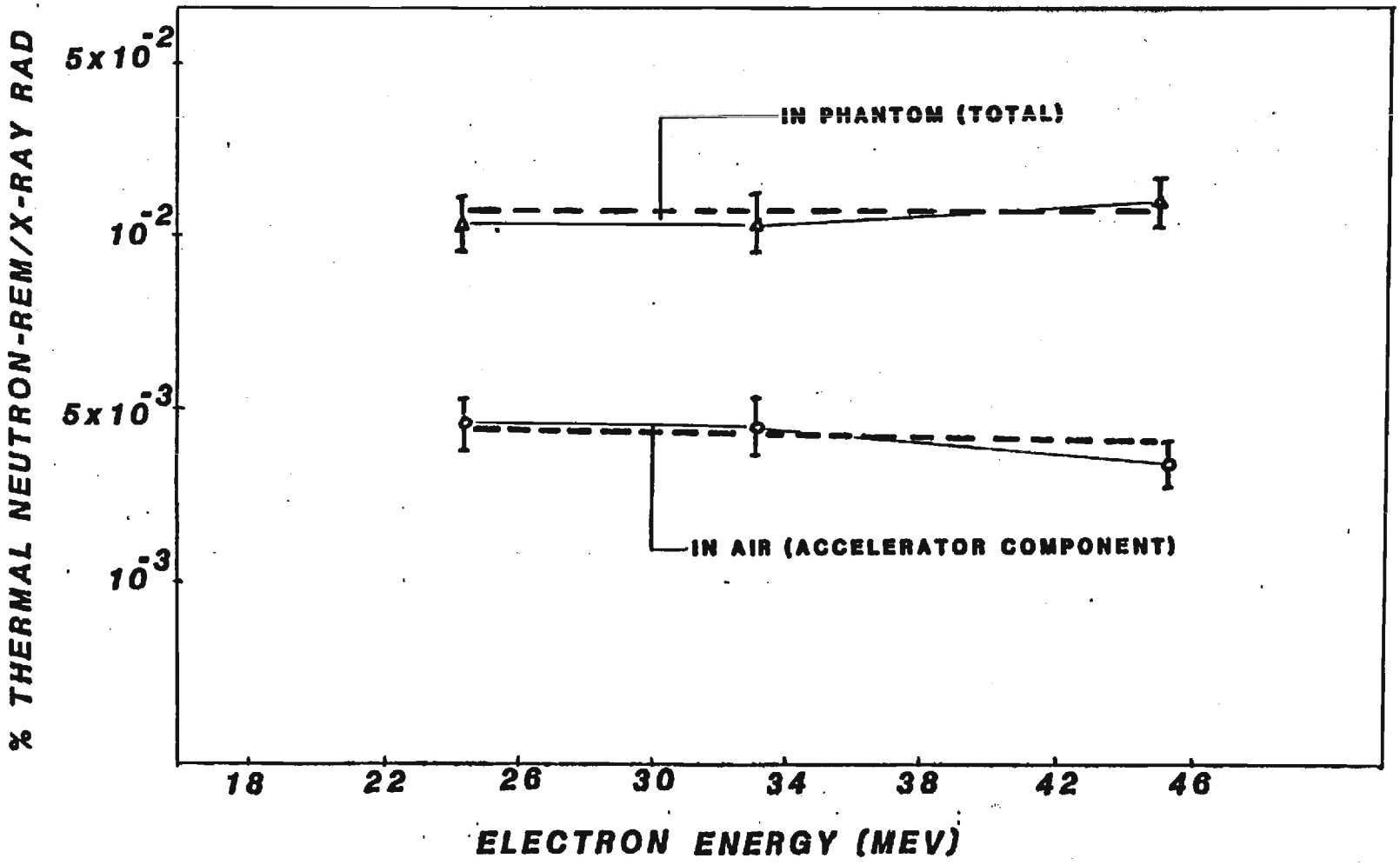

Figure 43. Additional Dose Deposited in the Patient Treatment Volume by Thermal Neutrons Produced in the Primary Beam of Several Accelerators and Measured by Damage-Track Dosimetry

relatively unchanged as the x-ray energy increases. Sohrabi (1975) showed that the bisphenol-A polycarbonate fast neutron dosimeter was insensitive to Co-60 photon irradiation up to doses of 10^6 rads. However, the use of bisphenol-A polycarbonate as a neutron detector in high-energy accelerator x-ray beams exposes the detector foil to not only intense x-ray fields but also high-energy x-rays which exceed the threshold energy for photoneutron production in the elements of which exceed the threshold energy for photoneutron production in the elements of which polycarbonate is made. There has been some question as to whether the larger photoneutron (> 1 MeV) dose-equivalent values measured by the damage-track method compared to other typically used methods (see Table 5) were due to actual higher doses present or to (x,n) reactions within the polymer volume which, in effect, induce a higher "background" in the foils. The polycarbonate used in the thermal neutron dosimeter is the same type of polycarbonate as is used in the fast neutron dosimeter. The fact that no increase in response is observed in the thermal neutron dosimeter as the x-ray beam energy is increased between 18 MV and 45 MV suggests that the polymer detector is insensitive to direct photon-neutron reactions within its volume in this x-ray energy range.

The dose-equivalent measurements made in this study showing the additional dose deposited in the treatment volume by neutrons with energies from thermal to 20 MeV is summarized in Figure 44. Actually, since the thermal neutron dose-equivalent values are more than two orders of magnitude smaller, the curves in Figure 44 are composed of only the intermediate and fast neutron measurements. The total dose-equivalent produced by accelerator component photoneutrons increases by only four percent (that is, from 1.77 percent neutron rem/x-ray rad to 1.84 percent neutron rem/x-ray rad) as

Table 5: Percent Additional Neutron Dose Deposited in the Treatment Volume per Unit Dose of X-Ray as Measured in Several Medical Accelerator X-Ray Beams by Etched Neutron Track Dosimeters (ENTD) and Compared to Measurements Made by Traditional Neutron Dosimeters

Accelerator	In-Activation (H_2O-Moderator)	In-Activation (Paraffin Moderator)	P_2O_5 Activation	ENTD	ENTD (Total)
Clinac-20	--	--	--	0.20	0.24
Allis-Chalmers 25 MeV Betatron	0.51	0.45	0.28	1.77	1.97
Brown-Boveri 45 MeV Betatron (33 MV Beam)	--	--	--	1.81	2.75
Brown-Boveri 45 MeV Betatron (45 MV Beam)	0.54	0.39	0.73	1.84	3.26

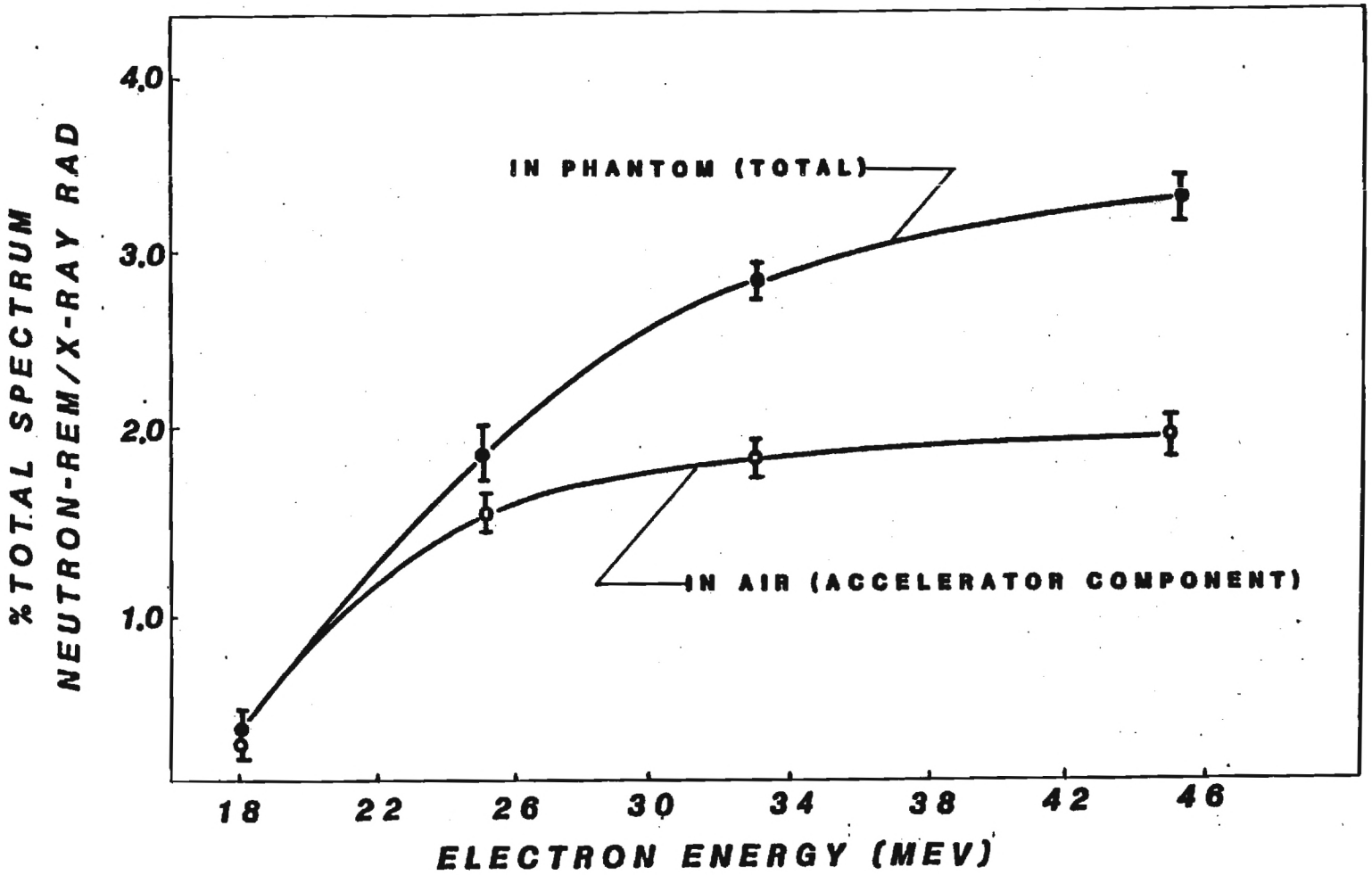

Figure 44. Additional Dose Deposited in the Patient Treatment Volume by the Whole Spectrum of Photoneutron Energies Produced in the Primary X-Ray Beam of Several Accelerators and Measured by Damage-Track Dosimetry

the x-ray beam energy increases between 25 MV and 45 MV. This compares to the $\sim$ 5 percent increase predicted by theory (McCall and Swanson, 1979). The total dose-equivalent measured due to the full spectrum of photoneutrons present in the x-ray beams is shown in the upper curve of Figure 44. The additional dose deposition in the treatment volume increases from 0.24 percent in the Clinac-20, 18 MV x-ray beam, to 3.26 percent in the 45 MV x-ray beam of the Brown-Boveri 45 MeV betatron. If a quality factor of approximately 10 is folded out of these data, the additional dose, in rad, deposited by all the photoneutrons produced in the x-ray beam and treatment volume is between 0.02 and 0.33 percent, depending on x-ray beam energy. These experimentally measured values compare favorably with theoretical calculations for a 30 MV accelerator x-ray beam, which predict an additional energy deposition due to photoneutrons within the treatment volume of 0.15 to 0.3 percent (Laughlin et al., 1979).

Figure 45 illustrates additional dose-equivalent deposition due to the full spectrum of photoneutrons measured in several accelerator x-ray beams as a function of depth in an elliptical thoracic phamtom. The additional photoneutron dose deposition at different depths may be thought of either as it relates to the x-ray dose at d_{max} (as shown by the solid-line curves in figure 45) or as it relates to the x-ray dose measured at the same dept a the neutron measurement (dashed-line curves in Figure 45). The latter method is more indicative of the local additional neutron dose deposition and more clearly reveals the primary problem presented to the patient by neutron contamination generated in the x-ray beam. The ratio of photoneutron dose to x-ray dose will begin to increase at some depth in the patient due to continuous generation of photoneutrons by the x-ray beam at all depths.

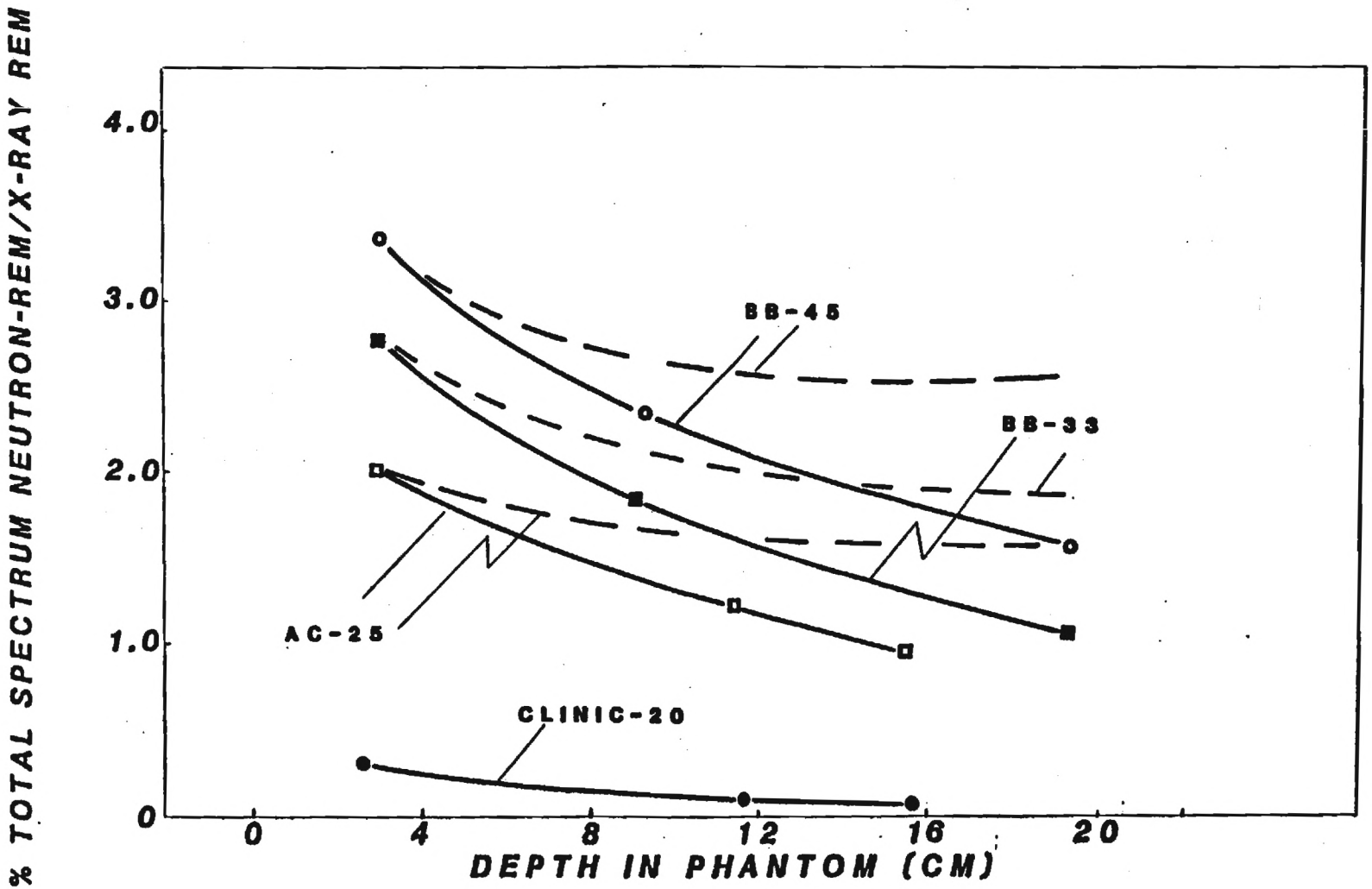

Figure 45. Additional Dose Deposited by Photoneutrons Produced in the Primary X-Ray Beam of Several Accelerators as a Function of Depth in a Tissue-Equivalent Phantom (The solid lines show the photoneutron dose at depth divided by the x-ray dose at d_{max} while the dashed lines show the photoneutron dose at depth divided by the x-ray dose at that same depth.)

While the neutron dose-equivalent measurements reported in this study are somewhat higher than those reported by conventional neutron fluence measurement techniques, they are still quite small when compared to the large dose of x-rays necessarily delivered to the treatment volume during high-energy accelerator radiotherapy. However, outside the treatment volume, where little or no x-ray dose is delivered, this investigation indicates that comparatively high neutron doses can be found. Figure 46 shows schematically a cross-sectional slice of the elliptical phantom used in this investigation. The lung phantom position and the treatment field of 22 cm x 22 cm at the phantom midline (10.5 cm) are also indicated. Neutron dose-equivalent measurements were taken at four different positions in this configuration for each of the investigated accelerator x-ray beams. Position A is located ∿3 cm perpendicularly outside the treatment volume, but still within the phantom. Position B is 6 cm perpendicularly outside the treatment volume and located on the outside of the phantom wall. Positions A'and B' are at the same respective distances outside the treatment volume; however, approximately 8 cm of lung-equivalent phantom has replaced the tissue-equivalent liquid. Table 6 presents the photoneutron dose-equivalent measurements at these positions and along the x-ray bem CAX. The dose-euivalent values given in the table have been normalized to an absorbed dose of 200 rad, which is typical of many x-ray prescriptions. As can be seen, at a point 6 cm distant from the treatment volume, -0.6 to 1.6 rem of neutrons can be measured per 200 rad, x-ray treatment, depending on the accelerator x-ray beam energy. This value is increased by 12-17 percent when measured through the lower-density lung phantom and is decreased by 3-12 percent when measured through a 2.5 cm diameter bone-equivalent phantom.

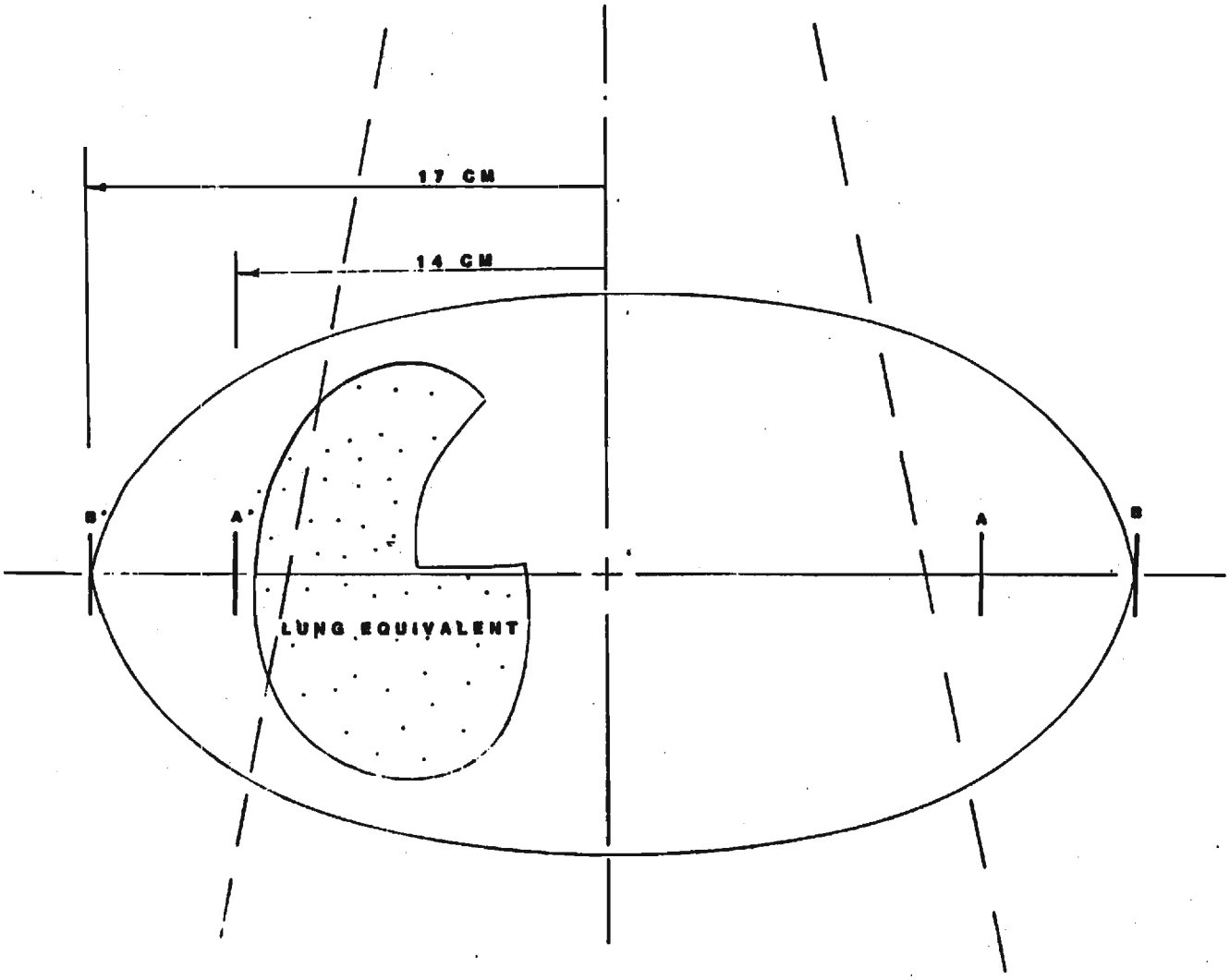

Figure 46. Schematic of Heterogeneous Phantom Cross-Section at Midline (A, A', B, and B' indicate points of neutron measurement.)

Table 5. Neutron Dose-Equivalent Measurements Found Outside a 20 cm × 20 cm Treatment Volume (22 cm × 22 cm @ 10 cm depth) Using Etched Neutron Track Dosimeters Within a Tissue-Equivalent Phantom

		Neutron Dose-Equivalent @ 10 cm on CAX (200 rad x-ray given dose)	Position (from Figure 46) A	A'	B	B'
A-C 25 MV Beam	> 1 MeV	2 Rem	0.34 Rem	0.5 Rem	0.65	0.6 Rem
	< 1 MeV	1 Rem			0.1 Rem	0.1 Rem
	thermal	0.02 Rem			0.9 mRem	0.9 mRem
BBC 33 MV Beam	> 1 MeV	2.6 Rem	1.24 Rem	1.5 Rem	1.06 Rem	1.22 Rem
	< 1 MeV	1 Rem			0.17 Rem	0.2 Rem
	thermal	0.02 Rem			0.6 mRem	0.6 mRem
BBC 45 MV Beam	> 1 MeV	4 Rem	1.42 Rem	1.77 Rem	1.2 Rem	1.51 Rem
	< 1 MeV	1 Rem			0.4 Rem	0.48 Rem
	thermal	0.015 Rem			0.2 mRem	0.2 mRem

3. DISCUSSION OF RESULTS

This research has consisted of two parts: (1) design and optimization of an intermediate neutron damage-track dosimeter, and (2) applications of the dosimeter to neutron measurements in air, within a tissue-equivalent phantom, and as an albedo dosimeter for different neutron spectra.

A simple, rugged, reliable damage-track dosimeter which is approximately rem-responding and useable in the 1 eV to 17 MeV neutron energy region has been developed. The dosimeter is based on the formation of neutron-induced damage-tracks near the surface and within the volume of thin foils made from the CR-39 monomer, allyl diglycol carbonate. The directly formed recoil track density recorded within the CR-39 foil volume is selectively boosted in track density by utilizing the $^{6}Li(n, \alpha)^{3}H$ reaction to shape the overall damage-track response to one of approximate dose-equivalence. Specially designed neutron "filters" made of Cd and In foils are utilized in conjunction with the $^{6}Li(n, \alpha)^{3}H$ 1/v cross-section variation with energy between 1 eV and 1 MeV to help approximate the rem-response of the system. The dosimeter design chosen in this research is shown in Figure 30 and its sensitivity response as a function of neutron energy is compared to the ICRP dose-equivalent curve in Figure 33. The directional dependence of the intermediate neutron dosimeter is displayed in Figure 35 and is comparable to or slightly better than that exhibited by other damage-track dosimeters using nonfissile charged particle radiators.

The selectively filtered intermediate neutron dosimeter designed in this research offers some advantages over other neutron measurement systems. These advantages include:

(1) a range suitable for both normal and accident applications, i.e., 0.001 to 1000 rem, by adjusting the ^{6}Li content of the ^{6}LiF-Teflon radiator;

(2) an insensitivity to other radiation, e.g., photons and beta particles;

(3) a reasonable spatial response;

(4) no post-irradiation fading;

(5) The dosimeter assembly is rugged, inexpensive, and the parts are readily available:

(6) CR-39 thin foils are inexpensive to process and easy to evaluate once processed;

(7) they are easy to wear and simple to use;

(8) they are capable of being used for dosimetry intercomparisons by mail;

(9) they cause negligible perturbation of the measured field;

(10) they offer an approximate rem-response and are useable in the 1 eV to 1 MeV neutron energy region;

(11) when used in conjunction with the fast (> 1 MeV) neutron damage-track dosimeter (Sohrabi, 1975) and the thermal neutron dosimeter (Su, 1979), they provide an approximate dose-equivalent response to neutrons of thermal to 20 MeV energies.

Much has been written about the variation in etch rate, damage-track response, and background response due to differences in the CR-39 polymer

foils obtained from different vendors, batchs, and even sheets (Durrani et al., 1981). During the course of this research, we have developed a procedure that has effectively eliminated most of these response variations. The most sensitive, lowest background material discovered during this investigation is the 400 μm thick CR-39 in the form of sheets which are protected on each side by 70 μm thick polyethylene film. Sheets, about 1 m^2 in size, are available from American Acrylics and Plastics, Stratford, Connecticut. Approximately 1300, 2.5 cm x 2.5 cm dosimeter foils canbe cut froma single sheet. This results in a cost per dosimeter, more expensive than the bisphenol polycarbonate, still quite inexpensive when compared to the cost of a single NTA emulsion.

Thickness variations within the same sheet of CR-39 were found to be as high as ± 40 percent in all of the CR-39 tested. We found that any response variations found due to thickness differences could be controlled by measuring the thickness of each 2.5 cm x 2.5 cm CR-39 foil, tagging the foils with the thickness, and using only those foils that were within ± 25 percent of a predetermined mean. This is a tedious exercise and effectively increases the cost per dosimeter; however, until CR-39 is manufactured under stricter tolerances, such additional care is required. Reproducible results within ± 10 percent were typically achieved using the criteria mentioned above.

The etchant resistant nature of the thermoset polymer, CR-39, compared to previously investigated thermoplastics such as bisphenol-A polycarbonate, necessitates the utilization and optimization of new etching procedures. During the course of this research the optimum parameters of a

combined chemical-electrochemical etching technique were determined as applied to neutron-induced alpha particle and recoil nuclei damage-tracks registered in thin CR-39 foils. A chemical etchant of 45 percent KOH at 60°C was found to allow the optimum blend of low background response and low etch product build-up on the foil surface. A chemical etch duration of two hours was chosen to etch both the neutron-induced alpha particle tracks on the foil surface and the neutron-induced recoil nuclei tracks within its volume to the dimensions most conducive to the electrochemical treeing process. The electrical treeing process and the resultant large damage-track amplification necessary for dosimetric evaluations were obtained by etching electrochemically the chemically-etched CR-39 foils in 45 percent KOH at 25°C, 2 kHz, and 23 kV/cm for two and one-half hours. The chemical etchant temperature of 60°C used in most of this research was 15°C lower than that which would have allowed the highest electrical treeing efficiency (see Figure 9). The 60°C etchant temperature was chosen because of the large build-up of the etch product, PAA, on the detector foil surface at higher temperatures. If a method could be devised to either eliminate PAA build-up on the CR-39, to filter it out of the etchant as it is produced, or to increase its solubility in the etchant, the electrochemical track revelation efficiency could be improved by about 50 percent.

When bisphenol-A polycarbonate is the damage-track recording polymer, addition of an organic solvent to the alkali hydroxide etchant bath significantly increases the electrtochemical etching sensitivity, efficiency, and etch rate found (Hassib et al., 1977; Somgyi, 1977; Su, 1979; Kumamoto, 1982). For CR-39 polymer, no enhancement, and in some cases inhibition, of damage-track revelation was found in this research when several solvents were added to the 45 percent KOH electrochemical etchant. This is thought

to be due to the thermoset nature of CR-39, where the smallest part of the polymer can no longer be thought of as being a long chain molecule, but is instead a three-dimensional matrix of intensely cross-linked polymer molecules. The etch product, poly allyl alcohol, is thought to inhibit the solvation action of the solvent by building up on the detector foil surface. However, another etch product, 2,2'-dioxyethanol, has been found to increase the etch rate of CR-39 when it is added to the alkali hydroxide etcant. Unfortunately, 2,2'-dioxyethanol suffers from being unstable in hot alkali hydroxide solutions. Future work to shorten CR-39 etching durations might be directed toward finding a molecule which gives the same etch enhancing behavior as 2,2'-dioxyethanol but is stable in hot alkali solutions.

The intermediate neutron dosimeter as decribed in this research primarily utilizes neutron-induced radiation alpha particles and recoil protons to form damage-track densities in CR-39 foils which are then related to dose-equivalence. Therefore, an investigation of the proton energy threshold for track formation and the etch of alpha energy as a function of chemical etching time on the sensitivity of damage-track revelation in CR-39 was completed. The proton energy threshold for track formation was found to be approximately 100 keV and corresponds well with the lowest energy neutrons measured by damage-tracks in CR-39.

The investigation into alpha damage-track sensitivty in CR-39 as a function of alpha energy and chemical etch duration has led to at least two interesting possibilities. The first is that CR-39 foils could be used as simple alpha spectrometers by calibrating the alpha energy track revelation sensitivity as a function of energy (as shown in Figure 24). The second

possibility is more germane to this research. It was found that higher energy alpha particle damage-tracks require longer chemical etch times to achieve the etch pit size and shape most condusive for electrochemical etching. Thus, since the alpha particle energies generate from the neutron-induced $^{6}Li(n, \alpha)^{3}H$ reaction by neutrons below 10 keV are lower than those generated by neutrons above 10 keV, the low neutron energy over-response seen in the intermediate neutron dosimeter might be reduced by adjusting the chemical etch parameters so that the alpha damage-tracks induced by $>$ 10 keV neutrons are preferentially shaped into the optimum etch pit dimensions for electric treeing. The alpha particle damage-tracks induced by $<$ 10 keV neutrons would also be chemically etched, of course, but they would be over-etched due to the chemical etch duration-alpha energy relationship and would not allow efficient electrochemical etching.

The intermediate neutron dosimeter was applied to dose-equivalent measurement in several neutron energy spectra during this research. The dosimeter has been shown to measure reliably the neutron dose-equvalent in a neutron spectrum rich in low-energy ($<$10 keV) neutrons to within a factor of two and in an energy spectrum with few neutrons below 10 keV to within $\pm$12 percent. The decreased dosimeter accuracy when measuring fluences of low-energy neutrons is due to an over-response of the dosimeter due to the rapid increase of $^{6}Li(n,\alpha)^{3}H$ cross-section and the constant quality factor below 10 keV. This measured over-response may possibly be decreased by adjusting the chemical etch parameters to preferentially etch only those alpha damage-tracks which have been induced by neutrons with energies above 10 keV. The dosimeter measured dose-equivalent to within $\pm$ 20 percent in the 8 MeV and 17 MeV average neutron energy spectra generated by the NASA

cyclotron. Although the dosimeter was designed to be used primarily in the neutron region between 1 eV and 1 MeV, its response in higher energy neutron spectra indicates that is is useable up to 17 MeV energies. However, above $\sim$ 4 MeV, the dosimeter does not provide as good a rem-response as bisphenol-A polycarbonate.

Perhaps the aspect of this investigation, that exhibits the advantages realized with this detection system most fully is that undertaken to determine the neutron contamination generated outside and within a heterogeneous phantom exposed to the primary x-ray beam of several high-energy electron accelerators used in medical radiotherapy. The dosimeter was required to measure neutrons contained within an intense, high energy x-ray beam. The dosimeter assembly was subjected to immersion in a tissue-equivalent liquid that dissolved the glue of the tape holding the dosimeter together and yet still gave the same track density response to within $\pm$ 10 percent of that of a dosimeter contained in a water-tight case.

The intermediate neutron dosimeter was used in conjunction with other approximately rem-responding damage-track dosimeters designed by Sohrabi (1975) and Su (1979) to measure the thermal to 20 MeV neutron dose-equivalent from neutrons generated in the accelertor x-ray beams by interactions with not only high-Z accelerator components but also the elemental constituents found within the patient. This heretofore unachievable investigation was realized because of the unique advantages of these damage-track dosimeters over other conventional methods to measure the neutron flux in photon fields. Some of the advantages obtained with these damage-track dosimeters are:

(1) little or no perturbation of the radiation field as seen with a remmeter or moderated neutron activation detector,

(2) response over the entire neutron energy range contained in the spectrum,

(3) measurement of an approximate dose-equivalent rather than just neutron fluence,

(4) ability to make measurements at interfaces,

(5) little or no response to low LET radiations, such a photons or electrons.

As can be seen in Table 5, the additional dose-equivalent deposited due to accelerator component-produced photoneutrons measured by the damage-track dosimeters is considerably higher than that suggested by techniques measuring only the neutron fluence. The total accelerator component plus phantom-produced additonal photoneutron dose deposited within the patient treatment volume increases from 0.24 percent of the x-ray dose found in the 18 MV Clinac-20 beam to 3.26 percent of the x-ray dose found in the 45 MV x-ray beam of the Brown-Boveri 45 MeV betatran. These mesurements offer the first experimental confirmation of the magnitude of additional dose deposited in the patient treatment volume due to photoneutron generation during high-energy acccelerator x-ray therapy as calculated by Laughlin (1979).

The investigation of photoneutron contamination in the primary beam during high energy accelerator x-ray therapy has shown, by utilizing the unique characteristics of rem-responding damage-track dosimeters, that the additional dose-equivalent deposited on the patient surface due to accelerator component produced photoneutrons is somewhat higher than that suggested by other neutron measurement techniques. The study has confirmed that photoneutron production does not increase appreciably in high-Z accelerator components exposed to an x-ray beam generated by electrons with

energy greater than 25 MeV. It has also been confirmed that the constituent elements of human tissue act as photoneutron generators during high-energy x-ray therapy and that most of these photoneutrons are produced when the x-ray beam is produced by electrons with energies greater than 20 MeV. The study has been the first to measure the total additional dose deposited within the patient treatment volume due to both accelerator component and tissue produced photoneutrons generated by the high-energy therapy x-ray bema. The accuracy of the measurements is substantiated by theory.

There is little that can be done to reduce the photoneutron dose generated within the patient treatment volume during therapy. This study has shown that up to 50 rem (see Table 6) of photoneutrons can be delivered to critical organs located 6 cm perpendicularly outside the patient treatment volume. The medical physicist and radiation therapist should keep this in mind when positioning the x-ray treatment fields on the patient. An example of a situation where this caution is applicable would be the lower mantle field irradiation treatment field positioning on a young man suffering from Hodgkin's disease. Even if the x-ray treatment field could not be adjusted to eliminate the possible photoneutron dose to the gonads, the patient should be advised to avoid procreation for a suitable period of time.

The intermediate neutron dosimeter designed in this research provides a method of measuring neutron dose-equivalent in the energy range between 1 eV and 1 MeV where polycarbonate detectors cannot be used due to their insensitivity. However, the over-response of the intermediate neutron dosimeter to neutrons with energies below 10 keV is a problem that has yet to be solved. As mentioned above, one possibility might be to "fine-tune" the chemical etch parameters so that the greater number of low energy

neutron-induced alpha tracks could be preferentially discriminated out. Another possible solution might be to space the radiator disc at some calibrated distance away from the CR-39 detector so that only the higher energy alpha particle could reach the foil surface.

A similar, but less pronounced, problem found with the intermediate neutron dosimeter is its under-response to neutrons with energies above $\sim$ 4 MeV. Possibly this problem could be eliminated by using an additional particle radiator that has an (n,α) or (n,p) cross-section threshold in this energy region. For example, ^{32}S could be mixed with the ^{6}Li to form a particle radiator disc that could be used in conjunction with CR-39 foil to form a detector which approximates more closely a rem-response at higher neutron energies.

The etching times necessary for damage-track revelation in CR-39 have yet to be satisfactorily shortened. The combined etch procedure, used in this research, lasted for four and one-half hours. Thus, future work should be devoted to decreasing this tedious process. One of the reasons for the long etching time is associated with build-up of the etch product, PAA, on the CR-39 dectector surface. Both the etch time and sensitivity of CR-39 dosimeters could be improved if a method could be devised that would eliminate this build-up completely.

The intermediate neutron dosimeter has been applied to dose-equivalent measurements in several situations during this research. However, there is no reason why it cannot be applied to any other neutron dosimetry measurement within its energy capability. Because of the large number of individuals working around power reactors, special consideration should be given to providing more information on the dosimeter response to neutron spectra typically found in power reactor environments.

4. FAST (> 1 MeV) NEUTRON DOSIMETRY

(Summary of Sohrabi (1975))

Neutron dosimetry is a problem of concern in many areas of health physics and radiotherapy. Considering the present state-of-the-art of fast neutron dosimetry, new developments and improvements in this area seemd desirable and justified a detailed experimental investigation. Among the numerous methods being studied are various track-etch methods in which the damage regions left by the passage of heavy charged particles in appropriate insulators are enlarged by subsequent etching procedures to make them more readily visible.

An electrochemical etching method for the amplification of fast-neutron-induced recoil particle tracks in polymers was investigated. The technique gave superior results oer those obtained by conventional etching methods especially when polycarbonate foils were used for recoil particle track amplification.

Elecrochemical etching systems capable of multi-foil processing were designed and constructed to demonstrate the feasibility of the technique for large-scale neutron dosimetry. Electrochemical etching parameters were studied including the nature or type of the polymer foil used, foil thickness and its effect on etching time, the applied voltage and its frequency, the chemical composition, concentration, and temperature of the etchant, distance and angle between the electrodes, and the type of particles such as recoil particles including protons. Recoil particle track density, mean track diameter, and optical density as functions of the mentioned effect on parameters were determined. Each parameter was found to have a distinct effect on the etching results in terms of the measured responses.

Several new characteristics of this fast neutron dosimetry method were studied, especially for personnel dosimetry using various radiation sources such as nuclear reactors, medical cyclotrons, and isotopic neutron sources. The dose range, neutron energy dependence, directional response, fading characteristics, neutron threshold energy, etc. were investigated.

The neutron dosimetry technique under investigation was relatively insensitive to high doses of x- and gamma rays (e.g. 10^4 rad); it had dose-equivalent response (rem) and it showed high spatial resolution. It was used for measurement of dose-equivalent of fast neutron contamination in high energy x-ray beams from medical betatrons and some results are reported here. Also some studies were conducted to compare the response of this dosimeter as a function of depth in bone-equivalent fluid and plastic and tissue-equivalent fluid inside an elliptical phantom. Both bone-equivalent materials performed equally well for fission neutrons; however, bone-equivalent fluid provides more flexibility for heterogeneity effect studies. Some results on the neutron dose distributions near bone-tissue and air-tissue interfacers inside a cubical phantom are reported also.

A neutron dosimetry technique is presented in which sensitivity and track diameter can be controlled by the parameters governing the electrochemical etching results. This neutron dosimetry approach provides simplicity, flexibility, and feasibility for large-scale neutron dosimetry. It has promising applications, especially for fast neutron personnel dosimetry since it provides many advantages over proton track registration in nuclear track emulsions and fission fragment registration techniques. As another approach, spark counting of recoil particle tracks in conventionally-etched thin polycarbonate foils (six μm) was also investigated, and did not prove to be as feasible as the above approach.

5. THERMAL NEUTRON DOSIMETRY

(Summary of Su (1979))

In the area of health physics and radiotherapy, neutron dosimetry has presented certain special difficulties both from the standpoint of theory as well as techniques and instruments. Registration of α-tracks and fast-neutron-induced recoil tracks by the electrochemical etching technique as applied to sensitive polycarbonate foils has provided a simple, sensitive, and inexpensive means of neutron dosimetry.

The track geometry during the electrochemical etching was studied to evaluate the bulk and track etching rates. Two optical devices--a transparency projector and a microfiche reader--were adapted to facilitate counting of the tracks appearing on foils. A Poison distribution was introduced for the determination of the foil track counting statistics. Background track reduction was studied by annealing the foils at different temperatures.

Experimental studies on the optimization of electrochemical etching parameters to obtain maximum sensitivity and to minimize etching time are described. Track density, mean track diameter, and optical density as a function of applied voltage, frequency, and etchant concentration were determined. It was discovered in these studies that an etching solution mixture of ethyl alcohol and 45% KOH aqueous solution offered considerable improvement over previous procedures.

Monoenergetic neutrons of $\sim$4.3 MeV,$\sim$ 14 MeV, and 22 MeV were produced by the reactions $^{7}Li(p,n)^{7}Be$, $^{3}H(d,n)^{4}He$ and $^{9}Be(d,n)^{10}B$, respectively, to

determine the detection efficiency for recoil particle tracks as a function of fast neutron energy. Results were compared with other studies using other sources and passive etching methods.

The efficiency of alpha track registration was determined by exposing foils a various distances from a 2.0 μCi ^{239}Pu source in air. Relative frequencies of track diameter distributions of diferrent alpha energies for different etching times under standard electrochemical etching conditions (1000 V, 2 kHz, 22°C, etching solution of 50% ethyl alcohol and 50% of 45% KOH) were plotted in histogram fashion to explain the track occurrences.

Lithium flouride radiators were made into tablets containing 0.07, 15.95, 31.90, 47.85, 63.77%, 80.85%, and 95.62% Li-6 abundances to produce the $^{6}Li\ (n,\alpha)^{3}H$ reaction for the thermal neutron measurement by the electrochemical etching system. Track density measurements as a function of ^{6}Li abundance in the radiators and of the duration of thermal neutron irradiation have been obtained.

The investigation was also extended to apply this thermal neutron dosimeter to the measurement of epithermal neutrons by utilizing the thermalizing properties of the body. Two lithium fluoride tablets containing 80.85% ^{6}Li in the first layer were put into a polyethylene holder, used as radiator, to respond to thermal albedo neutrons. Information about the neutron field can be obtained by using such a dosimeter.

6. ALPHA PARTICLE DOSIMETRY

(Summary of Stillwagon (1978))

The dosimetry of internally deposited alpha emitters, such as ^{239}Pu, has been of interest for many years as a means to determine directly such quantitites as maximum permissible body burden (MPBB) instead of the peresent practice of setting these values based upon comparison with ^{226}Ra. A new technique that will yield this dosimetry information directly by experimental measurement is a desirable task to perform and would provide data sorely needed by health physicists.

A procedure involving the electrochemical etching of polycarbonate foils to amplify the damage tracks produced by the alpha particles emitted by ^{239}Pu deposited in the skeletons of dogs and man was investigated to examine its feasibility for this application. This electrochemical etching technique was used to provide dose measurements and has been shown to be feasible for bone dosimetry applications of internally deposited alpha emitters. The technique delineated is general in nature and could be used for the dosimetry of other internally deposited alpha emitters, even in tissues other than osseous tissue.

During examination of the feasibility of the electrochemical etching system, several parameters were examined prior to the bone dosimetry application since the dosimetry system had not been calibrated for alpha particle dosimetry prior to this time. Several foil reading techniques were examined such as the transparency projector and microfiche reader. The compound microscope operated in the phase contrast mode was used for bone dosimetry.

Background reduction studies resulted in a background of 2.0 tracks/cm^2 of foil surface. Optimization of the electrochemical etching of polycarbonate foils, considering background and sensitivity, indicated 800 V, 2 kHz, 45% KOH etchant solution and four hours etching time provided low background and reasonable sensitivity. Sensitivity as a function of etching time and waiting time (time between irradiation and etching) were also examined. Efficiency of alpha particle track production as a function of energy was determined. A Bragg curve was achievable and the efficiency obtained at the peak of the Bragg curve was obtained when the energy of the monoenergetic alpha particle was lowered by the injection of 27-28 μ m of polycarbonate absorber between the source and detector, giving an efficiency of 1.0×10^{-3}%. A device called the vacuum-sealed alpha calibrator was designed for this purpose and housed a 2.0 μCi ^{239}Pu source as well as either polycarbonate foils or a surface barrier detector. Track diameter as a function of etching studies resulted in the discovery of two categories of track diameters appearing on foils irradiated by alpha particles and etched electrochemically. This effect was quantified as a function of incident alpha energy and a proposal offered to explain the effect. Reproducibility studies yielded an error of $\pm$ 15% in the dosimetry studies. These studies included foils etched weeks apart with different 45% KOH etchant solutions and different energies of alpha particles incident on the foils.

The bone dosimetry studies utilized undecalcified sections of beagle dog bones and decalcified human bone sections. The procedure used was as follows: (1) Polycarbonate foils were pressed tightly against the bone samples plus infinitely thick calibration sources and then etched electrochemically after appropriate exposure times. (2) Counting was

performed by randomly scanning the foils and counting tracks in a square 120 μm on each side. (3) Dose in rads/year was presented in two sets, one included the scans resulting in zero scans, D_o, the other did not, D_w. Efficiencies obtained from the infinitely thick calibration sources ranged from 2.22×10^{-3}% to 0.38%. Doses ranged from 16.7 rads/yr to 39580 rads/yr for D_o and 440 rads/yr to 317900 rads/yr for D_w. A factor was found that could be multiplied by the experimentally determined dose to make it equal to the ICRP permissible limit of 0.3 rad/yr (15 rem/yr). This value was them multiplied by the known skeletal burden to find an experimental maximum permissible skeletal burden for each bone section taking into account the mass difference of the dog and human skeleton. The average of these experimental maximum permissible skeletal burdens was one half the present ICRP value of 0.036 μCi, the maximum and minimum values were four time greater and 700 times less than the ICRP standard, respectively.

BIBLIOGRAPHY

Adams, J. H., Jr., "Automatic Track Measurements in CR-39," Nucl. Tracks 4, 67 (1980)

Aframian, A. and S. A. Durrani, "Semiautomatic Evaluation of Fast Neutron Fluences In Plastic SSNTDs Using a Double-Beam Microdensitometer," Solid State Nuclear Track Detectors, Vol. I, Proc. 9th Intl. Conf., Neuherberg/Munchen (1979)

Al-Najjar, S. A. R. and S. A. Durrani, "Electrochemical Etching of the CR-39 Plastic," Nucl. Instr. Meth. 173, 97 (1980)

Al-Najjar, S. A. R., R. K. Bull, S A. Durrani, "Electrochemical Etching of Al-Najjar, R-39 Plastic," Nucl. Tracks 3, 169 (1979)

Al-Najjar, S. A. R., M. Balacazar-Garcia, S. A. Durrani, "A Multi-Detector Electrochemical Etching and Automatic Scanning System," Nucl. Tracks 2, 215 (1968)

Anderson, M. E., "Increases in Neutron Yields of PuBe(α,n) Sources," Nucl. Applic.4, (1968)

Attix, F. H., W. C. Roesch, E. Tochilin, Radiation Dosimetry, Vol. I, II, III, Academic Press, New York City (1966, 1968, 1969)

Auxier, J. A., W. S. Snyder, T. D. Jones, "Neutron Interactions and Penetrations in Tissue," Chap. 6 in Radiation Dosimetry, Vol, I, Academic Press, New York City (1968)

Azimz-Garakani, D. and J. G. Williams, "Automatic Fission Track Counting Using Quantimet 720," Solid State Nuclear Track Detectors, Vol. I, Proc. 9th Intl. Conf., Neuherberg/Munchen (1979)

Barendsen, G. W., "Relative Biological Effectiveness (RBE)" in Encyclopedia of X-Rays and Gamma Rays, G. L. Clark, Reinhold, New York City (1963)

Becker, K. and M. Abd-El Razek, "Automatic Spark Counting of Fast Neutron-Induced Recoil-Particle Tracks in Polymer Foils," Nucl. Instr. Meth. 124, 557 (1975)

Becker, K., Solid State Dosimetry, CRC Press, Cleveland (1973)

Becker, K. "Neutron Personnel Dosimetry by Non-Photographic Nuclear Track Registration," Proc. ENEA Symp. Rad. Dose Meas., Stockholm (1967)

Benton, E. V. and R. P. Henke, "On Charged Particle Tracks in Cellulose Nitrate and Lexan," Dept. Physics, University of San Francisco, TR #19 (1972)

Benton, E. V., "A Study of Charged Particle Tracks in Cellulose Nitrate," USNRDL-TR-68-14 (1968)

Benton, E. V., "A Study of Charged Particle Tracks in Cellulose Nitrate," USNRDL-TR-68-14 (1968)

Benton, E. V., "Charged Particle Tracks in Polymers No. 4: Criterion for Track Registration," USNRDL-TR-67-80, Sana Francisco (1967)

Bewley, D. K., "Calculated Distribution of Fast Neutrons," Radiat. Res. 34, 437 (1968)

Blanford, G. E., Jr., R. M. Walker, J. P. Wefel, "Track Etching Parameters for Plastics," Radiat. Eff. 3, 267 (1970)

Bonfiglioli, G., A. Ferro, A. Mojoni, "Electron Microscope Investigation of the Nature of Tracks of Fission Products in Mica," J. Appl. Phys. 32 (1962)

Boyette, R. H., D. R. Johnson, K. Becker, "Some Studies of the Chemical Damage Mechanism Along Charged Particle Tracks in Polymers," Radiat. Res. 3, 1 (1970)

Briden, D. W. and R. D. Ice, "Neutron Measurements in Medical Betatron X-Ray Beams," 17th Annual Meeting of Health Physics Society, Las Vegas, 124 (1972)

Broerse, J. J. and G. W. Barendsen, "Recovery of Cultured Cells After Fast Neutron Irradiation," Intl. J. Rad. Biol. 15, 335 (1969)

BNL, Neutron Cross-Sections, BNL-325, Brookhaven Nat'l Lab (1953)

Burris, W. R. and V. V. Verbinski, "Fast Neutron Spectroscopy with Thick Organic Scintillators," Nucl. Instr. Meth. 153, 457 (1978)

Cartwright, B. G., E. K. Shirk, P. B. Price, "A Nuclear Track Recording Polymer of Unique Sensitivity and Resolution," Nucl. Instr. Meth. 153, 457 (1978)

Cassou, R. M. and E. V. Benton, "Properties and Applications of CR-39 Polymeric Nuclear Track Detectors," Nucl. Tracks 2, 173 (1978)

Cross, W. G. and H. Ing, "The Uses of ^{237}Np in Personnel Dosimetry for Fast Neutrons," Health Phys. 28, 511 (1975)

Cross, W. G. and L. Tommasino, "Electrical Detection of Fission Fragment Tracks for Fast Neutron Dosimetry," Health Phys. 15, 196 (1968)

DeSorbo, W., "UV Effects and Aging Effects on Etching Characteristics of Fission Tracks in Polycarbonate Film," Nucl. Tracks 3, 13 (1979)

DeSorbo, W. and J. S. Humphrey, "Studies of Environmental Effects Upon Track Etching Rates in Charged Particle Irradiated Polycarbonate Film," Radiat. Eff. 3, 281 (1970)

Diamond, W. T., A. E. Litherland, J. Goldenberg, H. L. Pai, A. H. Chung, Intl. Conf. on Photonucl. Reactions and Appl., Asilomar, CA (1973)

Dorschell, B. and V. Schuricht, "Calibration of Personnel Neutron Dosimetrs for Use in Different Neutron Fields," Intl. Sump. Adv. Rad. Prot., Stockholm IAEA (1979)

Durrani, S. and S. A. R. Al-Najjar, "Electrochemical Etching of CR-39 Plastic," Nucl. Instr. Meth. 173, 97 (1980)

Dutrannois, J., Proc. Intl. Con. Prot. Against Accel. and Space Rad., CERN-71-16, Vol. I, Cern, Geneva (1971)

Edmonds, E. A. and S. A. Durrani, "Relationship Between Thermnoluminescence, Radiation-Induced Electron Spin Resonance, and Track Etching of Lexan Polycarbonate," Nucl. Tracks 3, 3 (1979)

Eichholz, G. G. and J. W. Poston, Principles of Nuclear Radiation Detection, Ann Arbor Sciences Publishers (1980)

Eichhorn, R. M., "Treeing in Solid Extruded Electrical Insulators," IEEE Trans. Electr. Insul. EI-12, 2 (1977)

Eisen, Y., Z. Karpinowitz, A. Govron, A. Tol, Y. Itzkin, T. Schlesinger, "Development of a Polycarbonate Fast Neutron Dosimeter and Comparison with Conventional Emulsion Dosimetry," Health Phys. 38, 497 (1980)

Enge, W., R. Grabisch, R. Beaujean, K. P. Bartholoma, "The Mechanism of Etching Plastic Track Detectors," Proc. 8th Intl. Symp. Nucl. Photo, and Solid State Track Det., Bucharest (1972)

Fairman, L., Conf. Ser. Instr. Phys., 131 (1978)

Fisher, H. L., Jr. and W. S. Snyder, #ORNL Report, ORNL-4168, 245 (1968)

Fitzgerald, J. J., Applied Radiation Protection and Control, Vol. I, II, Gordon and Breach, New York City (1967)

Fleischer, R. L., P. B. Price, R. M. Walker, Nuclear Tracks in Solids, University of California Press, Berkeley (1975)

Fleischer, R. L. and H. R. Hart, Jr. "Fission Track Dating, Tracks and Problems," Rep. #70-C-328, General Electric Co., Schenectady, NY (197)

Fleischer, R. L., P. B. Price, R. M. Walker, E. L. Hubbard, "Criterion for Registration in Dielectric Track Detectors," Phys. Rev. 156, 353 (1967)

Fleischer, R. L., P. B. Price, R., M. Walker, "Tracks of Charged Particles in Solids,: Science 149, 333 (1965)

Fleischer, R. L., P. B. Price, R. M. Walker, "Track Registration in Various Solid State Nuclear Track Detectors," Phys. Rev. 133A, 1443 (1964)

Fleischer, R. L. and P. B. Price, "Tracks of Charged Particles in High Polymers," Science 140, 1221 (1963)

Gammage, R. B. and A. Chowdhury, "Electrochemical Etching of Fast Neutron-Induced Recoil Tracks in Cellulose Triacetate," Nucl. Tracks 4, 41 (1980)

Garry, S. M., P. S. Stansbury, J. W. Poston, "Measure of Absorbed Dose for Photon Sources Distributed Uniformly in Various Organs of Heterogeneous Phantom," USAEC Rep. ORNL-TM-4411 (1974)

Gibson, J. A. B., "A Neutron Dosimetry System in Use in Processing Plants," Intl. Symp. Adv., Rad. Prot. Monit., Stockholm (1978)

Gold, R. , R. J. Armani, G. K. Rusch, Th. D. Rhule, "Fast Neutron Personnel Dosimetry with Solid State Track Detectors," Nucl. Instr. Meth. 118, 383 (1974)

Goodman, L. J., "A Modified Tissue-Equivalent Liquid," Health Physics 16, 763 (1969)

Griffith, R. V. and D. E. Hankins, "A Systematic Approach to Personnel Neutron Monitoring," 5th Intl. Cong. IRPA, Jerusalem, 237 (1980)

Griffith, R. V. and J. C. Fisher, "Development of a Combined Albedo Electrochemical Track Etch Personnel Neutron Dosimeter," Rpt. UCRL-50007-76-2 (1976)

Griffith, R. V., Lawrence Livermore Lab. Rept. UCRL-51, 362 (1973)

Groenevald, K. O., E. Schopper, S. Schuman, "Atomic Displacement Effects from Heavy Ion-Induced Coulomb Explosions," Proc. 11th Intl. Confl SSNTD, Bristol, England (1981)

Gruhn, T. A., W. K. Li, E. V. Benon, R. M. Cassou, C. S. Johnson, "Etching Mechanism and Behavior of Polycarbonates in Hydroxide Solutions: Lexan and CR-39," Proc. 10th Intl. Conf. on SSNTD, Lyon, France (1980)

Gruhn, T. A., E. V. Benton, C. H. Andrus, "The Etching of Cellulose Nitrate Plastic," Nucl. Instr. Meth. 119, 131 (1974)

Gupton, E. D. and D. M. Davis, "Health Physics Instruments," Chap. 15 in Principles of Radiation Protection, K. Z. Morgan and J. E. Turner, Editors; Robert E. Kriehger Publ. Co., Huntington, NY (1973)

Hankins, D. E., "Progress in Personnel Neutron Dosimetry," Prod. 3rd Intl. Cong. IRPA, Washington, DC (1973)

Harvey, F. R. and S. Beynon, Proc. First Symp. Neut. Dosimetry in Biology and Medicine, Neuherberg/Munchen, Germany, 955 (1972)

Hassib, G. M., J. W. N. Tuyn, J. Dutrannois, "On the Electrochemical Etching of Neutron Induced Tracks in Plastics," Solid State Nuclear Track Detectors Vol. II, Proc. 9th Intl. Conf., Neuherberg/Munchen, Germany (1979)

Hassib, G. M., J. W. N. Tuyn, J. Dutrannois, Nucl. Instr. Meth. 147, 377 (1977)

Hilderbrand, D. and E. V. Benton, "The Chemical Etching Behavior of Cellulose Nitrate," Nucli. Tracks 4, 77 (1980)

Hildebrand, D., "Some Etching Aspects of Cellulose Nitrate," Nucl. Instr. Meth., 154, 19 (1977)

Hoy, J. E., "An Albedo-Type Personnel Neutron Dosimeter," Health Phys. 25, 385 (1972)

Hurst, G. S. and R. H. Ritchie, "Fast Neutron Dosimetry," Radiology 60, 864 (1953)

ICRP, "Data for Protection Against Ionizing Radiation from External Sources," Report #21, ICRP (1973)

ICRU, Neutron Dosimetry for Biology and Medicine, Report #26, ICRU (1977)

ICRU, Radiation Quantities and Units, Report #19, ICRU (1971)

ICRU, Neutron Fluence, Neutron Spectra, and Kerma, Report #13, ICRU (1968)

ICRU, Report 10C, NBS Handbook #85 (1964)

Ing, H. and W. G. Cross, "A Criticality Neutron Dosimeter Using $^{103}Rh(n,n)-^{103m}Rh$," Health Phys. 25, 291 (1973)

Johnson, D. R., "Mechanism and Application of Nuclear Track Formation in Polymers," PhD Thesis, University of Kansas (1970)

Kaplan, I., Nuclear Physics, Adison-Wesley Publ. Co. (1964)

Katz, R., "Track Structure Theory in Radiobiology and Radiation Detection," Solid State Nuclear Track Detectors Vol. I, Proc. 9th Intl. Conf., Neuherberg/Munchen, Germany (1979)

Katz, R. and E. J. Kobetich, "Energy Deposition by Electron Beams and Delta Rays," Phys. Rev. 170, 391 (1968)

Kawai, H. T. Koga, H. Moroshima, T. Niwa, Y. Nishiwaki, "Studies on the Characteristics of Nuclear Track Spark Counting for Neutron Monitoring," Intl. Symp. Adv. Rad. Prot. Mon., Stockholm, IAEA (1979)

Kenawy, M. A., M. El-Fiki, S. El-Konsol, M. A. Fadel, A. M. Basha, "Detection of Fast and Slow Neutrons by Etch Pit Method of Nuclear Track Registration in Plastics," Solid State Nuclear Track Detectors Vol. II, Proc. 9th Intl. Conf., Neuherberg/Munchen, Germany (1979)

Khan, H. A., R. A. Akbar, G. Hussain, "The Development of Plastic Track Detector," Solid State Nuclear Track Detectors Vol. II, Proc. 9th Intl. Conf., Neuherberg/Munchen, Germany (1979)

Kahn, H. A., "The Effects of Pre-Irradiation Annealing on Track Development Properties of Solid State Nuclear Track Detectors," Nucl. Instr. Meth. 125, 419 (1975)

Kahn, H. A., "An Important Precaution in the Etching of Solid State Nuclear Track Detectors," Nucl. Instr., Meth. 109, 515 (1973)

Khan, H. A. and S. A. Durrani, "Efficiency Calibration of Solid State Nuclear Track Detectors," Nucl. Instr., Meth. 98, 229 (1972a)

Khan, H. A. and S. A. Durrani, "Electronic Counting and Projection of Etched Tracks in Solid State Nuclear Track Detectors," Nucl. Instr., Meth., 101, 583 (1972b)

Kinoshita, K. and P. B. Price, "Method for Producing Thin Sheets of Proton Sensitive CR-39 Plastic Track Detectors," Rev. Sci. Inst. 51, 32 (1980)

Kruger, H., G. Trumbragel, R. Metzner, H. Koch, "Fast Neutron Dosimetry With Silicon Diodes," Proc Symp. Neut. Mon. Rad. Prot. Purposes,, Vienna, IAEA (1973)

Kumanoto, Y., "Measurement of Low Neutron Fluences with Polycarbonate Foils, Electrochemically Etched with Methyl Alcohol-KOH Solution," Health Physics 42, 497 (1982)

Laughlin, J. S., A. Reid, L. Zeitz, J. Ding, "Unwanted Neutron Contamination to Megavoltage X-Ray and Electron Therapy," Proc. Conf. Neutrons from Elec. Accel..., NBS 554, 1 (1979)

Levinger, J. S., Nuclear Photo-Disintegration, Oxford University Press (1960)

Lindhard, J., V. Nielson, M. Scharff, P. U. Thomsen, "Notes on Atomic Collisions," AECL-2059 (1963)

Mason, J. H., "Dielectric Breakdown in Solid Insulators," Prog. Dielectrics 1, 1 (1959)

Maurette, M., "Track Formation Mechanism in Minerals,' Radiat. Eff. 3, 149 (1970)

McCall, R. C. and W. P. Swanson, "Neutron Sources and Their Characteristics," Proc. Conf. Neutrons from Elec. Accel. NBS 554, 1 (1979)

McGinley, P. H. and M. Sohrabi, "Neutron Contamination in the Primary Beam," Proc. Conf. on Neut. from Elec. Med. Accel., NBS Spec. Publ. 554, 99 (1979)

Morgan, K. Z. and J. E. Turner, Principles of Radiation Protection, Robt. E. Krieger Publ. Co., Huntington, NY (1973)

Morgan, K. Z., "Instrumentation in the Field of Health Physics," Proc. Inst. of Radio. Eng. 37, No. 1 (1949)

Nagarajan, P. S. and P. Krishnan, "Neutron Personnel Monitoring-Correction Factors and a Suggested Device for Measuring Intermediate Energy Spectra," Health Phys. 17, 323 (1969)

NCRP, Protection Against Neutron Irradiation, Report #38 (1972)

NCRP, "Shielding for High Energy Electron Accelerator Installation," Natl. Council on Radiation Protection and Measurements, National Bureau of Standards NBS No. 97 and NCRP Rpt. No. 31 (1964)

Noonan, D. J. and J. L. Russell, Trans, 26th Annual Meeting of Health Physics Society, Louisville (1981)

Paretzke, H. G., "Heavy Ion Tracks in Plastics," Solid State Nuclear Track Detectors Vol. I, Proc. 9th intl. Conf., Neuherberg/Munchen, Germany (197)

Paretzke, H. G., T. A. Gruhn, E. V. Benton, Nucl. Instr. Meth. 107, 597 (1973)

Paretzke, H. G., "Some Remarks on the Formation and Development of Particle Tracks in Plastics," Proc. 8th Intl. Conf. Nucl. Photo, and Solid State Det., Budapest, Hungary (1972)

Paterson, H. W. and R. H. Thomas, Accelerator Health Physics, Academic Press, New York City (1973)

Pisch, E. and J. Jiasiac, "Automatic Spark Counting of Fast Neutron Induced Recoil Particles in Polymers," Solid State Nuclear Track Detectors Vol. I, Proc. 9th Intl. Conf., Neuherberg/Munchen, Germany (1979)

Piesch, E., "Developments of Radiophosphoressence Dosimetry," Chapter in Topics in Radiation Dosimetry, Suppl. I, F. H. Attix, Editor; Academic Press, New York City (1972)

Prêtre, S., "Personnel Neutron Dosimetry: Based on Automatic Fission Track, and Spark Counting, for Routine and Emergency Use," Proc. Symp. Neut. Mon. Rad. Prot. Purposes, IAEA, Vienna, Austria (1973)

Prêtre, S. "Measurement of Personnel Neutron Dosimetry by Fission Fragment Track Etching in Certain Plastics," Radiat. Eff. 5, 103 (1970)

Prêtre, S., E. Tochilin, N. Goldstein, "A Standardized Method for Making Neutron Fluence Measurements by Fission Fragment Tracks in Plastics," Proc. 1st Intl. Cong. IRPA (1968)

Price, P. B. and R. M. Walker, "Electron Microscope Observation of Etched Tracks from Spallation Recoils in Mica," Phys. Rev. Lett. I, 217 (1962)

Rossi, H. H. and G. Failla, "Tissue-Equivalent Ionization Chambers," Nucleonics 14, 32 (1956)

Sanders, M. E., K. Z. Morgan, P. H. McGinley, "Investigation of Contamination Neutrons Generated In and About High Energy Accelerator X-Ray Beams Used in Medical Therapy,' 15th Mid-Year Meeting of Health Physics Sociey, Orlando (1982)

Sanders, M. E., K. Z. Morgan, P. H. McGinley, "Measurement of Neutron and charged Particle Contamination in High Energy Medical X-Ray Beams Using Recoil Track Registration in Polycarbonate Foils," 25th Meeting of Health Physics Society, Seattle (1980)

Sanders, M. E., "Design and Application of a Damage-Track Neutron Dosimeter Useable in the lev or 17 Mev Neutron Energy Region", Ph.D. Thesis, Georgia Institute of Technology, (1982)

Schwartz, R. B. and C. M. Eisenhauer, "Use of a D_2O Moderated ^{252}Cf Source for Dosimeter Testing and Calibration," 8th DOE Workshop on Neutron Dosimetry, Louisville (1981)

Schwartz, R. B. and C. M. Eisenhauer, "The Design and Construction of a D_2O-Moderated ^{252}Cf Source for Calibrating Neutron Personnel Dosimetrs Used at Nuclear Power Reactors," NUREG/CR-1204 (1980)

Schwartz, R. B., "Calibration and Use of Filtered Beams," National Bureau of Standards Special Publication #493 (1977)

Seitz, F., "The Disordering of Solids by the Action of Fast, Massive Particles," Disc. Faraday Soc. 5, 271 (1949)

Silk, E. C. H. and R. S. Barnes, "Examination of Fission Fragment Tracks with an Electron Microscope,' Phil. Mag 4 (1959)

Sohrabi, M., "Electrochemical Etch Amplification of Low LET Recoil Particle Tracks in Polymers for Fast Neutron Dosimetry," PhD Thesis, Georgia Institute of Technology (1975)

Sohrabi, M. and K. Becker, "Fast Neutron Personnel Dosimetry by Fission Fragment Registration from ^{237}Np," Nucl. Instr., Meth. 104, 409 (1972)

Sohrabi, M. and K. Becker, "Some Studies on the Application of Track Etching in Personnel Fast Neutron Dosimetry," ORNL-TN-3605, ORNL (1971)

Somogyi, G. and I. Hunyadi, "Etching Properties of the CR-39 Polymeric Nuclear Track Detector,' Proc. 11th Intl. Conf. on SSNTD, Bristol England (1981)

Somogyi, G., "Etching Properties of the CR-309 Polymeric Nuclear Track Detector," Proc. 10th Intl. Conf. on SSNTD, Lyons, France (1980)

Somogyi, G., "A Study of the Basic Properties of Electrochemical Track Etching," Solid State Nuclear Track Detectors Vol. I, Proc. 9th Intl. Conf., Neuherberg/Munchen, Germany (1979)

Somogyi, G., "Processing of Plastic Track Detectors," Nucl. Tracks 1, 1 (1977)

Somogyi, G. and J. Gulyas, "Methods for Improving Radiograms i Plastic Detectors," Radioisotopy 13, 549 (1972)

Somogyi, G. and D. S. Srivastava, Proc. 7th Intl. Colloq. Nucl. Photo. and Solid State Track Detectors, Barelona (1970)

Spurny, F., Z. Prouza, I. Bucina, P. Galan, A. Hrabovocova, J. Kubeckova, D. Nikodenova, J. Singer, H. Solnicka, J. Trousil, K. Truek, "Czechoslavak Nuclear Accident Dosimetry System: Methods and Organization," Intl. Symp. Adv. Rad. Prot. Mon. Stockholm (1979)

Spurny, F. and K. Turek, "Neutron Dosimetry wit Solid State Nuclear Track Detectors," Nucl. Tracks 1, 189 (1977)

Stillwagon, G. B., "The Microdosimetry of Pu=39 in Bone Using Electrochemical Etching and Polycarbonate Foils," PhD Thesis, Georgia Institute of Technology (1978)

Stoddard, D. H. and H. E. Hootman, "^{252}Cf Shielding Guide," USAEC Rept. DP-1246 (1971)

Storer, J. B., P. S. Harris, J. E. Furchner, W. H. Langhorn, Radiation Res. 6, 188 (1957)

Su, S-J., M. Sanders, K. Z. Morgan, "Thermal Neutron Dosimetry," Proc. 24th Annual Health Physics Soc., Philadelphia (1979)

Su, S-J, "Neutron Dosimetry Using Electrochemical Etching," PhD Thesis, Georgia Institute of Technology (1979)

Swanson, W. P., "Calculations of Neutron Yields Released by Electrons Incident on Selected Materials," Stanford Linear Accelerator Center, Rpt. No. SLAC-Pub-2042 and Health Physics 35, 353 (1978)

Tobazeon, R. and E. Gartner, "On the Behavior of Ions at Insulator Liquid Interfaces and Its Consequences for Losses in Impregnated Insulators," Proc. Conf. Elec. Insul. and Dielec. Phenom. (1975)

Tommasino, L., G. Zapporili, E. V. Griffith, A. Mattei, "Electrochemical Etching: Mechanisms (I); Methods, Apparatus, and Results (II)," Nucl. Tracks 4 (1981)

Tommasino, L. G. Zapproili, R. V. Griffith, J. C. Fisher, "Electrochemical Etching CR-39 Foils for Personnel Neutron Dosimetry," 5th Intl. Cong. IRPA, Jerusalem (1980)

Tommasino, L. and G. Zapporili, "Further Investigation on Elecrochemical Etching for Personnel Neutron Dosimetry," 7th DOE Workshop on Pers. Neut. Dos., London (1978)

Tommasino, L., "Electrochemical Etching for Personnel Nuetorn Dosimetry," 6th DOE Workshop on Personnel Neutron Dos.. Oak Ridge (1977)

Tommasino, L. and C. Armellini, "A New Etching Technique for Damage Track Detection," Radiat. Eff. 20, 253 (1973)

Tommasino, L. "Method and Apparatus or Electrochemical Development of Damage Tracks Produced by Radiation Insulating Materials," Italian Pt. No. 51929A (1970)

Tripier, J., R. Opel, G. Remy, M. Debeauvais, "Fast Neutron Dosimetry by Means of a Cellulose Nitrate Detector," Nucl. Instr,. Meth. 125, 487 (1975)

Trousil, J., J. Singer, L. Kokta, Z. Prouza, "The Personnel Dosimetry Methods Introduced in the Czechoslovak National Laboratory," Intl. Symp. Adv. Rad. Prot. Monit., Stockholm (1979)

Vallario, E. J. and D. E. Hankins, "The USAEC Workshop on Personnel Neutron Dosimetry," Proc. Symp. Neut. Mon. Rad. Prot. Purposes, IAEA Vienna (1973)

Walker, R. M., P. B. Price, R. L. Fleischer, "A Versatile, Disposable Dosimeter for Slow and Fast Neutrons," App. Phys. Lett. 3, 28 (1963)

Yoshimura, N., F. Noto, K. Kikuchi, "Growth of Water Trees in Polyethylene and Silicon Rubber by Water Electrodes," IEEE Trans. Elect. Insul. E1, 411 (1977)

Young, D. A., "Etching of Radiation Damage in LiF," Nature 182 (1958)